T NO. UMTA-MA-06-0025-75-16.II

AN ASSESSMENT OF THE CRASHWORTHINESS OF EXISTING URBAN RAIL VEHICLES

Volume II: Analyses and Assessments of Vehicles Chapters 8 Through 12 and Appendixes and References

R.J. Cassidy
D.J. Romeo

NOVEMBER 1975
FINAL REPORT

Prepared for

U.S. DEPARTMENT OF TRANSPORTATION
URBAN MASS TRANSPORTATION ADMINISTRATION
Office of Research and Development
Washington DC 20590

Technical Report Documentation Page

1. Report No.	2. Government Accession No.	3. Recipient's Catolog No.
UMTA-MA-06-0025-75-16.II		

4. Title and Subtitle: AN ASSESSMENT OF THE CRASHWORTHINESS OF EXISTING URBAN RAIL VEHICLES. Volume II: Analyses and Assessments of Vehicles, Chapters 8 Through 12 and Appendixes and References

5. Report Date: November 1975

6. Performing Organization Code:

7. Author(s): R.J. Cassidy and D.J. Romeo

8. Performing Organization Report No.: DOT-TSC-UMTA-75-21.II

9. Performing Organization Name and Address:
Calspan Corporation*
P.O. Box 235
Buffalo NY 14221

10. Work Unit No. (TRAIS): UM604/R6745

11. Contract or Grant No.: DOT-TSC-681

12. Sponsoring Agency Name and Address:
U.S. Department of Transportation
Urban Mass Transportation Administration
Office of Research and Development
Washington DC 20590

13. Type of Report and Period Covered: Final Report
August 1973 - June 1975

14. Sponsoring Agency Code:

15. Supplementary Notes

*Under contract to: U.S. Department of Transportation.
Transportation Systems Center,
Kendall Square
Cambridge MA 02142

16. Abstract

The crashworthiness of existing urban rail vehicles (passenger cars) and the feasibility of improvements in this area were investigated by Calspan Corporation under contract to the Transportation Systems Center of the U.S. Department of Transtation in its role as systems manager for the Urban Mass Transportation Administration's Urban Rail Supporting Technology Program. Both rail-car structural configurations and impact absorption devices were studied. From this work, recommendations for engineering standards for urban rail vehicles will be developed.

This final report issued under the crashworthiness effort covers:

1. The development of analytical tools to predict passenger threat - environment during collision.
2. Criteria for predicting passenger injury due to train collisions.
3. An application of injury criteria and analytic models to predict passenger injuries resulting from collisions of trains that represent existing construction types.
4. A preliminary investigation of applying impact absorption devices to transit vehicles.
5. A design study of car structural configurations for improved impact energy management.
6. A review of engineering standards for Urban Rail Car Crashworthiness.

The report consists of three volumes:

Volume I: Analyses and Assessments of Vehicles, Chapters 1 Through 7
Volume II: Analyses and Assessments of Vehicles, Chapters 8 Through 12, Appendixes and References
Volume III: Train Collision Model User's Manual.

(Probably can't be found per UTM-53)

17. Key Words	18. Distribution Statement
Railway Car Crashworthiness, Train Crashes, Transportation Safety, Mass Transit, Urban Rail Car, Rapid Transit Car, Crashworthiness, Commuter Rail Car	DOCUMENT IS AVAILABLE TO THE PUBLIC THROUGH THE NATIONAL TECHNICAL INFORMATION SERVICE, SPRINGFIELD, VIRGINIA 22161

19. Security Classif. (of this report)	20. Security Classif. (of this page)	21. No. of Pages	22. Price
Unclassified	Unclassified	178	

Form DOT F 1700.7 (8-72) Reproduction of completed page authorized

PREFACE

In support of the Rail Technology Division of the Office of Research and Development of the Urban Mass Transportation Administration (UMTA), the Transportation Systems Center (TSC) has been assigned systems management responsibility for the UMTA Urban Rail System Supporting Technology Program.

As part of this program, TSC is conducting analytical and experimental studies directed towards improved urban rail system safety. A specific goal in the area of safety is reduction of both the number and the severity of injuries that may result from the collision of two trains.

On 16 August 1973, TSC contracted with Calspan Corporation to perform this study for the assessment of the crashworthiness of existing urban rail vehicles. This report presents a compilation of relevant background studies conducted prior to the start of this contract and an overall description of the work done during the course of this study conducted for the Rail Technology Division of the Urban Mass Transportation Administration under the TSC Urban Rail Supporting Technology Program.

This report is being published in three volumes. Volume I contains analyses and assessments of vehicles, Chapters 1 through 7. Volume II contains Chapters 8 through 12, all appendixes, and all references. Volume III contains a Train Collision Model User's Manual.

The authors take this opportunity to acknowledge the technical contributions to this report made by the program's technical monitor, Dr. Robert Raab of the Transportation Systems Center, U.S. Department of Transportation, Cambridge, Massachusetts; and by the Program Manager, Mr. Frederick Rutyna, also of the Transportation Systems Center.

The contributions of Mr. David J. Segal of Calspan Corporation are also recognized. Mr. Segal developed the computer program used for the analysis and applied this program to the many cases studied.

TABLE OF CONTENTS

TABLE OF CONTENTS (Cont.)

TABLE OF CONTENTS (Cont.)

LIST OF FIGURES

LIST OF FIGURES (Cont.)

LIST OF FIGURES (Cont.)

LIST OF FIGURES (Cont.)

VOLUME TWO

LIST OF FIGURES (Cont.)

LIST OF FIGURES (Cont.)

LIST OF TABLES

8. RAILCAR OVERRIDE

8.1 INTRODUCTION

A very general definition of an override collision is one in which the cars do not develop their full longitudinal strength potential. The classical form of override occurs when the overridden car is severely penetrated, with the primary longitudinal structure below the car floor left intact. Another form of "lateral override" occurs when major longitudinal structure of one or both colliding cars is displaced laterally during the collision without absorbing significant energy. Various forms of partial override occur in which the major structural elements below the car floor absorb some energy, but significantly less than their full potential.

It is noted in Chapter 5 that the relatively simple one dimensional car model being used in the present investigation is not capable of predicting the sometimes complex three dimensional behavior of a particular car in a collision. Its primary usefulness is in relating gross structural and interior car parameters to car crashworthiness, measured in terms of fatalities and injuries in a specified collision situation. In this context, an example of a gross car parameter is the effective longitudinal strength which is developed in a collision, regardless of the complex design characteristics which are involved in the development of this strength.

Because of the limitations of the one dimensional analysis, and the significance of the override problem, it is appropriate at this point to review what is known about override, from accident experience and from primarily qualitative analyses of typical car designs. Hence, an objective in this section is to identify structural design features and characteristics which appear to be "good" or "bad" in terms of likely override.

In Chapter 9, priority areas for the development of more crashworthy cars are examined. One of the major areas examined is the achievement of a controllable and predictable car force versus deflection characteristics. This portion of the study in Chapter 9 draws upon the override considerations in this section. However, an important objective of the overall study is to investigate the relationship between car design parameters and car crashworthiness. Hence, the reader primarily interested in these broad parametric aspects of the study may proceed directly from Chapter 7 to Chapter 9.

In the following sub-section, some significant collisions are reviewed. These collisions involved either full override, partial override or, at low speeds, failures which would appear to lead to override. In subsequent sections (8.3 through 8.7) qualitative and very approximate quantitative aspects of override are examined.

8.2 PREVIOUS COLLISIONS

Five collisions of identical or similar cars are summarized in Figure 8-1, and four additional collisions of dissimilar cars are summarized in Figure 8-2.

The Darien collision* (1969) occurred between two trains of identical equipment built to AAR specifications requiring anti-climbers, crash posts and locked trucks. The cars were multiple unit (MU) cars built in 1954. Car weight was approximately 157,000 pounds. A nine car train, (Train 49) weighing approximately 1,410,000 pounds, was travelling forward at an estimated speed of 30 mph at the time of impact with a three car train (Train 48) weighing approximately 470,000 pounds and also travelling forward at an estimated speed of 30 mph at time of impact. Estimated closure speed was therefor 60 mph. Inspection of the damaged cars indicated that Train 48 was overridden by Train 49 about midway

* Report NTSB-BAR-7d-3

Date	Place	Property	Type of Cars Involved	Est. Speed (Closure)	Over-Ride	Remarks
8/20/67	Darien, Conn.	P.C.R.R.	MU cars built in 1954	60 mph	Yes	Cars identical and conformed to AAR specifications. Nine car train over-rode 3 car train.
1969	Lindenwold, N.J.	D.R.P.A.	DRPA Rapid Transit Cars	22 mph	No	Not in revenue service
1972	Oakland, Calif.	BART	BART "A" Cars	25 mph	Apparently not	Not in revenue service
2/5/74	Philadelphia, Pa.	P.C.RR	Budd Silverliner & St. Louis Car Silverliner	10 mph	See Remarks	Oblique impact, main sill structure essentially intact but extensive damage to side of superstructure.
11/22/50	Rockville Ctr. Long Island, New York	LIRR	Identical commuter cars	High	Full Override	Over-ridden car completely destroyed

Figure 8-1. Study of Override-Previous Collisions of Identical or Similar Cars

Date	Place	Property	Type of Cars Involved	Est. Speed (Relative)	Over-Ride	Remarks
10/30/72	Chicago, Ill.	I.C.G. RR	Old style MU's and bilevels	45-55 mph	Yes	Collision posts failed on bilevel car. Half of car superstructure destroyed.
2/28/56	Swampscott,	B&M RR	RDC car and old style coach	50 mph	Yes	Coach over-ride RDC. severe damage and many fatalities
1970	New York City	LIRR	Old and new style MU's	about 15 mph	Yes	Center sill of old car bent upwards
10/13/39	Napier, Mo.	CB&Q RR	Burlington Zephyr, Old coach	High	Yes	Most of coach destroyed

Figure 8-2. Study of Override-Previous Collisions of Dissimilar Cars

through the crash. Total crush of Train 48 was 30 feet. Approximately the first 13 feet of crush appeared to be well controlled, with crushing of the underframe as well as the superstructure taking place. However, in the final 17 feet of crush, the underframe of Train 48 was left intact, with continuing crushing of the superstructure. In Train 49, only moderate damage occurred to the underframes of five trailing cars and in Train 48, moderate damage occurred to the two trailing cars. Significant crush of the lead car underframes occurred before climbing took place; hence the collision posts apparently functioned well in the early stages of the collision.

The collision between two identical Delaware River Port Authority (DRPA) cars in 1969 is of interest because the 22 mph closure speed was sufficiently moderate that the failure sequence was not obscurred. The cars struck at the anti-climbers, causing one anti-climber to crush about 5 inches while maintaining alignment. One draft sill system yielded and buckled, however, permitting about 1 inch of additional travel. It is assumed that the 6 inches of crush which took place changed the speed of the moving car from 22 mph to 11 mph. The average force level can be calculated based upon equating the kinetic energy expended in the crash to the work done in deformation and yields a value of approximately 250,000 pounds. Since the cars were designed to resist a buff load of 200,000 pounds, the anti-climbers apparently functioned well in this collision.

The collision between two BART cars which occured in Oakland, California, in nonrevenue service in 1972 is also significant because the relatively low closure speeds left sufficient structure intact to analyze failure modes. Each of the colliding cars was pushed inward about 2 feet at draft gear level. The 2 feet of longitudinal deformation occurred as intended by the designers, with the sides of the draft gear (center sill) box beam peeling away at the junction of the center sill and the car body bolster, as shown in Figure 8-3. Using a common velocity after car crush which was one half the striking velocity (from conservation of momentum), the striking velocity can be computed from energy dissipation considerations. Weight of the BART car was approximately 60,000 pounds, and the center sill was designed to fail at about 200,000 pounds.

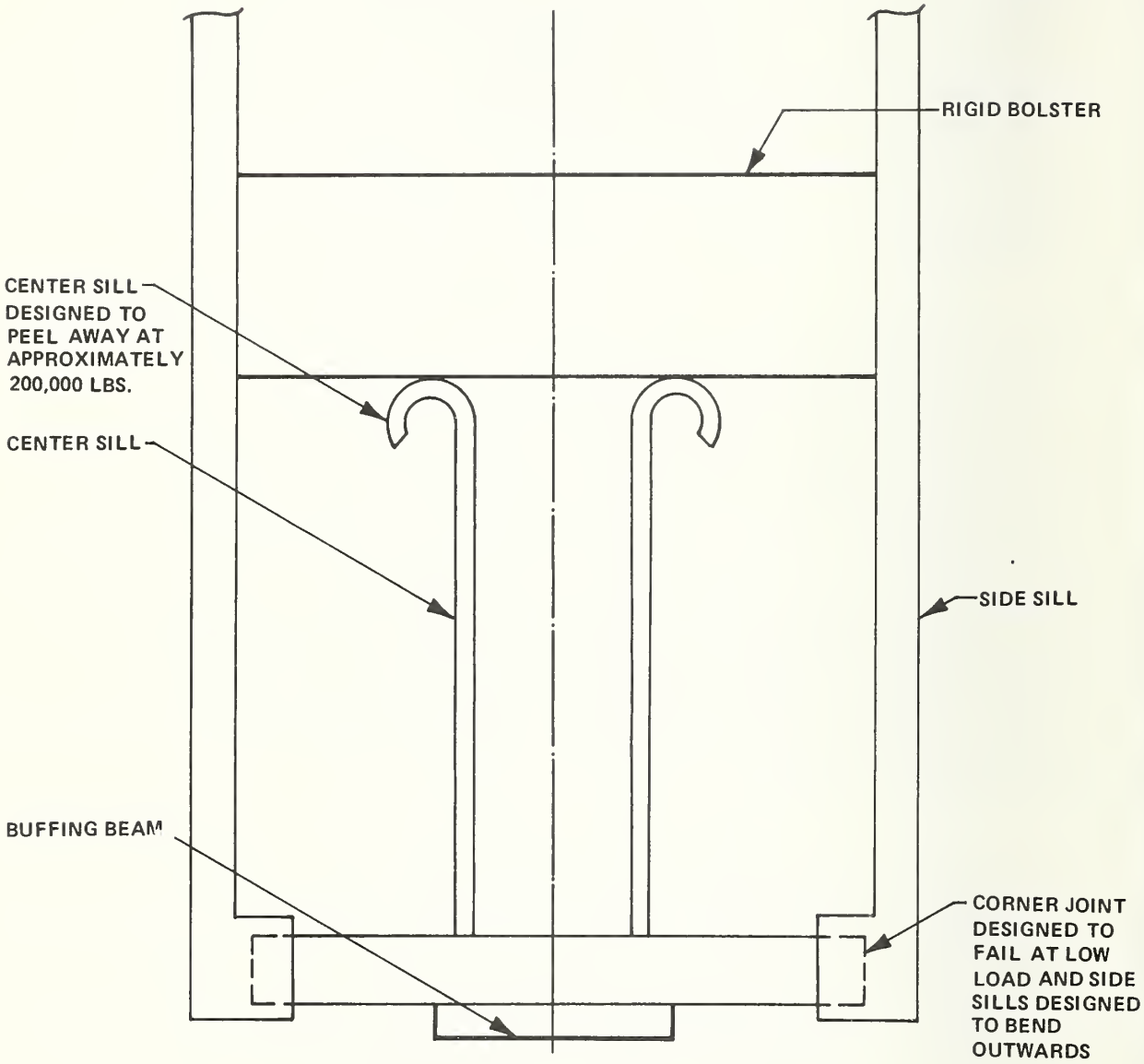

Figure 8-3. Schematic of BART Energy Absorber

Based on the estimated 2 feet of crush for each car, the striking velocity would be 28 mph. Estimates of the striking velocity ranged from 25 mph to 40 mph; however the lower figure appears to be more accurate, as a 40 mph striking velocity would have required that each car crush a distance of approximately 4 feet, about twice the amount which the damage indicated. The calculations above are based on retention of the initial 200,000 pound crush load over the full 32 feet. Inspection of BART car failures in low speed collisions* shows that the center sill tends to be bent significantly upwards or downwards in the process of failing. The BART car has no collision post requirements and the actual collision post is light structure with no rigid vertical load path from the draft sill structure into the collision post structure. If this vertical flexibility were to lead to override in a 40 mph frontal collision of long trains, significantly more than 32 feet of the car structure would be vulnerable.

The collision in Philadelphia in 1974 between a Budd Silverliner and a St. Louis Car Silverliner was an oblique impact which occurred at low speed (10 mph) during a switching operation. Classical override did not occur. However the collision is significant because the oblique impact resulted in considerable damage and penetration of the side of one of the Silverliners. The operator and a passenger several feet behind the operator on the penetrated side were severely injured. The Silverliner has a vestibule at the front end, and the car has typical vestibule construction features. The side door and steps result in elimination of the side sill structure in the vestibule area. Corner posts are relatively light and not adequate to prevent penetration in the type of oblique impact which occurred. No significant damage was done to the draft sill of either car.

---

* The low speed collision described above and an additional collision in which a BART car engaged a sand pile barrier after control malfunction had caused the car to run off the end of the track.

The very severe frontal collision between identical MP-54 cars on the Long Island Railroad at Richmond Hill, Queens, in November 1950, resulted in complete override of one car. The overridden car was completely destroyed, contributing to 77 fatalities and 153 injuries.* Because of the degree of destruction, failure sequence could not be inferred. The significance of this accident is that it demonstrates that full, catastrophic override can occur between identical cars. However, the cars did not have anti-climbers. There was no significant underframe damage on the overriding car.

A collision on the Long Island Railroad in 1970 between old and new style Multiple Unit Cars** may shed some light on the structural behavior of the cars in the severe Richmond Hills accident. The old style cars in this accident were MP 54 cars, similar to the cars in the Richmond Hills accident. In this accident the sill bent upwards in the MP car. This type of failure would lead to severe override at higher speeds.

The 1972 Illinois Central Gulf Railroad collision in Chicago occurred between entirely dissimilar cars. In this collision, the new style bilevel car was overridden by an old style single level car. The collision posts failed on the bilevel car and its superstructure was destroyed. The accident report*** discusses in considerable detail the attachment of the collision posts to the end underframe of the bilevel car. Indications of weakness and imperfections in the welded attachment were found. It was also noted that the attachment was designed primarily for shear between the collision post and the end underframe, with no strong provisions for loads normal to the shear plane.

---

* A formal agency report on the accident has not been located, and may not exist. Details of the accident were obtained from New York newspapers published subsequent to the crash on Nov. 22, 1950.

** The cars are classified as dissimilar cars. Therefore the accident is summarized in Figure 8-2.

*** Anon., "Collision of Illinois Central Gulf Railroad Commuter Trains, Chicago, Illinois--Oct. 30, 1972", Railroad Accident Report NTSB-RAR-73-5, National Transportation Safety Board, Washington, D.C., 28 June 1973.

The B&MRR collision in Swampscott, Massachusetts (1956) involved overriding of a Rail Diesel Car (commonly called "RDC Car") by an old style coach. Damage to the RDC Car was severe, resulting in 13 fatalities. In the accident report shown below, the RDC Car is CAR #6150, and the old style coach is CAR #3684.

> "The destruction of Car #6150 resulted from the unusual combination of forces and circumstances which occurred at and immediately following the moment of impact. Apparently the trailing end of the last car (#3684) of the stopped train was lifted up off its trucks (no locking king pins on this ex-Reading Car) and at the same time the whole end frame unit was sheared and broken off the front end of car #6150. The momentum of car #6150 and the following three cars then pushed car #6150 on under car #3684, sheering off the left side frame at the floor and the roof above the letterboard on the right side. The end underframe of car #6150 was broken at the rear draft stops and at the connection to the stainless steel center sill, and connections of bolster ends to side frames were broken, but end underframe remained connected to truck, and the underframe remained about at its normal location with relation to the remainder of the floor, except rotated nearly 90°. Car #3684 finally came to rest on top of the trailing end of car #6150 immediately adjacent to the end frame and in partial contact with the front end of the second car."

The 1939 collision in Napier, Missouri, was between a Burlington Zephyr locomotive and an old style coach. The coach was overridden and most of it was destroyed, resulting in 45 fatalities. The locomotive buffing beam was above the underframe of the old car. Override occurred with little underframe resitance.

From this review, the following observations appear to be significant.

(1) Override can occur between cars of the same design. Anti-climbers are effective at low speeds but lose their effectivity when significant underframe crush is involved.

(2) The likelihood of severe override appears to increase in higher speed collisions.

(3) In low speed collisions, where relatively minor override occurred or where override tendencies were indicated, (Oakland, L.I.R.R. in New York City) failures in the end underframe structure and/or its attachment to adjacent structure resulted in significant deformation of the end underframe in the vertical plane.

(4) In higher speed collisions where severe override or structural spreading occurred (e.g., Darien, Chicago, Swampscott) very large deformations of the end underframe were observed.

(5) In high speed accidents, (closure speeds of 40 mph to 60 mph) severe second collision injuries to passengers in undeformed car sections have not been reported. These accidents have generally involved trains of approximately equal weight.

In regard to observation (2), specific accidents were not found which could demonstrate the effectiveness of conventional transit car anti-climbers at closure speeds significantly in excess of 20 mph. In discussions with experienced operating engineers in the transit properties, the view was expressed that anti-climbers are not effective in high speed accidents. This appears to confirm observations of damaged cars which indicate that anti-climbers and buffing beams can be made ineffective by excessive vertical deformation and failures in the anti-climber back up structure.

Observations (3) and (4) appear to have considerable significance, in terms of existing railcar design. In the following section, an elementary review of the kinematics of override tends to confirm accident observations - that severe override must be accompanied by significant structural deformations, generally extending over a significant length (measured from the front end) of one or both colliding cars.

8.3 KINEMATICS OF OVERRIDE

Override (climbing) and subsequent telescoping of a rail car during a collision may, in theory, occur without any vertical deformation of the car structure (Figure 8-4 [a]) or, at the other extreme, may occur wholly as a result of vertical deformation (Figure 8-4 [b]). For this range of collision situations, we are interested in studying the relationship between vertical climb accelerations and longitudinal accelerations of the car. These accelerations are of interest because they relate directly to the longitudinal and vertical forces imposed on the car structure during collision.

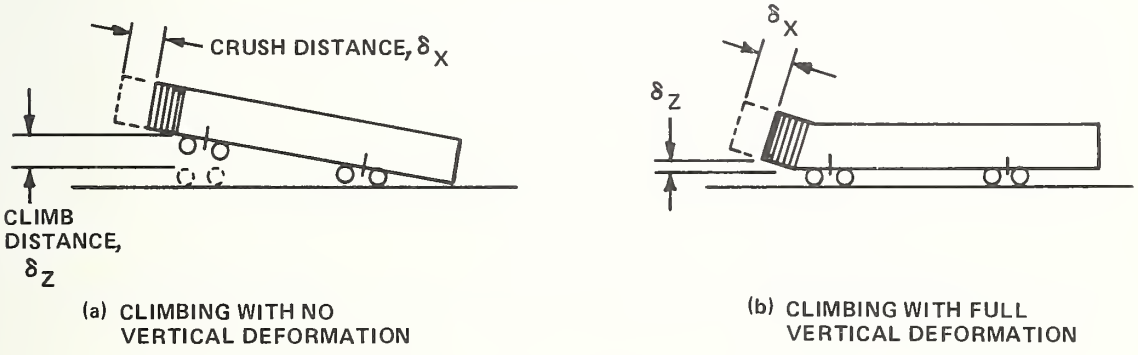

Figure 8-4. Kinematics of Rail-Car Climbing

To keep the analysis simple, two assumptions were made:

The rail car has a perfectly plastic crush-force-versus-longitudinal-deflection (force/deflection) curve, resulting in constant car deceleration in the longitudinal direction.

The vertical acceleration at the front of the rail-car body during climbing is also constant.

The effect of these assumptions on the analysis is discussed later.

For impact velocity, V_c, the crush distance, δ_X, is related to time, t, by

$$\delta_X = V_c t - \frac{1}{2} a_X t^2 \tag{8-1}$$

where a_X is the constant longitudinal deceleration.

From Equation 8-1,

$$t = \frac{V_c - \sqrt{V_c^2 - 2a_X\delta_X}}{a_X} \tag{8-2}$$

For constant vertical acceleration, a_Z, the vertical acceleration is related to the distance of vertical climb, δ_Z, by

$$a_Z = \frac{2\,\delta_Z}{t^2} \tag{8-3}$$

Substituting expression 8-2 for t into Equation 8-3,

$$n_Z = \frac{a_Z}{g} = \frac{\delta_Z\, a_X^2}{V_c^2 - V_c\sqrt{V_c^2 - 2a_X\delta_X} - a_X\delta_X}\left[\frac{1}{g}\right] \tag{8-4}$$

Equation 8-4 shows that the vertical acceleration at the front of the car (number of g's, n_Z) can be expressed as a function of

a_X, longitudinal deceleration
δ_X, longitudinal crush distance
δ_Z, distance of vertical climb
V_c, impact velocity

We note that δ_X and δ_Z are instantaneous values of crush and vertical displacement at some time t at which the velocity, V, of the rigid portion of the car is given by

$$V = V_c - a_x t$$

Equation 8-4 is plotted in Figure 8-5 for the following two cases:

(1) a_x = 32 feet/sec/sec (1 g)
δz = 1 foot
V_c = 30 mph

(2) a_x = 32 feet/sec/sec
δz = 1 foot
V_c = 45 mph

The selection of 32 feet/sec/sec for a_x represents a typical crash deceleration for trains; however, we will see that the general conclusions from this analysis are the same at significantly higher or lower decelerations. A value of 1 foot is selected for climb height (δz) because many car-end underframes and main-sill structural components are about this height; in a crash which is characterized by full climbing in the vertical direction, these structures would achieve a position in which the end underframe of one colliding car has passed over the top of the end underframe of the other colliding car.

Figure 8-5 shows that extremely large vertical accelerations at the car end would be required to result in full climbing, unless the climbing takes place over a significant length of horizontal travel. The numbers tabulated below, taken from Figure 8-5, illustrate this.

HORIZONTAL TRAVEL (ft)	VERTICAL ACCELERATION (g's)	
	V_c = 30 mph	V_c = 45 mph
	>100	>100
2	30	65
4	7.2	16.5
8	1.6	4.0
12	0.66	1.7

High vertical accelerations are required to achieve the 1-foot climb height at relatively small horizontal travels because of the extremely small time associated with these small travels. If the car deceleration during the crash is greater than assumed in cases 1 and 2 above, rigid-body car velocity is reduced more rapidly, resulting in longer time periods for the crash and in

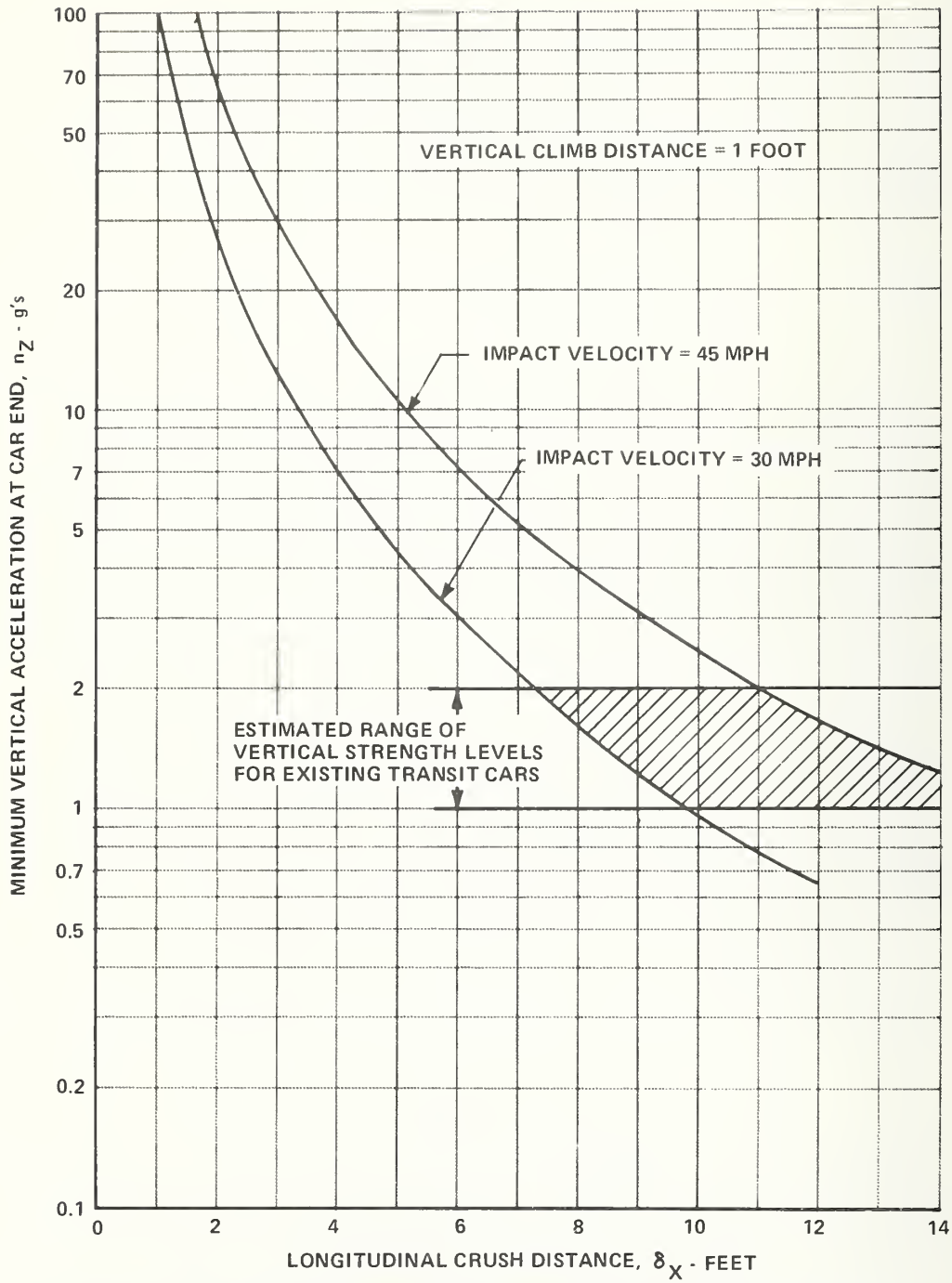

Figure 8-5. Minimum Vertical Acceleration Versus Longitudinal Crush Distance

lower vertical accelerations required to achieve a given climb height. However, even if train strength-to-weight ratio is such that relatively high decelerations are experienced, vertical accelerations associated with climbing still tend to be very high. For example, if the car deceleration level is 4 g's (instead of 1 g, as previously assumed), the vertical acceleration level associated with 4 feet of horizontal travel is 5.4 g's -- which is lower than the level of 7.2 g's associated with 1-g horizontal deceleration, but still quite high.

Note that the original assumptions (constant vertical and horizontal accelerations during crash) result in the lowest possible peak vertical acceleration, given that climb height (δ_Z) is achieved in the crush distance (δ_X). Thus, peak vertical accelerations will tend to be even higher than shown in Figure 8-5.

The high level of these vertical accelerations is illustrated by the fact that existing rapid-transit cars, as well as commuter and intercity cars, are not designed to resist vertical end accelerations significantly greater than 1g; in almost all cases, the available vertical strength at the car end is less than 2g's. (This will be shown in subsequent analysis of the available vertical strength at the ends of existing cars.)

Several significant conclusions may be drawn:

Climbing cannot take place without significant vertical deformation of one or both colliding cars (i.e., the high accelerations and resulting high vertical forces associated with zero vertical car deformation cannot be sustained by the car structure).

Because the available vertical strength at the ends of existing cars is relatively low, climbing -- when it does take place -- must occur over significant horizontal distances (generally, 10 feet or more) even at speeds as low as 30 mph.

The previous conclusions indicate further that severe climbing situations are characterized by significant vertical deformations which may occur anywhere in the end portion of the car back to a point at the truck bolster, which, for most designs, is about 10 or 12 feet from the end of the car.

These conclusions are particularly significant because rail-car structural specifications have put little or no emphasis on vertical strength and rigidity of car bodies in the end underframe area. Crash-post specifications are a good example. When crash-post specifications are included in car-body structural specifications (and, frequently, they are not included), the strength of the crash-post-to-end-underframe attachment is specified in the longitudinal direction, but never in the vertical direction.

While the previous analysis indicates that the vertical strength of car bodies in the end underframe area has not been properly emphasized, considerably more investigation is required to determine (1) the source of vertical loads which lead to car-body vertical failures and ultimate climbing, (2) the magnitudes of these loads, and (3) the level of vertical strength and stiffness required to prevent such failures.

Basic elements in the climbing problem can be identified by referring to Figure 8-6, where the elementary problem of longitudinal crash dynamics (sketches [a] and [b]) is compared to the elementary problem of crash dynamics during climbing (sketches [c] and [d]). The simplest model of longitudinal impact (Figure 8-6 [a]) involves rigid bodies, resulting in infinite accelerations at impact. A rough understanding of the problem is obtained from Figure 8-6 (b), where the weightless impacting surfaces are supported longitudinally by springs having a given effective stiffness. The element of climbing is introduced in Figure 8-6(c); however, it is evident that vertical forces and accelerations are infinite in this model because the vehicle masses must undergo a discontinuity in the vertical component of velocity. The simplest elementary model to reflect a climbing situation with any degree of realism is shown by Figure 8-6(d), where the weightless striking surface is supported by springs having given effective stiffness in the longitudinal and vertical directions.

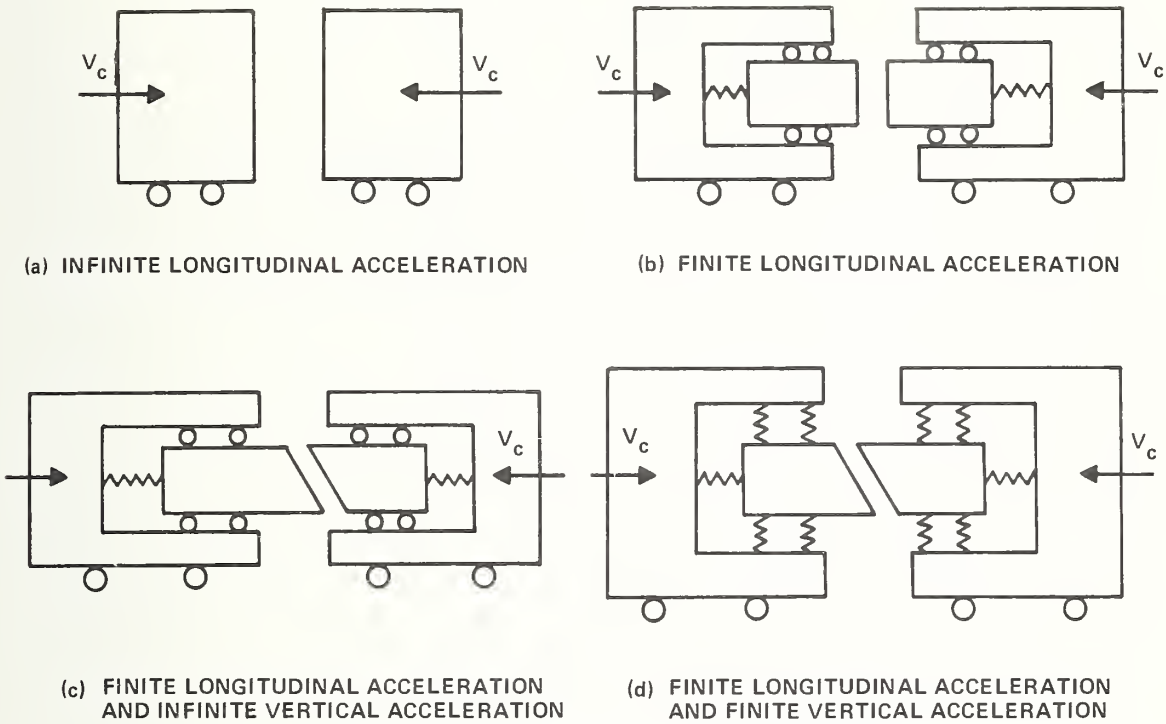

Figure 8-6. Elementary Models for Longitudinal and Vertical Acceleration in Crash

Climbing models similar to that shown in 8-6(d) can be used to obtain some understanding of the relationship between climbing loads and motions and the strength, stiffness and mass characteristics of the car end structure. Before using a relatively simple model to investigate these factors it is appropriate to identify means by which climbing loads and motions between cars of the same design, or similar designs, can be initiated.

8.4 INITIATION OF CLIMBING LOADS BETWEEN CARS OF THE SAME DESIGN

There appear to be several ways in which climbing loads between cars of the same design can be initiated. We first consider situations in which climbing is initiated at or near the instant of impact. Figure 8-7 shows a possible failure progression at impact of identical anti-climbers of the type used on most transit cars. In sketch 8-7(a) anti-climbers are shown meeting head on, with zero or negligible initial eccentricity. At this instant, the two anti-climbers, if perfectly rigid in all directions, would undergo infinite deceleration. Therefor, for any finite degree of rigidity, local deformation (whether due to brinelling, compression instability, bending or a combination of these) of the engaging tangs would take place. This deformation can take place in such a way as to produce a progressive wedging action, as shown in Figures 8-7(b) and 8-7(c). The vertical loads induced by this action will be transmitted further into the car structure, with the possibility of further vertical yielding and failure occurring.

Figure 8-7 illustrated how climbing can be initiated due to a particular anti-climber geometry, and given a striking situation in which the tangs strike directly, either head on or with slight initial eccentricity. Figures 8-8 through 8-11 illustrate a mechanism by which climbing may be initiated at impact without depending on local deformation of anti-climbing tangs. In Figure 8-8(a), the anti-climbers strike in such a way that the tangs miss entirely. In terms of conditions at initial impact, this situation can be similar to striking of vehicles having buffer plates (Figure 8-8(b)) instead of conventional transit car anti-climbers. (The BART car employs buffer plates instead of anti-climbers). For this situation, we want to investigate the stresses and deformations in the identical sections A-A and B-B, when the construction and the local dynamic loads are such that crushing occurs at this section. A simplified elastic-plastic stress strain curve for the material at this section is assumed, as shown in Figure 8-9. Figures 8-10(a) and 8-10(b) show the identical cross sections A-A and B-B displaced from each other by the

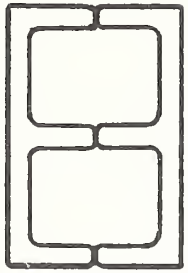

A

STANDARD ANTICLIMBERS
MEETING HEAD ON

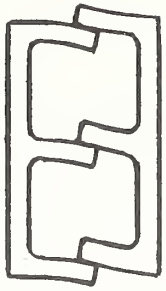

B

POSSIBLE DEFORMATION
OF ANTICLIMBERS
INSTANT AFTER - A

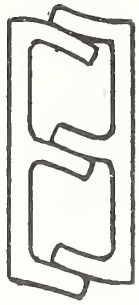

C

POSSIBLE DEFORMATION
OF ANTICLIMBERS
INSTANT AFTER - B

Figure 8-7. Possible Failure Mode of Standard Anticlimbers

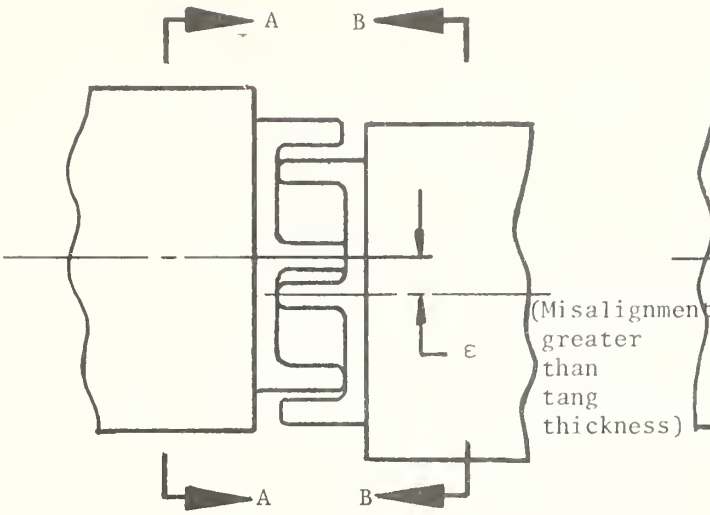

Figure 8-8a

Anticlimbers Meeting with Eccentricity-ε

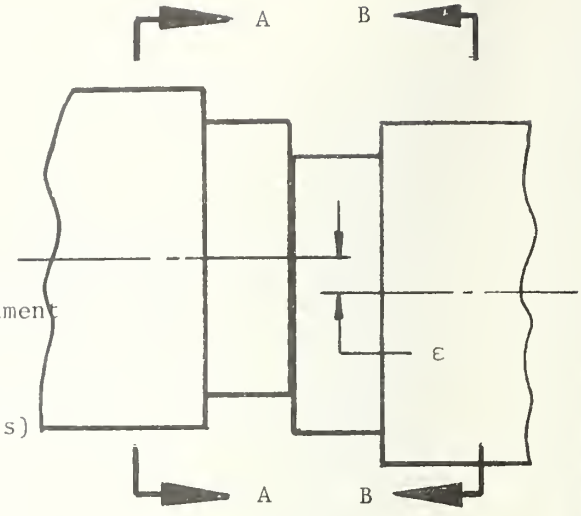

Figure 8-8b

Flat Face Buffers Meeting with Eccentricity-ε

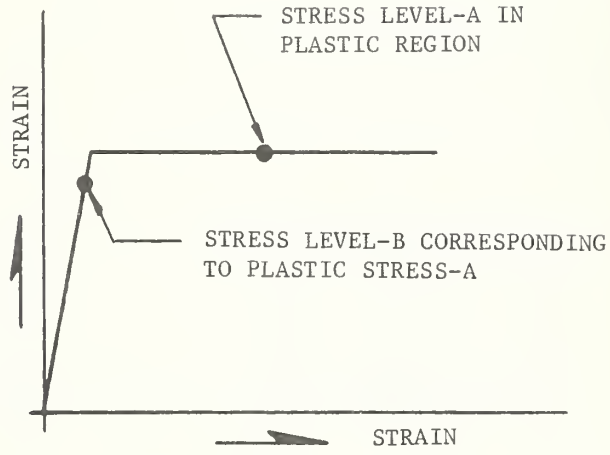

Figure 8-9. Pure Elastic-Plastic Stress Versus Strain

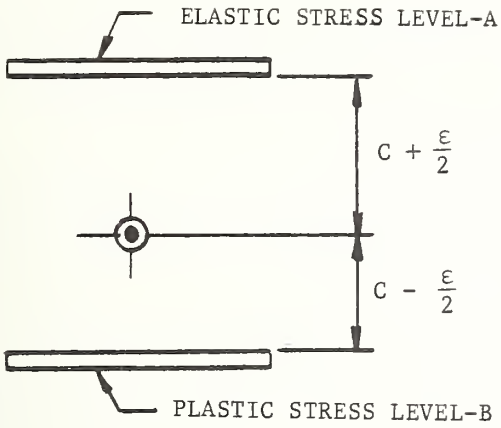

Figure 8-10a
Section A-A
(Ref. Figure 8-8)

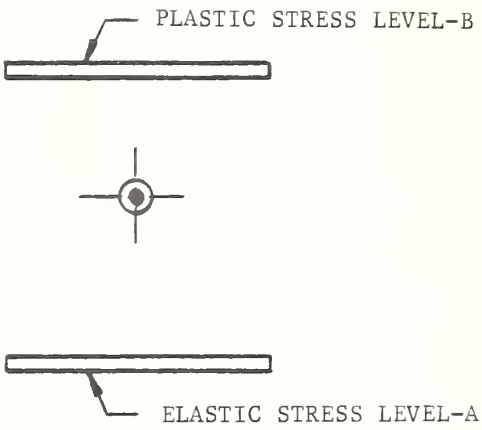

Figure 8-10b
Section B-B
(Ref. Figure 8-8)

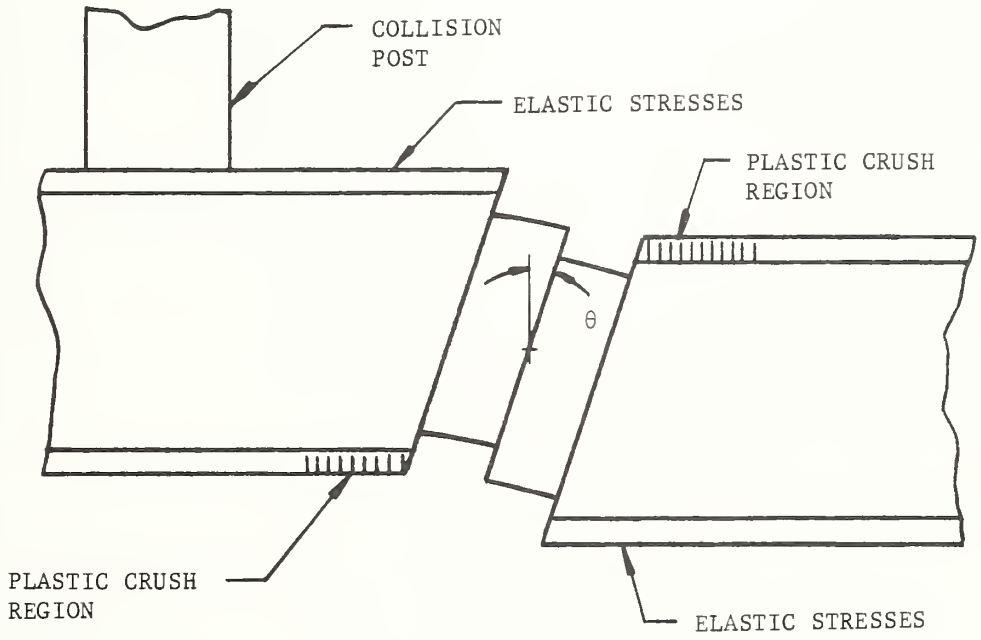

Figure 8-11. Wedge Angle Due to Structural Crush Forward of Collision Post

small misalignment ϵ. For this situation the load line during impact is displaced downward with respect to the centroid of A-A by 1/2 ϵ, and upward with respect to the centroid of B-B by the same amount 1/2 ϵ, as shown in the figure. Each section is subject to a moment given by

$$M_{AA} = -M_{BB} = \frac{1}{2} P\epsilon \qquad (8\text{-}5)$$

where P is the axial load in the sections at the instant of interest. In Section A-A, this moment requires that the stress level in the lower portion of the section be greater than that in the upper portion, whereas in Section B-B, the reverse is true. Hence, when the load P reaches a particular level during the impact, the first material to crush will be the bottom portion of Section A-A, and the top portion of Section B-B. This will result in the introduction of a wedging angle θ, as shown in Figure 8-11. For the simplified stress-strain curve in Figure 8-9, this angle will continue to increase indefinitely. In an actual collision, the angle θ might come to equilibrium as a result of other forces and motions arising from large plastic deformation. (e.g., vertical motions which would null the eccentricity, or a positive slope existing at some point in the plastic region of the stress-strain curve.) It is also noted that a wedge angle would result from small differences in material hardness and strength in section A-A and/or section B-B, and does not necessarily depend on any initial eccentricity.

The sources of climbing cited so far involve local plastic deformations forward of the collision post which can cause climbing angles and vertical forces to occur in the immediate instant after impact. Plastic deformations aft of the collision post can cause climbing conditions to be induced some period of time after initial impact, as indicated by Figures 8-12(a) and 8-12 (b). In the symmetrical crash condition shown in Figure 8-12(a), significant plastic deformation (measured in feet rather than inches) of the end underframe structure aft of the collision post leads to a pitch rotation of the collision post with accompanying large end moments occurring in the joint between collision post and end underframe, and vertical deformations at the end underframe. Such a

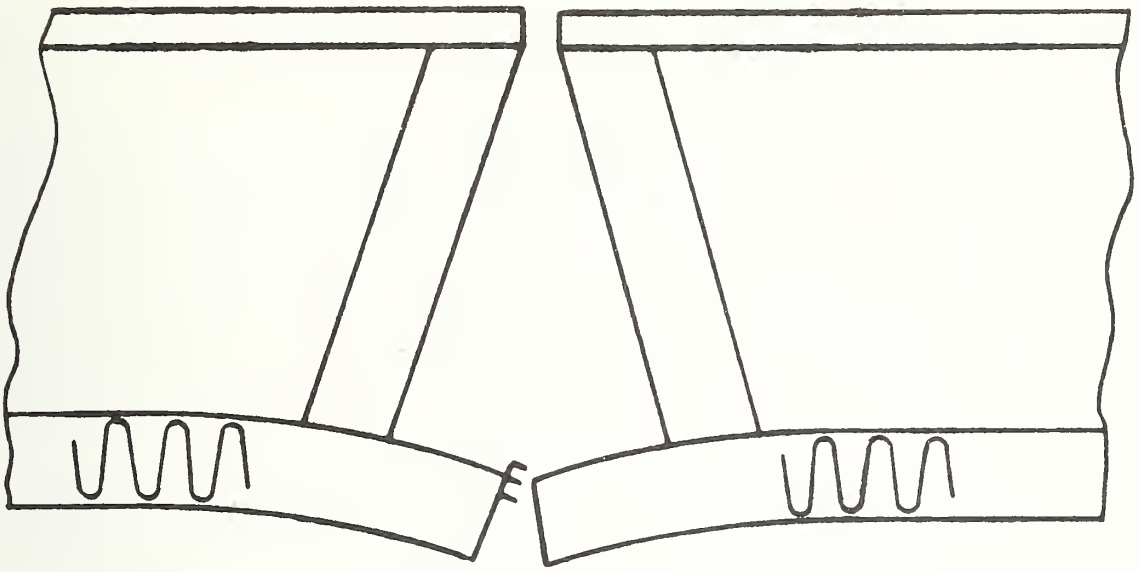

Figure 8-12a. Symmetrical Failure Mode due to Plastic Deformations Aft of Collision Post

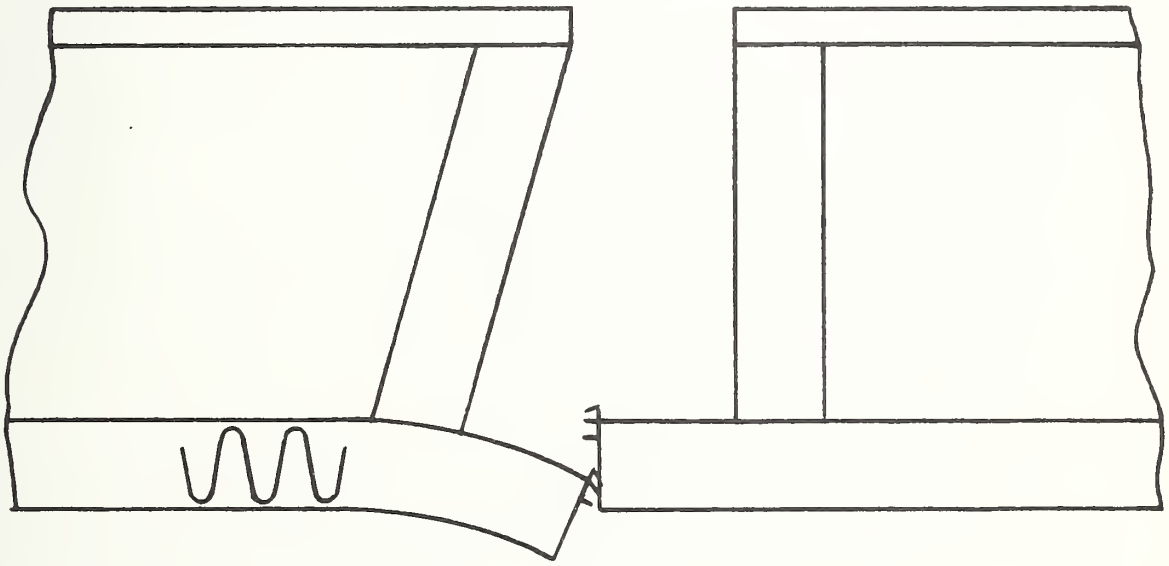

Figure 8-12b. Unsymmetrical Failure Mode due to Plastic Deformations Aft of Collision Post

failure mode would not likely lead to complete override unless the end moment on the collision post was sufficient to cause failure of the joint, and resulting complete beam column failure of the end underframe. However, we have noted that existing specifications and existing construction practice are limited to providing a given level of shear strength between collision post and end underframe; hence large end moments and tensile stresses in the joint caused by large end underframe plastic crush are likely to cause joint failure.

An unsymmetrical failure mode due to plastic deformation in the end underframe aft of the collision post is shown in Figure 8-12(b). Such an unsymmetrical failure can occur on cars of the same design because of small differences in material strength of the two colliding end underframes. Considering again the simplified elastic-plastic stress-strain curve in Figure 8-9, a small difference in crush strength level (say 5 percent or less) between the two structures can lead to significantly more vertical deformation on the weaker structure.

The mechanisms we have discussed deal only with possible means by which cars having the same or similar designs can develop forces and wedge angles during impact which can lead to override. The magnitude of these forces and wedge angles is highly dependent on the non-linear yield and crush characteristics of the material and the very localized distribution of dynamic stresses during impact, as well as the identifiable geometric and material characteristics of the design. It is anticipated that the only way to understand and quantify this is through an empirical approach involving small scale or full-scale tests on representative front end configurations, in parallel with more detailed analysis of the dynamics of the impact.

While quantification and the development of capability to predict the behavior of the immediate front end structure will require development of this empirical capability, it is nonetheless possible to identify design characteristics or design trends which appear to be "bad" or "good" in terms of the development of climbing forces and wedge angles at impact. An example of this is suggested by the discussion of Figures 8-7 through 8-11. When crushing takes

place forward of the collision post, the tendency for the development of significant wedging angles is reduced when the section modulus at the cross section where crushing occurs is increased. In the case of Figures 8-10(a) and 8-10(b), this suggests that the section have the highest practicable dimension, c, and that the section be symmetrical about a horizontal reference line.

Finally, we note that significant climbing between two identical or similar colliding structures requires that two things occur: (1) that wedge angles and resulting vertical forces are produced to initiate climbing (e.g., the examples illustrated by Figures 8-8 through 8-12) and (2), that basic vehicle structural characteristics are such that the climbing process, once initiated, is continued to the extent that climbing significantly reduces the capacity of the structure to resist the collision impact. In the following section, we review means by which climbing can be initiated and/or contained (discontinued after initiation) at successively severe stages in the collision.

8.5 CLIMBING CONDITIONS AT SUCCESSIVELY SEVERE STAGES OF THE COLLISION

It is convenient at this point to describe collision events in terms of three successively severe stages of the collision:

First Stage — Vehicle crush distance δ = 6 inches or less

Second Stage — 6" < δ < 1.5 ft.

Third Stage — δ > 1.5 ft.

The crush distance for the first stage (6 inches or less) corresponds generally to small deformations of the vehicle sill structure which occur during the first instants after the impact. These small deformations would generally occur forward of the collision post as in Figure 8-13(a), but could also occur aft of the collision post, as in Figure 8-13 (b).

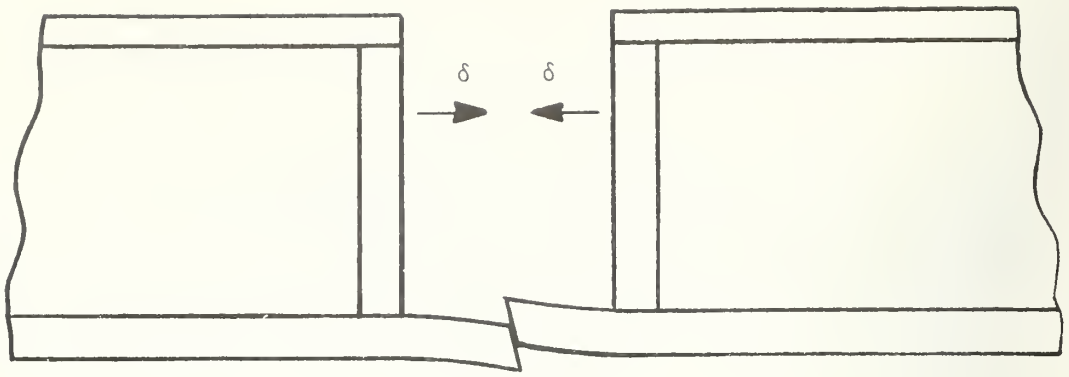

Figure 8-13a. First Collision Stage δ < 6" Climbing Conditions Initiated

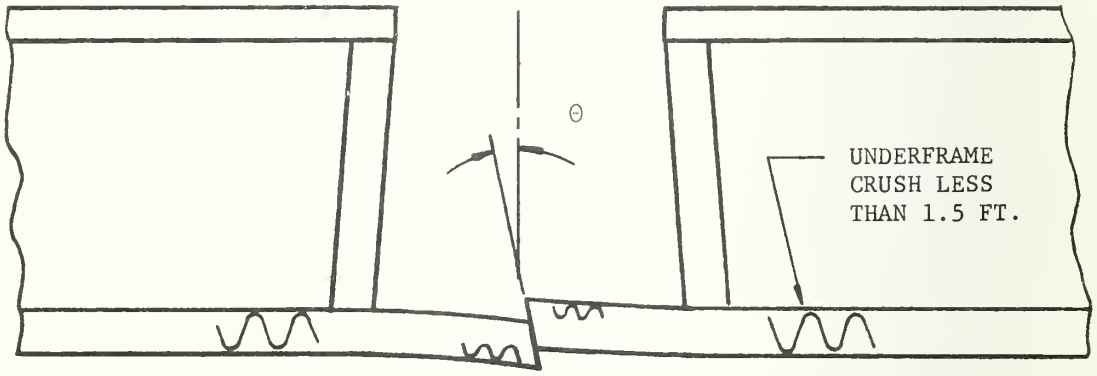

Figure 8-13b. First or Second Collision Stage δ < 1.5 Ft. Climbing Forces Sustained

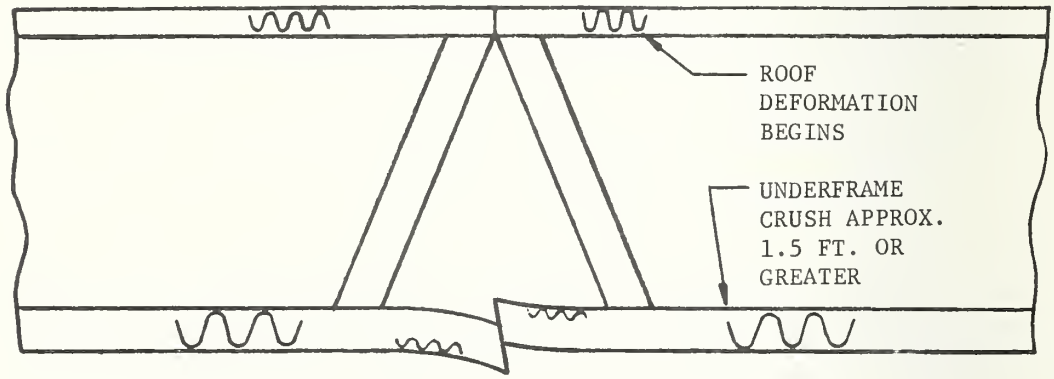

Figure 8-13c. Progression to Third Collision Stage δ > 1.5 Ft. Climbing Forces Sustained

The upper limit of the crush distance for the second stage corresponds to the point at which the sill structure is sufficiently crushed that the roof structures make contact, as in Figure 8-13(c). For most transit cars, this is generally greater than one foot and generally less than three feet. The third stage of the collision applies to any period of time after which sufficient crush has taken place to permit the roof structures to contact.

In the previous section, several means were described by which climbing can be initiated in the first or second stages. Climbing can also be contained (discontinued) in the first or second stage, as indicated by Figure 8-13(b). Containment occurs when the ratio of longitudinal to vertical contact load is sufficiently high in the period after initial impact that gross vehicle longitudinal crush begins before vertical yield of the structure takes place. That severe climbing will tend to stop in this type of sequence can be seen by considering a particular wedge angle θ, and zero friction at the contacting surfaces (for a given wedge angle, zero friction provides the least resistance to climbing). If gross vehicle crush (such as shown aft of the collision post in Figure 8-13(b)) occurs before vertical yield, a "plateau" or levelling off point for longitudinal load has been reached. Since the maximum vertical load is related to the maximum longitudinal load by the wedge angle θ, the vertical load will also reach a plateau at a force level lower than that required to cause vertical deformation. Because of the presence of the vertical load, rigid body climbing will continue. However it was noted in Section 8.3 that this type of climbing proceeds at a relatively low rate, because the mass of the entire car resists pitch rotation. Moreover, retention of vertical structural integrity permits the collision post to stay fixed to the underframe, so that all climbing is ultimately stopped by the shear rigidity of the collision post.

When climbing is contained in the first or second stage of the collision, gross longitudinal crush will continue through the second stage, until the third or flat face stage of the collision is reached, as shown in Figure 8-13(c). If significant climbing has not occurred at this point in a severe

collision, this third stage in the collision is critical, since most of the car penetration is yet to occur. Climbing motion can be initiated during this stage, or it can be renewed if it has been initiated and stopped in the earlier stages. The Darien collision, discussed previously in section 8.2, is an example where the major climbing motions were initiated in the third stage. Gross longitudinal crush can give rise to rotational or vertical motions at the contacting surfaces, particularly when the longitudinal crushing and associated penetration of structural components into one another cause destruction of existing vertical or lateral strength and stability. An example of this sort of behavior would be the destruction of the end bulkhead, either because of deformations normal to its plane of rigidity as shown in Figure 8-13(c) or because of penetration by collision debris. This bulkhead normally provides vertical rigidity to the car structures by transmitting vertical loads from the collision post to the side frame structure, which is several orders of magnitude stiffer than the end underframe in the vertical direction. Failure of the end bulkhead can therefore lead to beam column failure of the entire end underframe forward of the car body bolster, resulting in climbing: (A structural approach to prevent this type of catastrophic failure is discussed in Section 9.2.1).

If climbing forces and motions are not contained in the second stage of the collision, the third stage does not begin with flat face crushing shown by Figure 8-13(c). Partial or full override will occur in the second stage, as depicted in Figures 8-13(d) and 8-13(e). Figure 8-13(d) shows the result of continued climbing motions in the second stage. When climbing has progressed to the point shown in Figure 8-13(d), development of full car longitudinal resistance is dependent on collision post strength; in particular the shear strength between the collision post and the end underframe. Specifications and construction practice are generally such that the shear strength of the joint is less than the strength which can be developed by the end underframe and sill structures in longitudinal crush; hence the collision post is likely to be sheared off with resulting override and deep penetration.

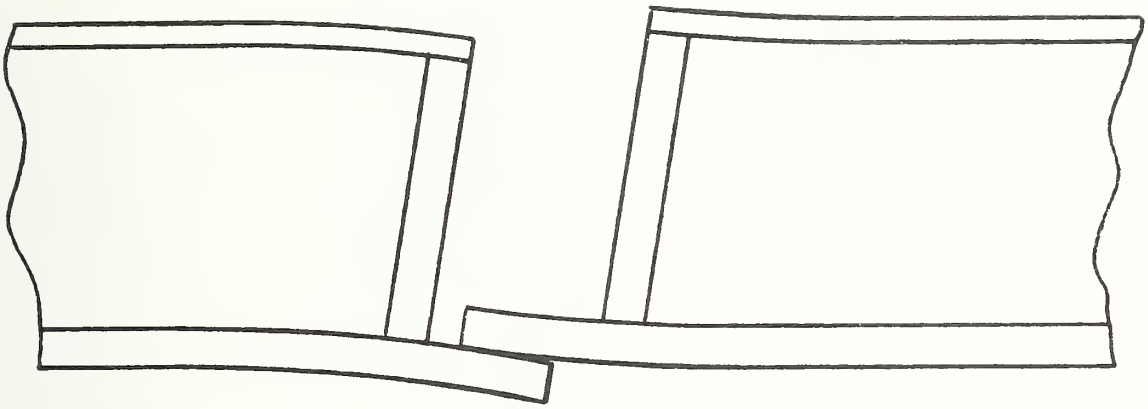

Figure 8-13d. Potential Full Climbing Reached in Second Collision Stage

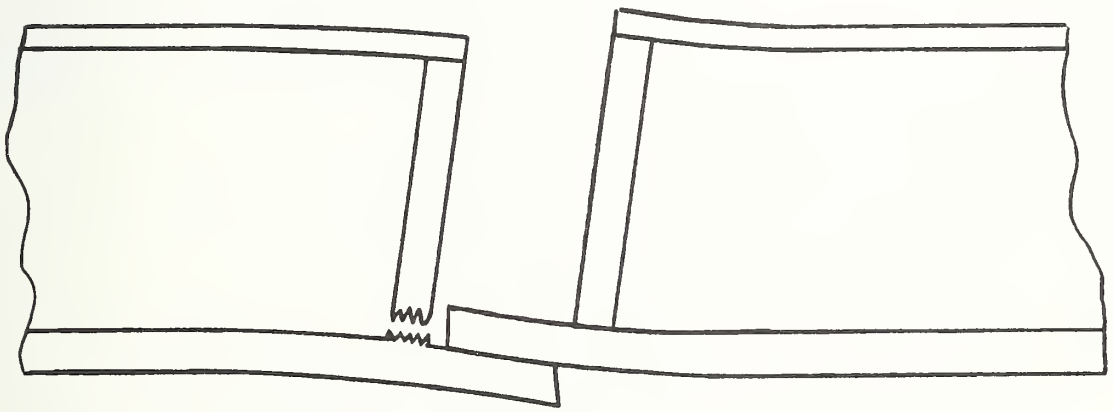

Figure 8-13e. Full Climbing Permitted by Tension and Bending Failure of Collision Post

Figure 8-13(d) shows that the total vertical displacement between the colliding end underframes can be represented as the sum of displacements resulting from two deformations, (1) relatively local deformation of the end underframe forward of the collision post and (2), deformations in the forward end of the car structure aft of the collision post. Vertical loads required for significant vertical deformation of the car structure may be sufficiently high to cause a combined tension and bending failure of the joint connecting the collision post to the end underframe, as shown in Figure 8-13(e). This type of failure may also be induced earlier in the collision before vertical displacements are sufficient to permit overlapping of the end underframes. If this happens, vertical displacements of the underframes will increase rapidly, because of the loss of vertical rigidity which had been provided by the load path from the end underframe through the collision posts and end bulkhead to the side frame structure, which has far greater stiffness in the vertical direction than the end underframe. This can lead to bending or beam column failure of the end underframe, with override likely to result.

It is apparent from the preceding discussions that override can be initiated because of deformations and rotations occurring on the anti-climber and buffing beam structure at the instant of impact, and that progression of the override process is highly dependent on these car structural characteristics:

Stiffness and strength level for vertical loads

Relationship between vertical strength level and longitudinal strength level

Because of the nature of the typical car structure, there is a strong interaction between stiffness levels and strength levels. Vertical loads are initially generated because of structural deformations. If vertical loads exceed vertical strength levels, failures will occur which reduce vertical stiffness levels resulting in larger vertical deformations and further overriding.

Prediction of the events in the override process, and quantitative prediction of the degree of override, will require development of complex collision models and a thorough program of validation tests, because of the different stages in the collision process, and the fact that each collision stage progresses in a highly non-linear manner. Nonetheless, it is believed that an elementary collision model can be useful in showing how gross car geometry, strength and inertia characteristics affect the collision and overriding process. In the following section, an elementary model is formulated. The approach is to start with particular overriding conditions after the first instant of impact (particular wedge angle θ) and to investigate the progression of dynamic forces and motions and how they are affected by car strength, stiffness and inertia characteristics in the longitudinal and vertical directions.

8.6 ELEMENTARY OVERRIDE MODEL

The forward end of a typical transit car is depicted in the upper portion of Figure 8-14. The approach in constructing a very elementary override model is to assume that the structure of the vehicle is weightless,* and the vertical inertia at the forward end of the vehicle is represented by a concentrated mass located midway between the anti-climber and the car body bolster as shown in the figure.

The actual model is shown in the lower portion of Figure 8-14. Key elements in the model are

Striking structure with initial wedge angle θ

Spring k_z, representing the elastic vertical stiffness of the car structure between the anti-climber and a point at distance ℓ aft of the anti-climber.

Mass m_z, representing the vertical inertia of the portion of the car structure forward of the body bolster.

Spring k_z, representing the elastic vertical stiffness of the car structure between the mass k_z, and the body bolster

* Ratio of structural weight to maximum weight of a loaded transit car is typically about 1 to 5.

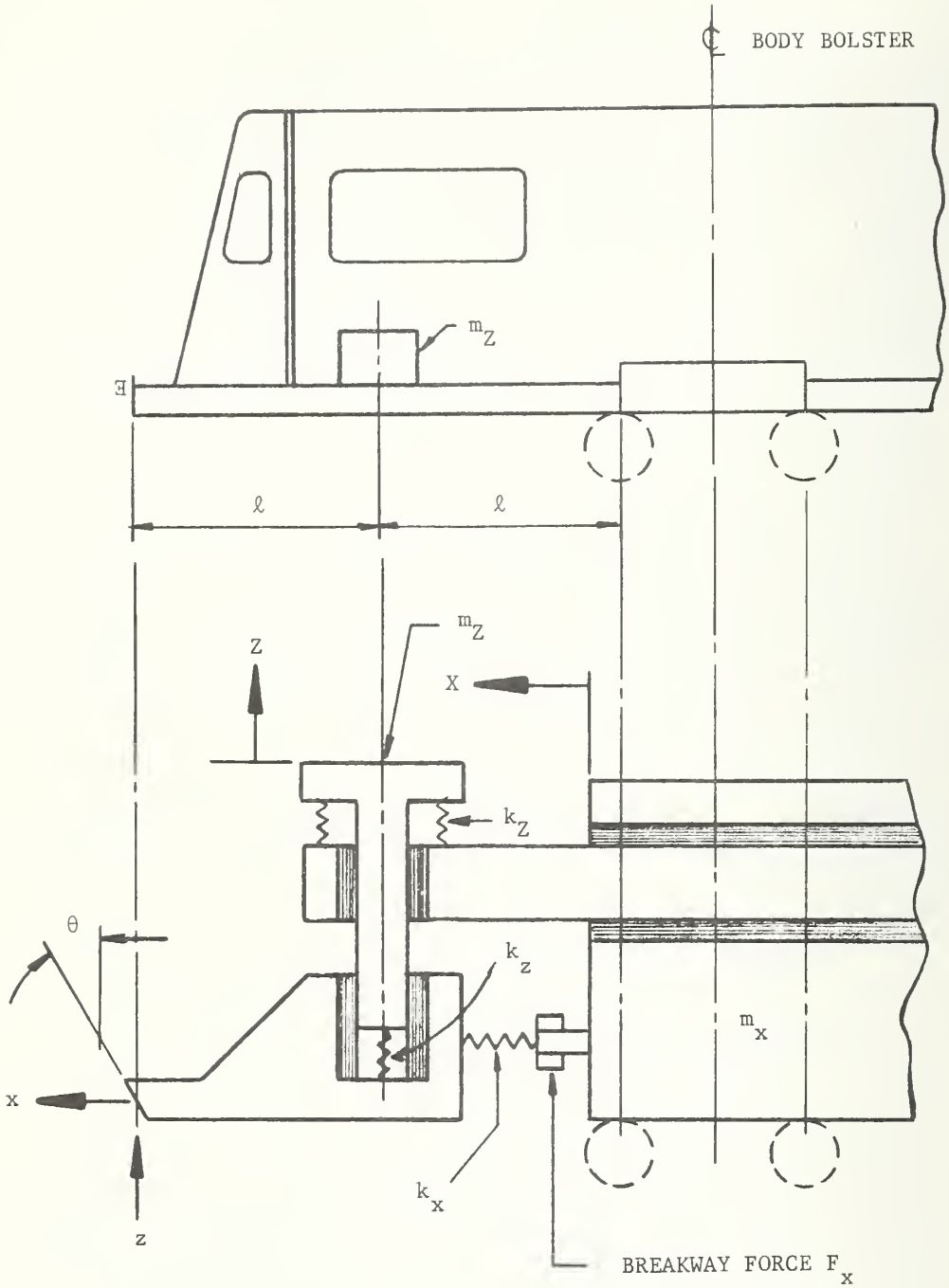

Figure 8-14. Forward End of Transit Car and Simplified Override Model

Spring k_x, representing the longitudinal elastic stiffness of the car body

Force generator F_x, representing the longitudinal crush force level of the car body structure

Mass m_x, representing the effective longitudinal inertia of the train

The idealized striking structure is free to move up and down in coordinate z, opposed by car structural spring stiffness k_z. Mass m_Z is free to move up and down through the coordinate Z, opposed by car structural spring stiffness k_Z. The assembly consisting of the striking surface, effective mass m_Z and flexible structural elements k_z and k_Z, is free to move aft against the longitudinal elastic structural spring k_x and, ultimately, opposed by the fixed crush force level F_x. Longitudinal coordinates consist of the forward motion of the striking surface (depicted by x) and the forward motion of the effective train mass, (depicted by X).

The free body of the striking structure is shown in Figure 8-15. From inspection of Figure 8-15, the longitudinal and vertical components of load at the striking surface can be related to the normal force at the surface as follows:

$$F_z = F\ (\cos\ \theta - \mu \sin\ \theta) = FA_1 \qquad (8\text{-}6)$$

$$F_x = F\ (\sin\ \theta + \mu \cos\ \theta) = FA_2 \qquad (8\text{-}7)$$

where μ is the ratio of shear force acting on the surface to normal force acting on the surface.

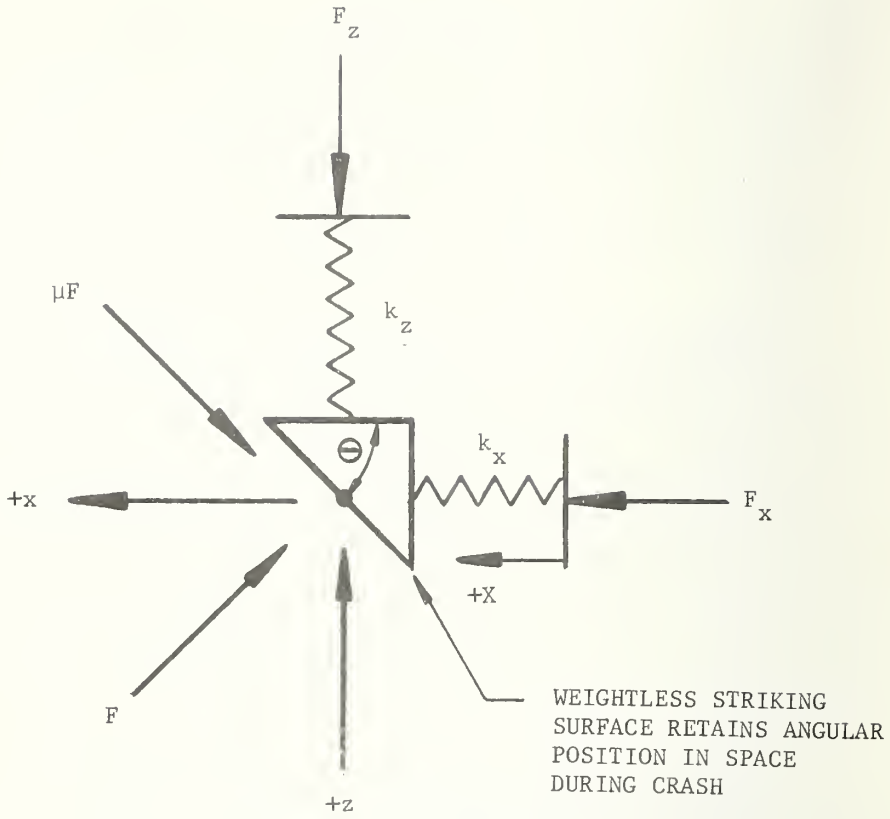

Figure 8-15. Free Body of Striking Surface

The equations of motion and force-geometry relationships for the override model can be written from inspection of Figure 8-14:

$$F_{Zm} = m_Z \ddot{Z} \tag{8-8}$$

$$F_x = - m_x \ddot{X} \tag{8-9}$$

$$F_{Zm} = k_1 z + k_2 Z \tag{8-10}$$

$$F_x = k_x (- x + X) \tag{8-11}$$

$$\frac{x}{z} = \tan \theta \tag{8-12}$$

where $k_1 = k_z$

and $k_2 = - k_z - k_Z$

Note that equation (7) is based on an anti-symmetrical collision. This implies equal and opposite vertical motions of the striking masses, which will initially occur in collisions between identical vehicles, because the equal and opposite forces F_z will produce equal and opposite motions on the identical spring-mass systems.

In equations (3) and (4), m_Z and m_x represent the effective vertical and longitudinal inertias, respectively.

Equations 1 through 7 can be reduced to the following fourth-order differential equation in Z:

$$\ddot{Z} + B_3 Z = 0 \tag{8-13}$$

where B_3 is given by

$$B_3 = \left[\frac{A_2/A_1}{m_x} - \frac{k_2}{k_1} \frac{\tan\theta}{m_Z} \right] \left[\frac{1}{\frac{\tan\theta}{k_1} + \frac{A_2/A_1}{k_x}} \right] \tag{8-14}$$

Longitudinal motion X is related to Z by

$$X = \ddot{Z}B_1 + ZB_2 \tag{8-15}$$

where B_1 and B_2 are given by

$$B_1 = m_Z \left[\frac{A_2/A_1}{k_X} + \frac{\tan\theta}{k_1} \right] \tag{8-16}$$

$$B_2 = -\frac{k_2}{k_1} \tan\theta - \frac{A_2}{A_1} \frac{k_z}{k_x} \tag{8-17}$$

The general solution to Equation 8 is

$$Z = C_1 \frac{1}{B_3} \cos\sqrt{B_3}\, t + C_2 \frac{1}{B3} \sin\sqrt{B_3}\, t + C_3 t + C_4 \tag{8-18}$$

Four initial conditions exist at time, $t = 0$:

$$Z = 0 \qquad \ddot{Z} = 0$$
$$\dot{Z} = 0 \qquad \dot{X} = V_c$$

The constants of integration determined by application of these boundary conditions are

$$C_1 = 0$$
$$C_2 = -V_c \frac{1}{B_1\sqrt{B_3}}$$
$$C_3 = V_c \frac{1}{B_1 B_3}$$
$$C_4 = 0$$

The resulting solutions for motion of the concentrated mass (Z), net vertical force acting on the concentrated mass (F_{Zm}), vertical motion at the striking surface (z) and vertical force at the striking surface (F_z) are given by

$$Z = V_c \frac{1}{B_1 B_3} \left[t - \frac{1}{\sqrt{B_3}} \sin \sqrt{B_3}\, t \right] \tag{8-19}$$

$$F_{Zm} = V_c m_Z \frac{1}{B_1 B_3} \left[\sqrt{B_3} \sin \sqrt{B_3}\, t \right] \tag{8-20}$$

$$z = \frac{F_{Zm}}{k_1} - Z \frac{k_2}{k_1} \tag{8-21}$$

$$F_z = k_1 (z-Z) \tag{8-22}$$

Since the constant B_1, B_2 and B_3 are expressed in terms of the initial climbing conditions (A_1, A_2, θ from equations 1 and 2) it is possible to determine the climbing force at the striking surface (F_z) and the amount of vertical climb at the striking surface (z) as a function of time. From this information, the climbing force can be obtained as a function of climb height.

In the following section, we use equations 14 through 17 to calculate climbing force for a range of initial climbing conditions and car structural characteristics.

8.7 CALCULATION OF OVERRIDE FORCES AND MOTIONS

Typical car geometry is shown by Figures 8-16(a) and 8-16(b). It is desired to establish upper and lower bounds for the effective vertical stiffness and strength of cars with the cross section geometry shown in Figure 8-16(b). In the previous section, the stiffness coefficient k_z is used to represent the vertical stiffness of the car structure between the anti-climber and a point at distance ℓ from the anti-climber, and the spring constant k_Z is used to represent the vertical stiffness of the car between a point at distance ℓ from the anti-climber and a point at distance 2ℓ from the anti-climber. The distance ℓ represents half the distance from the anti-climber to the car body bolster, as shown in Figure 8-16(a).

The upper bound for vertical car stiffness and strength corresponds to the full car cross section, including side sill and roof structure. For this upper bound to exist, it is necessary that all structural elements in the bending load path are sufficiently strong to deliver to the roof structure the axial stresses due to vertical bending. Key elements in this load path include:

End underframe

Collision post and its attachments to the end underframe and the end bulkhead

End bulkhead and its attachments to side frames

Side frame shear material, reinforcements for window and door cutouts, connection of side frame shear material to roof structure

Any additional transverse members which serve to deliver vertical loads from the end underframe to the side frame.

For typical transit car construction, the amount of bending material in the roof and corner purlins is less than the amount of bending material below the floor (center sill and/or side sill, and sub floor members). Therefore, the

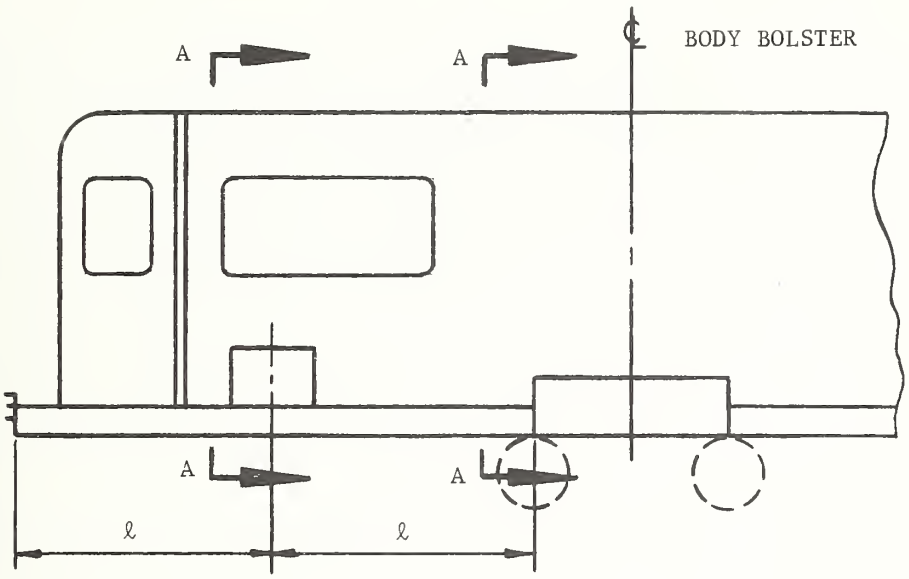

8-16a

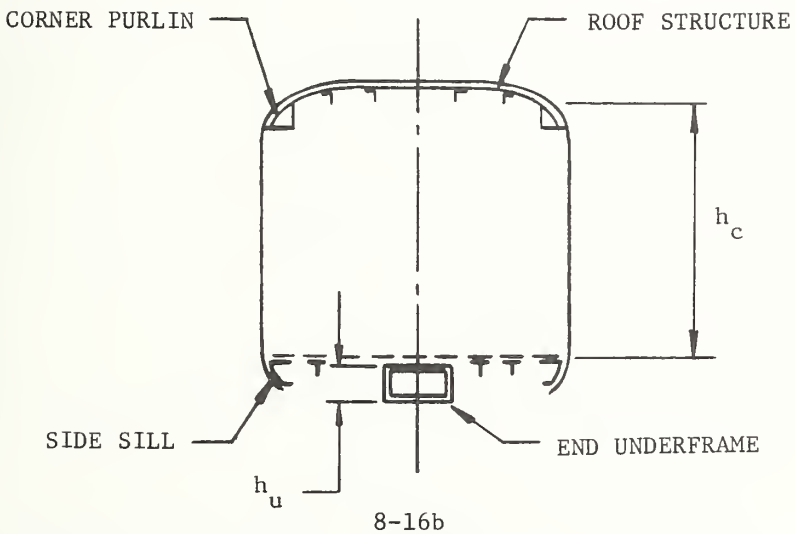

8-16b

SECTION A-A

Figure 8-16. Typical Car Geometry

effective section inertia existing in a bending failure due to vertical loads is controlled by roof longitudinal strength. For the cross section shown in Figure 8-16(b), typical effective roof area, including corner purlins, is taken as seven square inches (this corresponds to a roof longitudinal strength of 210,000 pounds, at a material strength of 30,000 psi). The effective section inertia of the car body at failure is given by

$$I \approx A_R \frac{h_c^2}{2} \tag{8-23}$$

where

A_R = effective roof area

h_c = distance from centroid of roof area to centroid of sill structure area, shown in Figure 8-16(b).

A typical value for h_c is about 90 inches. From equation 18, the car body section inertia is given by

$$I = 7 \frac{(90)^2}{2} = 28,350 \text{ in}^4$$

The stiffness coefficients k_z and k_Z are determined by considering the car body acting as a cantilever beam over distance ℓ. For a cantilever beam,

$$k_z = k_Z = \frac{3EI}{\ell^3} \tag{8-24}$$

Using steel having a modulus of elasticity (E) of 30×10^6 psi and using 60 inches for ℓ,

$$k_z = k_Z = \frac{3(30)(10)^6(28350)}{(60)^3} = 11.8\ 10^6 \text{ pounds per inch}$$

The effective section modulus for calculation of bending strength is

$$\frac{2I}{h_c} = \frac{2(28350)}{90} = 630 \text{ in}^3$$

The lower bound for vertical car stiffness and strength corresponds to a situation in which no effective load path exists between the end underframe, where the collision loads are initially applied, and the side frame. The situation may exist at the instant of impact in designs where no effective load path exists, or it may occur shortly after impact due to failure of an element in the vertical load path to the side frame caused by relatively high vertical loads at impact associated with significant wedge angle at the striking surface. For these situations, the available vertical stiffness and vertical strength is limited to the end underframe structure. For the lower bound for stiffness and strength, the end underframe structure is assumed cantilevered from a rigid car body bolster, with no additional vertical support provided. For an end underframe structure having approximately 12 inches of height and ten square inches of bending material on the compression and tension surfaces of the beam, the effective section inertia is given by equation 18.

$$I = 10\,\frac{(12)^2}{2} = 720 \text{ in}^4$$

The stiffness coefficients are determined from equation 19 in the same manner as for the full car body section:

$$k_z = k_Z = \frac{3(30)(10)^6(720)}{(60)^3} = 300{,}000 \text{ pounds per inch}$$

The effective section modulus for calculation of bending strength is

$$\frac{2I}{h_u} = \frac{2(720)}{(12)} = 120 \text{ in}^3$$

The longitudinal stiffness coefficient (k_x) for both upper and lower vertical strength levels is taken as the longitudinal stiffness of one full car body:

$$k_x = \frac{A_b E}{\ell_B} \qquad (8\text{-}25)$$

The effective cross sectional area of the car body (A_B) is taken as 14 square inches, and the effective length (ℓ_B) is taken as one car body length (900 inches). From equation 20

$$k_x = \frac{14(30)(10)^6}{900} = 466{,}000 \text{ pounds per inch}$$

The mass for simulating vertical inertia effects (m_Z) is based on a total weight of 10,000 pounds forward of the car body bolster, and the mass for simulating longitudinal inertia effects (m_x) is based on a total car body weight of 70,000 pounds:

$$m_Z = \frac{10{,}000}{386} = 25.9 \ \frac{\text{pound sec}^2}{\text{inch}}$$

$$m_x = \frac{70{,}000}{386} = 181 \ \frac{\text{pound sec}^2}{\text{inch}}$$

Summarizing, the car body structural characteristics taken for the upper and lower vertical strength bounds are:

	Upper Bound	Lower Bound
Inertia of Bending Section	28,350 in^4	720 in^4
k_z	11.8 million pounds per inch	300,000 pounds per inch
k_Z	11.8 million pounds per inch	300,000 pounds per inch
Section Modulus for Bending Section	630 in^3	120 in^3
k_x	466,000 pounds per inch	466,000 pounds per inch
m_Z	25.9 $\frac{\text{pound sec}^2}{\text{inch}}$	25.9 $\frac{\text{pound sec}^2}{\text{inch}}$
m_x	181 $\frac{\text{pound sec}^2}{\text{inch}}$	181 $\frac{\text{pound sec}^2}{\text{inch}}$

Values of the vertical force and deflection (F_z and z) at the striking surface are obtained from equations 14 through 17. The necessary constants B_1 and B_3 in equations 14 and 15 are calculated by inserting the spring and mass properties shown above into equations 9 and 11. Assuming a 45° wedge angle and zero friction ($A_2/A_1 = 0$ and $\tan \theta = 1$), the calculated maximum values of F_z and z are

	Maximum Values of:	
	z (inches)	F_z (pounds)
Upper Bound	.086	539,000
Lower Bound	18.4	2,840,000

Referring to Figures 8-16a and 8-16b, the maximum bending moment in the car structure is given by

$$M_{max.} = F_z \ell + F_{Zm} \ell \qquad (8\text{-}26)$$

The maximum bending stress is given by

$$f_b = \frac{M_{max}}{I/C} \qquad (8\text{-}27)$$

From Equations 21 and 22, the maximum moment and the maximum bending stress in the upper bound (full monocoque) structure and the lower bound (end underframe) structure can be calculated, provided that the length ℓ and the section modulus I/C are known. In this example, these values are

	ℓ	I/C
Upper Bound	60 in.	630 in^3
Lower Bound	60 in.	120 in^3

Inserting these values into Equations 21 and 22, the maximum vertical moment and maximum bending stresses are

	Maximum Values of	
	M (in.lb.)	f_b (psi)
Upper Bound	36.5 million	60,800
Lower Bound	180 million	1,500,000

The condition taken (θ = 45° and zero friction) is extremely severe. However it is significant that the calculated stress in the lower bound structure (end underframe acting alone) is approximately 25 times as large as that for the upper bound structure (full monocoque car section acting). This large difference is primarily due to the fact that the relatively flexible end underframe structure when acting alone, deflects far more than the full monocoque structure. (A maximum theoretical vertical deflection* of 18.4 inches for the former, versus only .086 inches for the latter). In this simplified example, it is evident that the end underframe structure would fail long before the maximum vertical deflection of 18.4 inches is reached. (For a failure stress of 60,000 psi, the end underframe structure would fail at a vertical deflection of approximately 0.73 inches.)

The extreme simplicity of the model should be emphasized. Accurate prediction of vertical forces and deflections in a collision will require a much more complex multi-degree of freedom model. Nonetheless, the extremely large vertical force and deflection in the end underframe when it is not

* In this case, this is the maximum elastic deflection, provided that material failure does not occur before this deflection is reached.

effectively attached to the full monocoque structure is significant. End underframe failure and subsequent climbing are likely to occur if an adequate vertical load path from the end underframe to the full monocoque structure is not provided. In addition, the monocoque structure itself must also have adequate vertical strength.

In regard to the available longitudinal and vertical strengths which are actually specified for existing urban rail cars, it is of interest to review Table 8-1. This table shows an overview of structural specifications and other structural characteristics of the five cars studied in this program plus two additional cars: the R-46, being built by Pullman-Standard for the New York City Transit Authority (NYCTA); and the RTC-1, built by The Budd Company for the Chicago Transit Authority (CTA). In regard to car structural specifications, the following points are noted:

(1) The transit cars all have significantly lower buff-load requirements than the Silverliner commuter car, which is specified per AAR requirements for main-line (commuter or intercity) cars.

(2) Half of the urban rail cars have no collision-post shear requirements. The maximum collision-post shear requirement is, again, the AAR requirement for the Silverliner; among urban rail cars, this requirement is met only by the latest NYCTA car, the R-46. (Collision-post shear refers to the longitudinal strength of the attachment of the collision post to the underframe.)

(3) Half of the urban rail cars have no requirement for anti-climbing or any vertical load. Again, the R-46 car is the only car whose specifications meet the AAR anticlimbing load requirement. This requirement is for 100,000 lb of

TABLE 8-1. RAIL-CAR SPECIFICATIONS AND STRUCTURAL CHARACTERISTICS

RAIL CAR	USER	MANUFACTURER	CONSTRUCTION		BUFF LOAD (lb)	ALLOWABLE STRESS AT BUFF LOAD*	TEST REQUIRED ?	COLLISION-POST SHEAR (lb)	ANTI-CLIMB VERTICAL LOAD (lb)	REMARKS
			SIDE SILL ?	CENTER SILL ?						
SILVERLINER	PENN CENTRAL RR, READING CO.	THE BUDD COMPANY	YES	YES	800,000	F_y	YES	300,000 EA	100,000	PER AAR, LOAD APPLIED TO DRAFT GEAR CENTERLINE
R-33	NYC TRANSIT AUTHORITY	ST. LOUIS CAR DIV.	YES	YES	200,000	$0.5\ F_y$	NO	NO REQUIREMENT	NO REQUIREMENT	
R-44	NYC TRANSIT AUTHORITY	ST. LOUIS CAR DIV.	YES	NO	250,000	$0.5\ F_y$	YES	NO REQUIREMENT	NO REQUIREMENT	
BART	SAN FRANCISCO BART	ROHR INDUSTRIES	YES	NO	180,000	$0.9\ F_y$	YES	NO REQUIREMENT	NO REQUIREMENT	
SILVERBIRD	MASS. BAY TRANSP. AUTH.	PULLMAN-STD DIV.	YES	NO	200,000	$0.9\ F_y$	YES	200,000 EA	75,000	35,000-lb LOAD TO EACH COLLISION POST 18 IN. ABOVE FLOOR
R-46	NYC TRANSIT AUTHORITY	PULLMAN-STD DIV.	?	?	400,000	$0.8\ F_y$	YES	300,000 EA	100,000	300,000 lb TO EACH CORNER POST ALSO
RTC-1	CHICAGO TRANSIT AUTH.	THE BUDD COMPANY	YES	YES	200,000	$0.9\ F_y$	YES	SEE REMARKS	NO REQUIREMENT	Z_{TOTAL} OF COLLISION POSTS $\geq$ 22.5 CUBIC INCHES

*WHERE F_y IS THE YIELD STRENGTH

vertical strength "assigned to the buffer beam construction, the anticlimbing arrangement, and the coupler carrier arrangement."

It is significant that only three of the cars shown in Table 8-1 have vertical-load requirements. The maximum requirement is 100,000 lb (for the Silverliner and R-46) and represents a small percentage of the longitudinal (buff) load requirement. Further, no test is required to demonstrate compliance to this requirement.

Summarizing, the vertical strength at the ends of the urban rail cars studied is generally in accord with specification requirements for the individual cars. However, these requirements appear to be very lenient, or nonexistent. For such constructions, climbing is likely to occur under adverse conditions of initial misalignment. Further study and tests are required to establish adequate vertical strength requirements.

9. PRIORITY AREAS FOR THE DEVELOPMENT OF COST EFFECTIVE IMPROVED CAR STRUCTURES

9.1 INTRODUCTION

At this point in the study, specific areas for the development of cost effective improved car structures are selected and investigated.

In Section 9.2, three priority areas are selected, primarily on the basis of a subjective review of the collision simulation results shown in Chapter 7. Parameters associated with these priority areas (e.g., S/W is associated with strengthening of car) are identified, and the relationship between these parameters and crashworthiness benefits are studied. These benefits are measured in terms of numbers of lives saved and reductions in severe injuries for specified collisions.

In Section 9.3, specific design concepts which apply to the priority areas are described. Car body structure concepts are based on structural principles discussed in Section 8. Emphasis is placed on achieving a controlled and predictable force-deflection curve, and minimizing the likelihood of climbing. Design features in the end underframe and in the superstructure for achieving these goals are discussed. Energy absorber concepts are based on first order relationships between car strength to weight ratio and length of crush.

In Section 9.4, approximate weight and cost estimates for the design concepts are made. The estimates include initial and recurring costs. Initial costs are associated with particular unit construction costs (e.g. 1, 2, 3 dollars per pound, etc.). Recurring costs include power system costs and other costs associated with added weight. The annual costs of providing end-free space and providing several types of energy absorbers are compared. On the basis of this comparison, a specific energy absorber concept is selected. In Section 10, specific design applications of the selected energy absorber concept are investigated.

9.2 RELATIONSHIP OF DESIGN CHARACTERISTICS OF TRAIN CRASHWORTHINESS

In Chapter 7, car crashworthiness was assessed in terms of four design parameters: strength to weight ratio of car (S/W), amount of passenger unoccupied space at car ends, distance between passenger and impacted object (s) and the effective crush distance occurring on the impacted object upon passenger impact (d). These parameters were varied independently to determine their separate effects on injuries and fatalities occurring under specified collision conditions. The results are shown in Figures 7-1 through 7-28 and are discussed in the accompanying text in Chapter 7.

It was observed in Chapter 7 that the car force-deflection curves used in the collision model resulted in considerably more sharing of crush (between cars in the train) than has generally been observed in accidents, where all or almost all of train crush has occurred in the lead car. A strong factor leading to the type of crush behavior which has been observed is believed to be the tendency of the lead car to fail at force levels less than would be predicted, because of transverse (vertical and lateral) failures induced by initial crash deformations. Even if the crush force level of the lead car is not significantly reduced from that which would occur in a well controlled longitudinal failure (and frequently it is significantly reduced) this sort of crush behavior causes increased fatalities because crush is not distributed to a number of car ends, where several feet of space is frequently either unoccupied or sparsely occupied by passengers, because of the interior layout. It is concluded that an extremely important structural design characteristic to achieve is a well controlled and predictable force - deflection characteristic. Accordingly this is identified as a priority area for the development of improved car structures.

Another significant result shown in Chapter 7 was that the number of first collision fatalities was very significantly reduced by the provision of passenger-free space at the car ends, particularly at collision speeds of 40 mph and less, where a relatively small amount of unoccupied space at the end of the lead car (from 2 feet to 10 feet) provides large percentage reductions in first collision fatalities. It is evident that the provision of an energy absorber on the lead car would have a similar effect. Therefore the energy absorber is a potential priority area for the development of more crashworthy cars. We note, however, that the feasibility of the energy absorber depends on its cost. To be feasible it must, for example, be less costly than merely providing unoccupied passenger space at the end of the normal car outline. Later in this section we deal with this subject in more detail.

On the basis of the results in Chapter 7 a third priority area for achieving more crashworthy cars (not any less important than the other two priority areas which have been identified) is the development of safer car interiors. Interior safety is dependent on passenger travel (s) to the impacted object, and object crush distance (d). Results in Chapter 7 show that both of these parameters have extremely strong effect on car crashworthiness. An increase of d from 1 inch to 2 inches, for example, is sufficient to eliminate all severe injuries as well as all fatalities for all standing passengers in the second collision, at all closure speeds up to 40 mph for accidents between similar trains having cars with strength to weight ratio as high as 12. The significance of improved interior safety is that it permits the use of stronger car structures, thus reducing first collision fatalities, while avoiding an increase in second collision severity associated with the increased car decelerations caused by the stronger structures.

To provide a basis for evaluating the effect of design improvements in these three areas (improved car structures, energy absorbers, improved interiors) the performance of four baseline designs, without improvements, is shown in Figure 9-1 for collisions of identical eight car trains at 40 mph closure speed. In the figure, first collision fatalities, second collision fatalities

Baseline Design	S/W (Note 1)	d (Inches) (Note 2)	S Feet (Note 3)	Free Space (Feet) (Note 4)	Fatalities and Injuries (Note 5)		
					First Collision Fatalities	Second Collision Fatalities	Second Collision Injuries
1	4	1	2	2	4.3	0	0
2	4	1	12	2	4.3	0	25
2	8	1	2	2	2.1	0	0
4	8	1	12	2	2.1	37.5	87.5

NOTES:

(1) S/W is strength to weight ratio of car

(2) d is effective crush distance of impacted object (inches)

(3) S is distance between passenger and impacted object (feet)

(4) Free space is unoccupied space at car ends (feet)

(5) Fatalities and injuries are given in percentage of train occupants Percentages for second collision are based on assumption that passenger travels distance S unimpeded.

Figure 9-1. Incidence of Fatalaties and Severe Injuries for Baseline Designs in 40 MPH Collision of 8 Car Trains

and second collision injuries are summarized for the baseline designs. The baseline designs consist of cars with strength to weight ratios of 4 and 8, each with passenger spacing of 2 feet (generally representative of seated passengers) and 12 feet (taken here as representative of standing passengers).

In Figures 9-2 through 9-5 predicted improvements (in terms of reduced fatalities and injuries) for each of the baseline designs are listed, for the following specific improvements in the three priority areas.

Improved Structures - The improvement consists of controlled car crush such that total crush is distributed between cars as shown by the computer models, as opposed to all of the crush in the lead car.

Energy Absorber - The improvement consists of the addition at the front end of the lead car of an energy absorber having 7 feet of effective stroke, and force level approximately three quarters of car strength.

Improved Interiors - The improvement consists of an increase of interior object crush distance from 1 inch, which is used in the baseline designs, to 2 inches.

Fatalities and injuries in Figures 9-2 through 9-5 are given in percentage of total train occupants. It is noted that a relatively small percentage for an eight car train with 200 passengers per car results in a relatively high number of fatalities or injuries (in this case, 2.5% of 1600 passengers is equal to 40 passengers).

Oesign Oescription	PREOICTIONS First Collision Fatalities	Second Collision Fatalities	Second Collison Injuries	PREOICTEO IMPROVEMENT First Collison Fatalities	Second Collision Fatalities	Second Collison Injuries
Baseline 1	4.3	0	0	---	---	---
Structural Improvement[2]	2.5	0	0	1.B	0	0
Energy Absorber[3]	0	0	0	4.3	0	0
Interior Improvement[4]	4.3	0	0	0	0	0

Figure 9.2

(Baseline Design 1 Used as Reference)

Oesign Oescription	PREOICTIONS First Collision Fatalities	Second Collision Fatalities	Second Collison Injuries	PREOICTED IMPROVEMENT First Collision Fatalities	Second Collision Fatalities	Second Collision Injuries
Baseline 2	4.3	0	0	---	---	---
Structural Improvement	2.5	0	2S	I.B	0	-25
Energy Absorber	0	0	0	4.3	0	0
Interior Improvement	4.3	0	0	0	0	0

Figure 9.3

(Baseline Design 2 Used as Reference)

Oesign Description	PREOICTIONS First Collision Fatalities	Second Collision Fatalities	Second Collision Injuries	PREOICTED IMPROVEMENT First Collision Fatalities	Second Collision Fatalities	Second Collision Injuries
Baseline 3	2.1	0	0	---	---	---
Structural Improvement	0.6	0	0	1.5	0	0
Energy Absorber	0	0	0	2.1	0	0
Interior Improvement	2.1	0	0	0	0	0

Figure 9.4

(Baseline Design 3 Used as Reference)

Oesign Description	PREOICTIONS First Collision Fatalities	Second Collision Fatalities	Second Collision Injuries	PREDICTEO IMPROVEMENT First Collision Fatalities	Second Collision Fatalities	Second Collision Injuries
Baseline 4	2.1	37.5	B7.5	---	---	---
Structural Improvement	0.6	37.5	B7.S	1.5	0	0
Energy Absorber	0	20	50	2.1	17.S	37.5
Interior Improvement	2.1	0	0	0	37.S	B7.5

Figure 9.5

(Baseline Design 4 Used as Reference)

NOTES

(1) Fatalities and injuries are in percentage of train occupants.

(2) Improved Structures - The improvement consists of controlled car crush such that total crush is distributed between cars as shown by the computer models, as opposed to all of the crush in the lead car.

(3) Energy Absorber - The improvement consists of the addition at the front end of the lead car of an energy absorber having 7 feet of effective stroke, and force level approximately three quarters of car strength.

(4) Improved Interiors - The improvement consists of an increase of interior object crush distance from 1 inch, which is used in the baseline designs, to 2 inches.

Figures 9-2 through 9-5. Effect of Design Improvements on Fatalities and Severe Injuries in 40 MPH Collision of 8 Car Trains

9.3 DESIGN CONCEPTS

In Chapters 5, 6 and 7, design parameters (e.g.; S/W, s, d, force deflection curve shape, provision of crush space and energy absorbing characteristics) which affect predicted fatalities and injuries in specified collisions were identified and investigated. As a result of these studies, three design-related areas (development of controlled and predictable force-deflection characteristics, energy absorbing, and interior safety) have been identified as priority areas to be investigated further. At this point, specific physical design concepts which apply to these areas are studied. Design concepts relating to controlled force deflection characteristics within the structure of the car body are discussed in Section 9.3.1. Design concepts for energy absorbing are discussed in Section 9.3.2.

9.3.1 Body Construction

Design parameters which are influenced by body construction are strength to weight ratio, and the shape of the force-deflection curve. It is evident (see Chapter 5) that the potential for extremely large variations in these parameters exists in all of the generic construction types represented by the five study cars. In practice, collision experience has indicated that car structures fail to behave in a predictable or repeatable manner. This lack of predictability relates to the longitudinal force developed during the collision. It appears to be due to override, or the general tendency of car structures to become unstable (i.e., to fail in directions other than the direction of collision impact) as a result of local structural failures associated with large longitudinal deformations. These effects were discussed in Chapter 8.

It is evident that improvements in car construction should be directed at achieving a predictable resistance force level during collisions. This requires that the construction be such that the liklihood of override and transverse deformation is minimized. This in turn requires that major longitudinal elements in the structure fail in a controlled and predictable manner,

and that key transverse elements in the structure retain their stabilizing function as the large longitudinal deformations progress.

Structural principles which might be employed to achieve predictable and repeatable force-deflection characteristics in a collision are illustrated by figures 9-6 through 9-13.

Figure 9-6 shows a design concept in which the buffing beam or anti climber structure (1) is backed up by crushable material (2). The design intent is for element (2) to crush first, and by yielding in a controlled manner to prevent excessive deformations in (1) at the instant of impact which would lead to wedge angles and development of climbing forces. Determination of the required strength levels of (1) and (2), and weight of (1), to insure this kind of failure mode would have to be made by employing a relatively fine grid dynamic analysis, as described in Section 5.3. Full crushing of element (2) is designed to occur with no significant deformation or failure in collision posts (4) and end bulkhead(5). Immediately following full crushing of element (2), side sill structure (6) and draft sill structure (7) are designed to crush simultaneously. The side sill crush strength and the bending strength of the transverse structural member (3) must be such that (3) does not yield during the crushing process. This member, together with the attached collision post (4) and end bulkhead structure (5) are intended to translate aft as an undeformed integral structure during crushing of the side sill and center sill structures and the roof structure. To permit this to happen, the collision post is designed to engage the collision post of the opposite striking car simultaneously with engagement of buffing beams, as indicated by Figure 9-7*.

* This ideal situation applies only when both striking cars are designed to the same specifications. However, collision posts of existing cars could be retrofitted with bearing elements as shown at the top of the collision post in Figure 9-7.

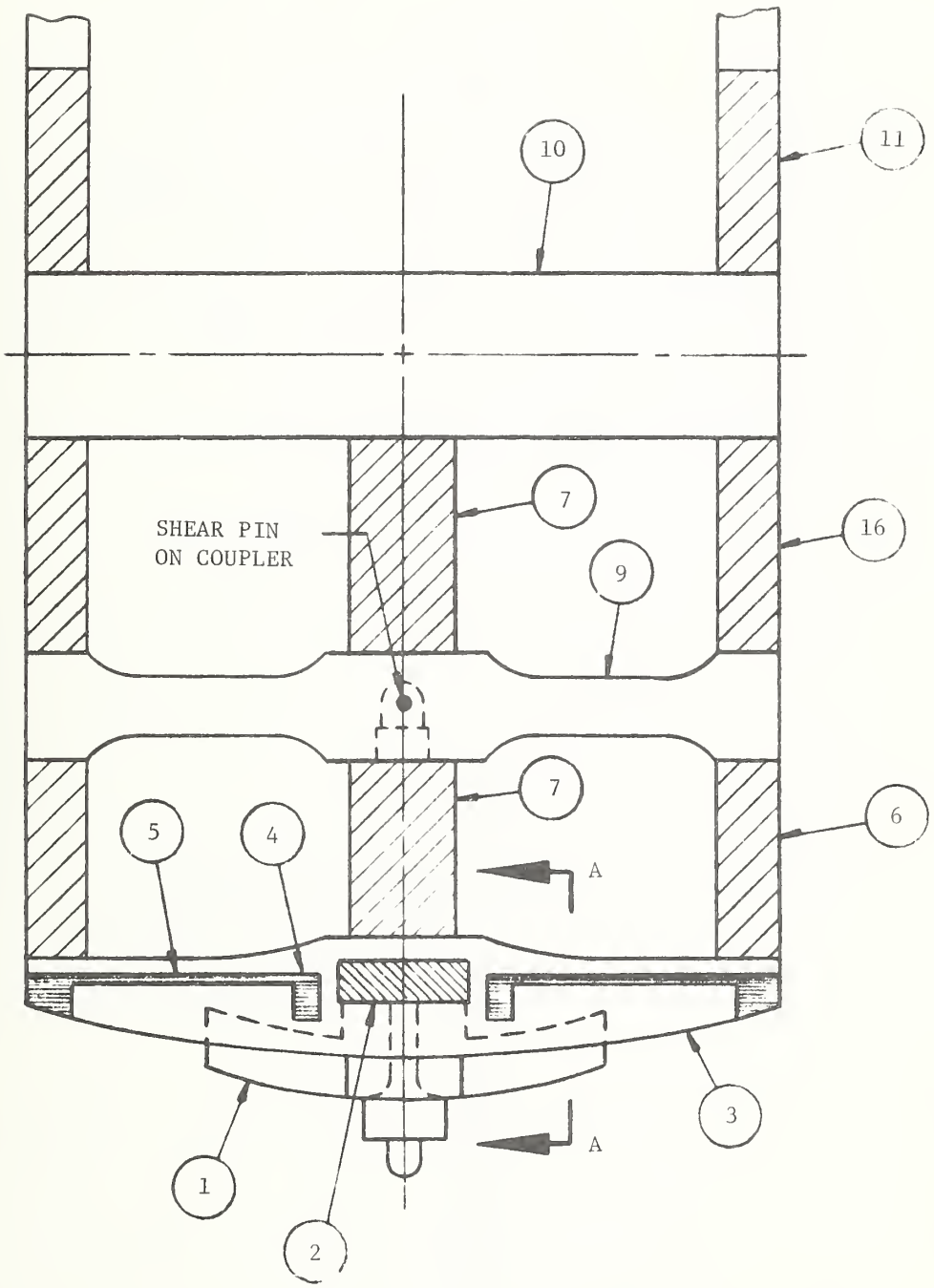

Figure 9-6. Design Concept 1

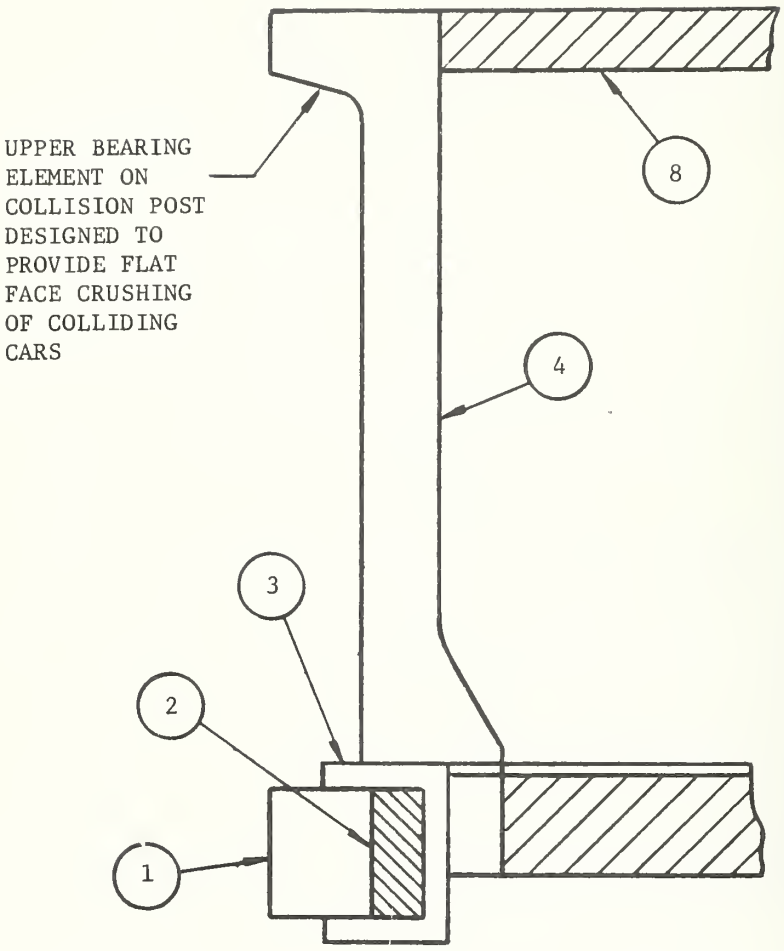

SECTION A-A FROM FIGURE 9-6

Figure 9-7. Collision Post Concept

In order for the integral structure consisting of the collision post, the transverse element (3) and the end bulkhead to retain its integrity during the collision it must have sufficient strength to withstand the forces exerted by the crushing longitudinal members. Assume for example that a relatively high strength to weight ratio of 12 is to be realized during simultaneous crushing of (6), (7) and (8).* For a car weighing 70,000 pounds, the sum of the longitudinal forces in these members is given by:

$$F_6 + F_7 + F_8 = 12\ (70{,}000) = 840{,}000 \text{ pounds}$$

A reasonable distribution of forces would be as follows:

Side Sill (6)	(160,000 lb per side)	320,000 lb
Draft Sill (7)		320,000 lb
Roof (8)		200,000 lb
Total		840,000 lb

For this force distribution, element (3) must have sufficient bending strength at Section A-A to resist the moment exerted by the 160,000 pound crush force of the side sill. For typical cars, the effective moment arm is about 50 inches. The moment at Section A-A is approximately:

$$M_{AA} = 160{,}000\ (50) = 8 \text{ million in. lb.}$$

Based on a safe elastic stress level of 20,000 psi in element (3), the required section modulus at Section A-A is

$$\frac{I}{C} = \frac{M}{f} = \frac{8 \times 10^6}{2 \times 10^4} = 400 \text{ in}^3$$

* During simultaneous crushing of these sub-floor and roof elements, the effective neutral axis is at the center of area of elements 6, 7 and 8.

This section modulus can be provided by the section geometry shown below

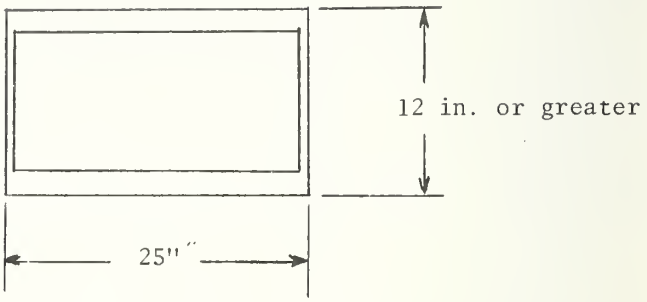

The section modulus is provided primarily by the lateral flanges. Considering only the lateral flanges

$$\frac{I}{C} = 2\,\frac{b\,t^2}{6} = \frac{2\,(2)\,(25)^2}{6} = 417\ in^3$$

An additional feature in the design concept shown in Figure 9-6 is the transverse stabilizing member (9). This member provides lateral stability for members (6) and (7). On most existing designs, members (6) and (7) are connected by a relatively thin shear web. Such a shear web has significant shear capacity in its undeformed state, and serves to transfer buff loads from the draft sill to the continuous side sill members. However, when significant crush occurs, the shear web will be extensively deformed, and will not provide stability to the side sills. This can lead to instability failure of the side sill, which is frequently designed as an "open" section (channel type section as opposed to a closed box).

Figure 9-8 shows a variation of the design shown in Figure 9-6. In this design a center sill structure does not exist, and the side sill must carry the entire portion of the crush load taken by longitudinal members below floor level. To achieve the strength-to-weight ratio of 12, the side sill crush load is increased to 320,000 pounds, requiring that the section inertia of element (3) be doubled.

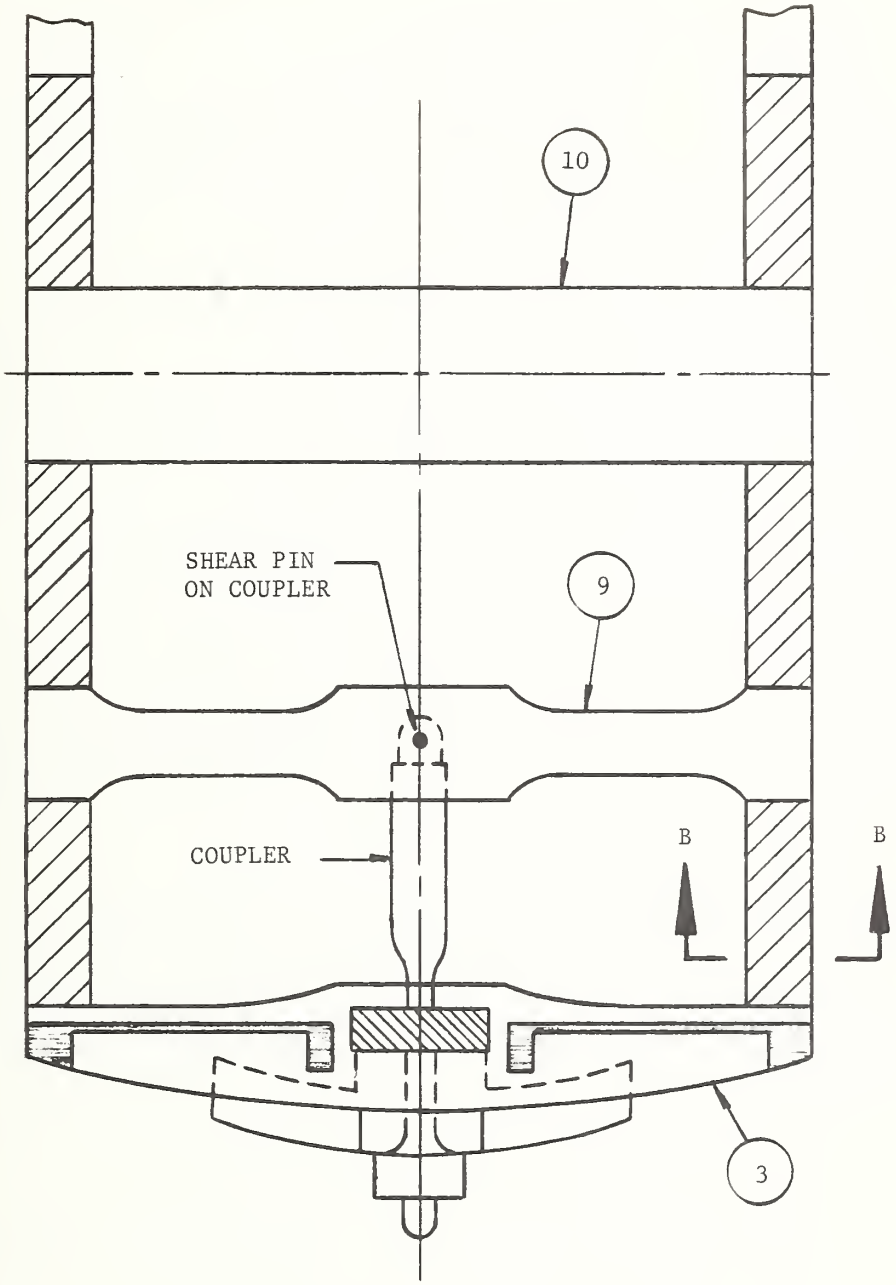

Figure 9-8. Design Concept 2

It is instructive to check the column stability requirements for the side sill, shown in cross section in Figure 9-9. The closed box section with dimensions shown has an area given by

$$A \approx 4\ (8)\ (.16) \approx 5.4\ \text{in}^2$$

and the stress at crush load is

$$f_C = \frac{160{,}000}{5.4} \approx 30{,}000 \text{ psi}$$

The moment of inertia I of the section is approximately equal to

$$I_{XX} = I_{YY} \approx \frac{(8)^4}{12} - \frac{(7.68)^4}{12} \approx 50\ \text{in}^4$$

The Euler column stability load, for a long pin ended column, is given by

$$P_{CR} = \frac{\pi^2 EI}{\ell^2}$$

Assuming that a transverse stabilizing member does not exist (i.e., transverse beam (9) does not exist), the effective column length (ℓ) extends from transverse frontal member (3) to the transverse bolster structure (10). For most transit cars, this distance is approximately 100 inches. For aluminum ($E = 1 \times 10^7$ psi) the Euler column load is given by

$$P_{CR} = \frac{(3.14)^2\ (10)^7\ (10)^2\ (0.5)}{10^4} = 493{,}600 \text{ pounds}$$

For steel ($E \approx 3 \times 10^7$ psi) the Euler column load is given by

$$P_{CR} = \frac{(3.14)^2\ (3)\ (10)^7\ (10)^2\ (0.5)}{(10)^4} = 1{,}480{,}000 \text{ pounds}$$

It is evident that, for reasonably proportioned closed sections, such as that in Figure 9-9, column buckling is not a failure mode.* Even more stability is provided by transverse beam (9), which serves to reduce the effective column length by one half, and quadruple the Euler column load. More significantly, beam (9) serves to hold the shape of the gross car cross section by preventing lateral motion of the side sills under lateral loads produced by the collision.

A drawback of the designs shown in Figures 9-6 and 9-8 is that the structural assembly consisting of the frontal transverse beam, crash post and front bulkhead (elements (3), (4) and (5) respectively) is relatively vulnerable to damage from crash debris, particularly in crashes where longitudinal deflections are large. Puncturing of (5) bulkhead, for example, would destroy the major vertical load path between striking element (1) and the gross car section, consisting of center and side sills, side frame, and roof. The effective vertical stiffness and vertical strength of the car would be severely reduced, and the likelihood of climbing would be vastly increased. Such a design might behave well for relatively small longitudinal deformations, perhaps two to three feet or less, but its performance for significantly larger deformations would be questionable.

The performance of the design under large deflections could be significantly improved by providing substantial rigidity to transverse beam (9). If this beam were designed with section modulus approximately equivalent to that of the center sill,** a relatively rigid load path would be provided from the center sill to the monocoque car section, and the likelihood of climbing as a result of end bulkhead destruction would be considerably reduced.

A potentially stronger solution to the problem of such climbing is indicated by the design shown in Figures 9-10 and 9-11. In this approach, the

---

* Present design practice is generally to design tranverse members in this area as relatively light stiffinners.

** The square shape shown in Figure 9-9 may be difficult to obtain in the region of the truck because of required truck clearance.

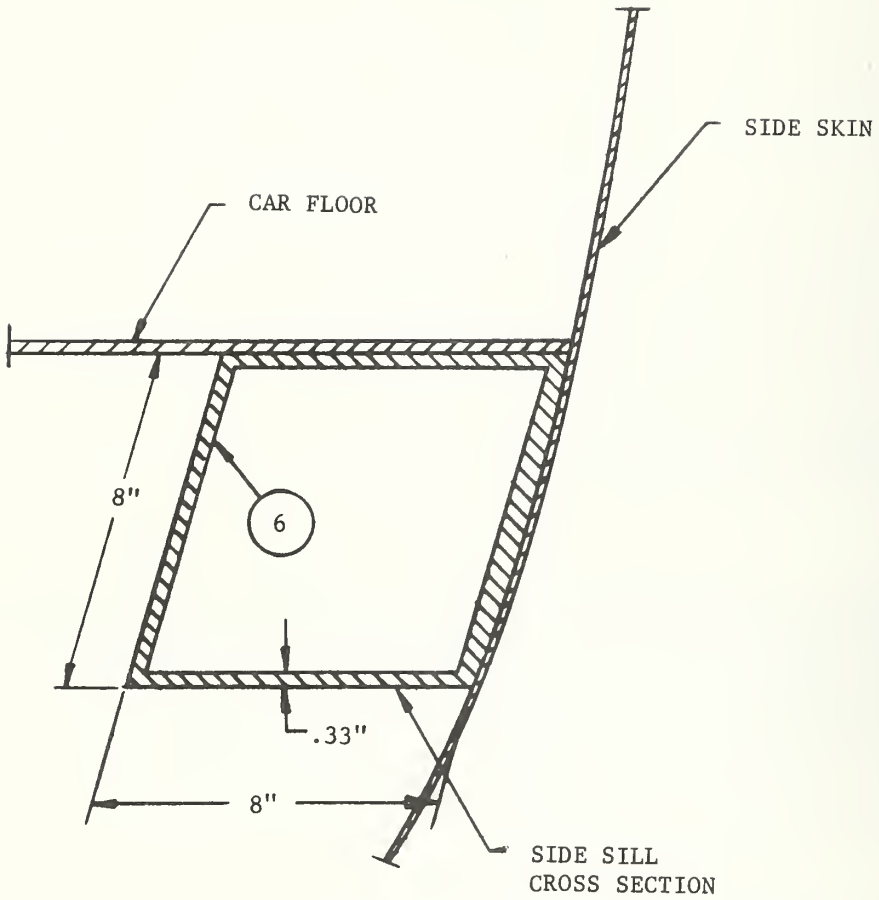

Figure 9-9. Section B-B from Figure 9-8

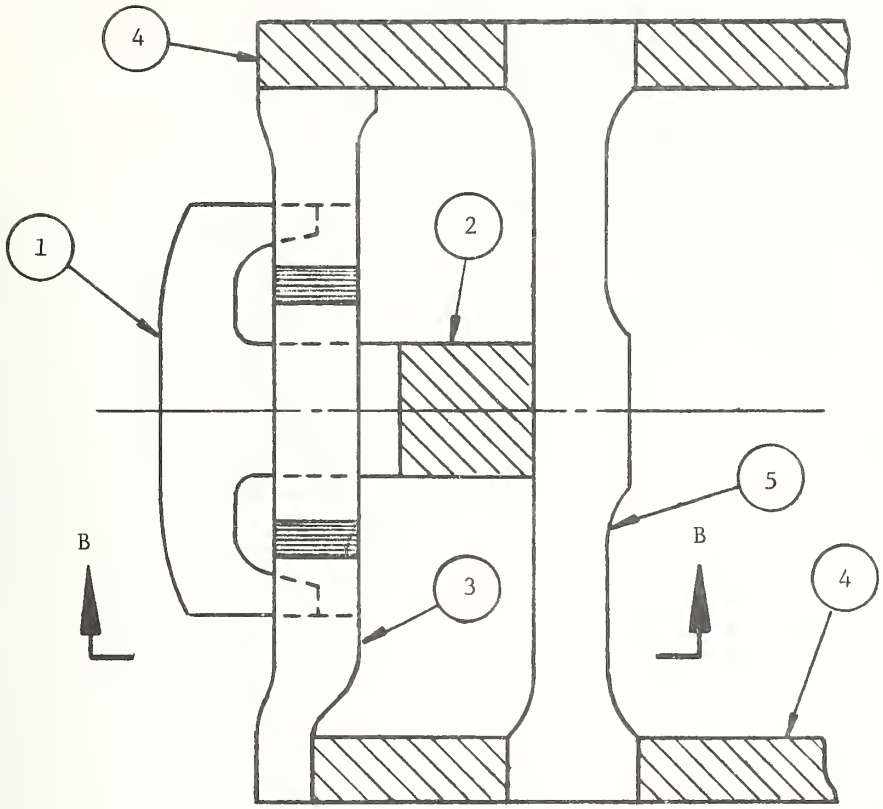

Figure 9-10. Concept 3

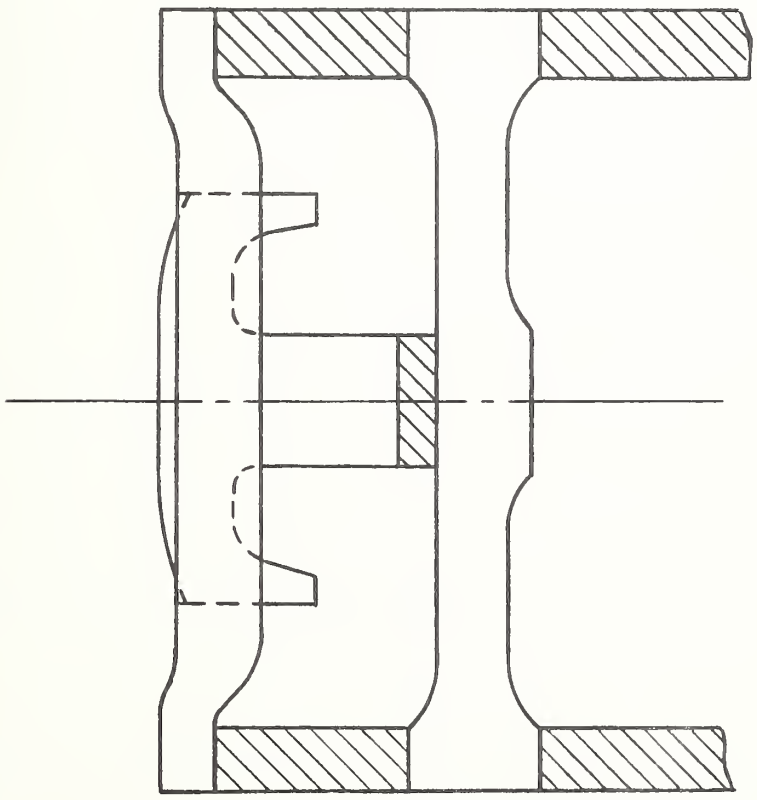

Figure 9-11. Flat Face Position

striking element (1) is designed to deflect sufficiently, through crushing of element (2), to achieve a "flat face" bearing condition as shown in Figure 9-11. At this time, collision loads are transmitted directly to the crushable side sills (6). The side sills are inherently stable in the vertical direction, being supported by the side frame which extends to the roof. Stability of the side sills in the lateral direction is provided by transverse beam (9) which is relatively compact (not vulnerable) and separated from the face of the crash. This beam is likely to retain its integrity over longer crush distances than will the bulkhead assembly of Figures 9-6 and 9-8.

Further improvement may be achieved by the design concept shown in Figure 9-12. In this approach, the striking element (1) is backed up by two crushing elements (2), affording increased lateral stability. The transverse frontal beam (3) serves to house the assembly consisting of (1) and (2), and provides sufficient bending to distribute the crash loads to the side sills during crush of elements (2). When the "flat face" position is achieved (Figure 9-13), cross beam (3) has served its purpose. Since the side sills are stabilized vertically by the side frames, and laterally by cross beam (9), destruction of cross beam (3) subsequent to achieving the flat face position should not result in climbing.

9.3.2 Energy Absorbers

In Section 9.2, it is noted that energy absorption can be obtained within the normal car body outline simply by eliminating passenger space for a given distance (x) at the forward end of the lead car. The potential for various lengths of energy absorbers to reduce collision fatalities can be determined by counting fatalities for particular lengths of passenger-free crush space. This is done in Chapter 7 (see Figures 7-6 and 7-7) for car crush lengths determined by means of employing generalized force-deflection curves as inputs to the dynamic train model described in Chapters 4 and 5.

In reviewing the results of the train model collisions, we note in Section 9.2 that the generalized force-deflection curves used in the train

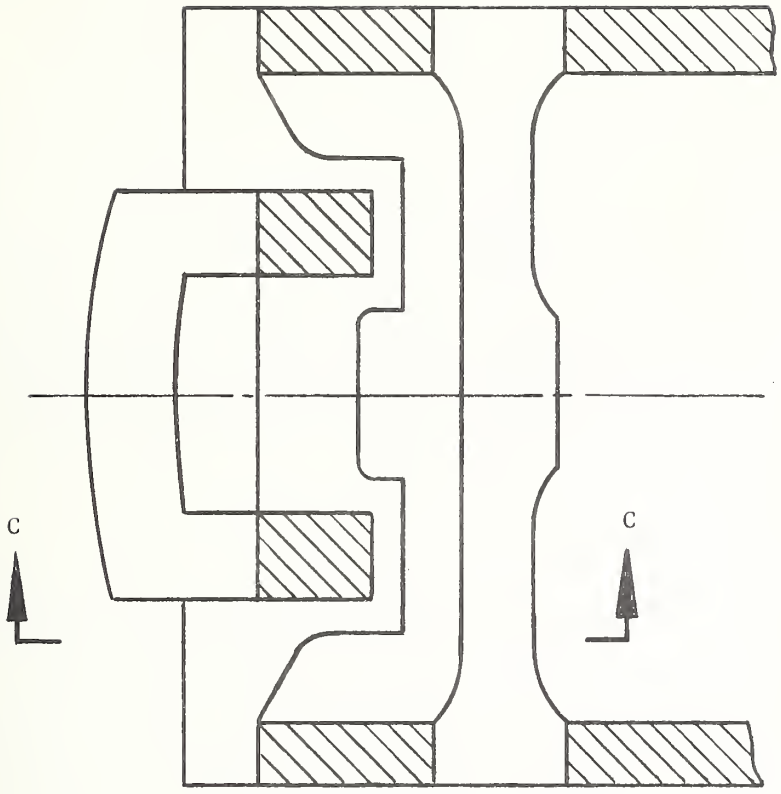

Figure 9-12. Concept 4

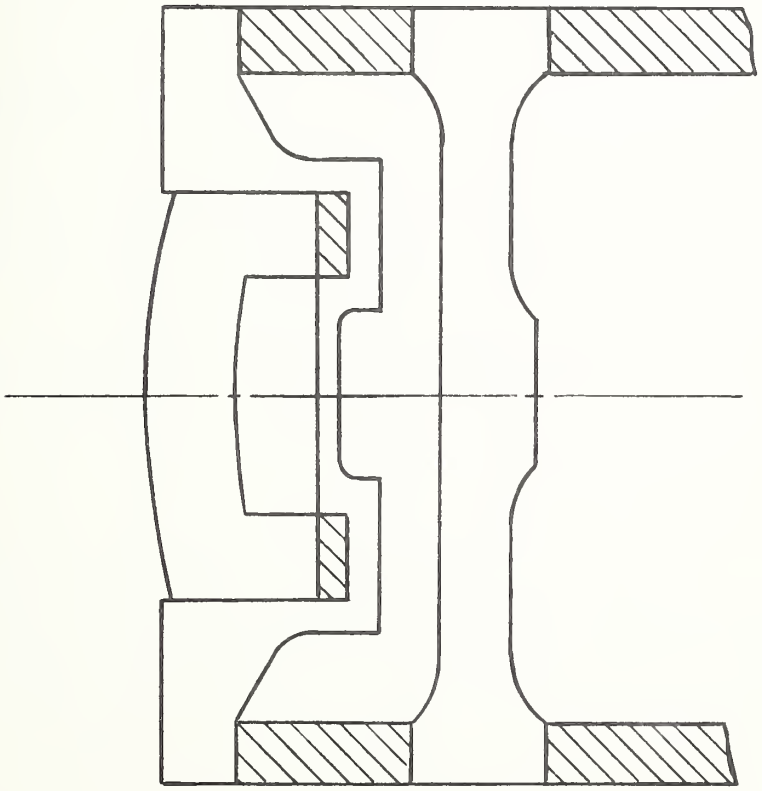

Figure 9-13. Flat Face Position

model resulted in considerably more sharing of crush between cars than has generally been observed in accidents. This is attributed, at least in part, to the tendency of colliding cars in actual accidents to fail to develop full crush force potential because of local structural failures induced at the initiation of impact or during the longitudinal deformation process which lead to various degrees of vertical (or lateral) misalignment - generally referred to as override.

An illustrative example of the potential of an externally mounted energy absorber for reducing injuries and fatalities is given in Section 9.2. In this example, a baseline car is used in which all of the crush occurs at the lead car, thus approaching actual accident conditions more closely than the idealized model. In figures 9-2 through 9-5, estimated reductions in fatalities and injuries are shown for a specific absorber characteristic (7 feet of crushable length and force level equal to car strength) and for a particular collision condition (collision of identical eight car trains at 40 mph closure speed).

In this section, we investigate the potential of three energy absorber designs. In order to determine their full potential, no limitiations are initially set for design closure speed or length of absorber. Before identifying the three design concepts, it is appropriate to review the basic relationships between crushable length of energy absorber (x), car strength to weight ratio (S/W), number of cars in the train (n) and collision velocity V. If the average force in the energy absorber is three forths of the car crush strength, the energy absorbed can be equated to train kinetic energy as follows

$$\frac{3}{4} S x = \frac{1}{2} \frac{w}{g} n V_b^2 \qquad (9\text{-}1)$$

where V_b is equivalent barrier velocity (equal to one half the closure velocity for collisions of identical trains), all crush is assumed to take place at the lead cars, and equal crush occurs on the identical lead cars. Equation (9-1) can be rewritten as follows

$$V_c = \sqrt{\frac{3}{2} g} \sqrt{\frac{x}{n}} \sqrt{S/W} \qquad (9\text{-}2)$$

Units for equations (9-1) and (9-2) are feet, pounds, and seconds. For V_c expressed in miles per hour, and x expressed in feet, equation (2) reduces to

$$V_c = 4.74 \sqrt{\frac{x}{n}} \sqrt{S/W} \qquad (9\text{-}3)$$

Equation (9-3) expresses the maximum equivalent barrier velocity (in mph) which can be absorbed by an energy absorber of crushable length x feet attached to a train having n cars with car strength to weight ratio S/W. Equation (9-3) is plotted in Figure 9-14 for an eight car train with available crush lengths of 8 feet, 16 feet and 50 feet. The ordinate in Figure 9-14 is closure velocity which, as has been noted, is twice equivalent barrier velocity for collisions of identical trains.

Three conceptual approaches to energy absorbing are shown in Figures 9-15 through 9-17.

Figure 9-15 illustrates an energy absorbing vehicle which is coupled to the lead car by a normal coupler. The energy absorbing vehicle can be as long as the standard car, and requires two trucks, as on the standard car.

In Figure 9-16, the energy absorbing vehicle is articulated to the lead car through an adapter attached to the lead car. This type of energy absorber can be approximately as long as the lead car, but requires only one conventional truck. Additional dolly wheels are provided to permit the energy absorber to move when not attached to the lead car.

In Figure 9-17, the energy absorber is cantilevered to the lead car. For this arrangement, the length of the energy absorber is limited by lateral clearance requirements. For transit properties having minimum curve radius of 145 feet, the maximum usable crushable length of a cantilevered absorber is

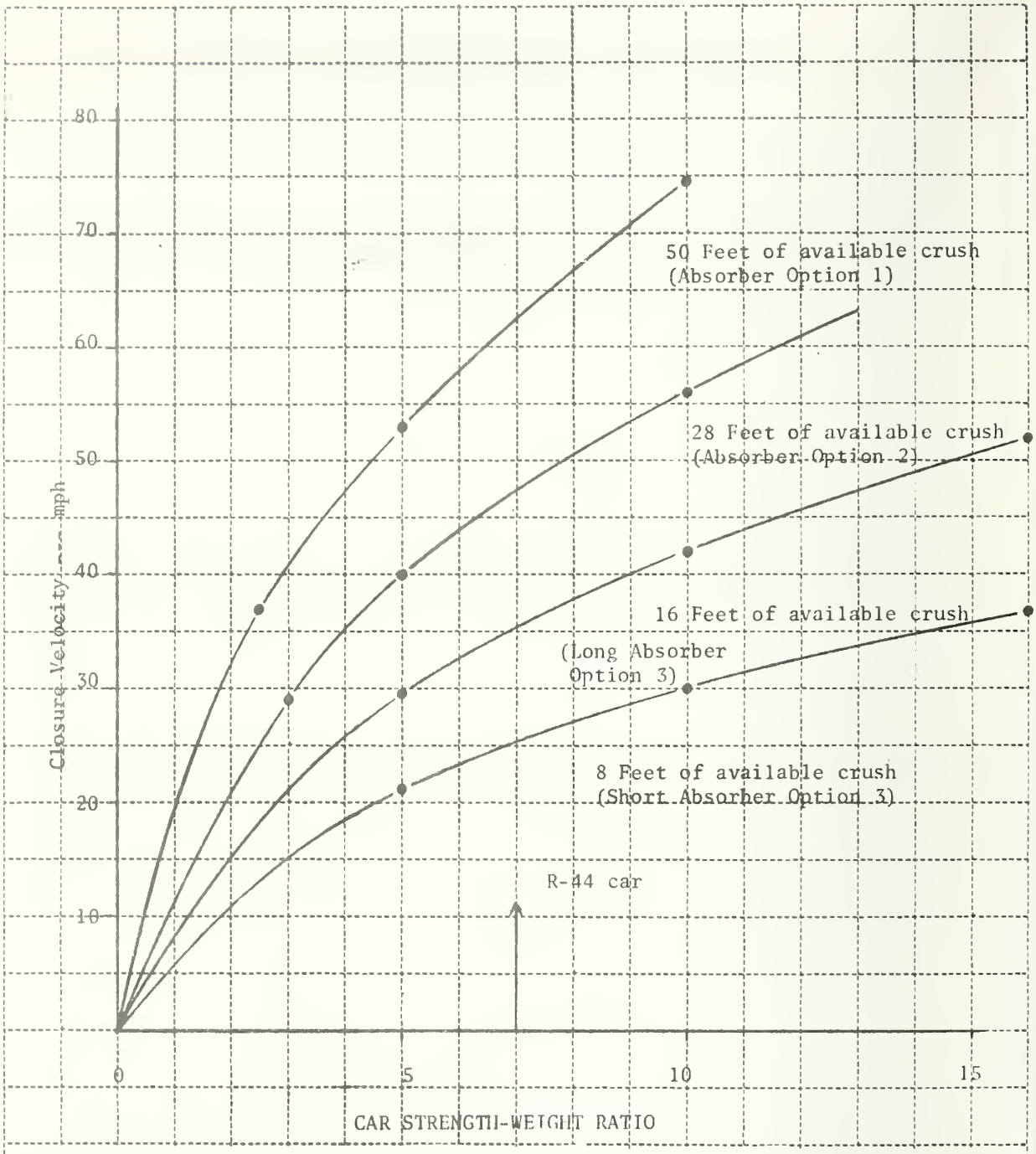

Figure 9-14. Maximum Closure Velocity Versus Strength-Weight Ratio (8 Car Train)

Figure 9-15. Separate Energy Absorbing Vehicle Option-1

Figure 9-16. Articulated Energy Absorbing Vehicle Option-2

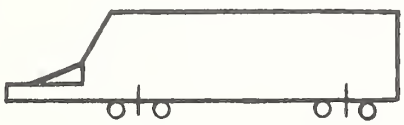

Figure 9-17. Cantilevered Energy Absorber Option-3

generally about eight feet, and on properties having minimum curve radius of 250 feet, the maximum usable crushable length can be as long as 16 feet. (The clearance problem for cantilevered absorbers is studied in detail in Chapter 10.)

For the first configuration (Figure 9-15) the usable crushable length is estimated at two thirds of the total length of the absorber. If the latter is 75 feet (a typical transit car length) the maximum usable crush length is therefore about 50 feet. The upper curve in Figure 9-14 indicates the potential of such an absorber. For car strength to weight ratio of five, the 50 foot energy absorbing vehicle can absorb the full energy of a 52 mph closure collision between identical eight car trains. For a strength to weight ratio of ten, the minimum velocity increases to approximately 75 mph.

For the second configuration (Figure 9-16,) a total length of 43 feet is chosen for purposes of illustration. A usable crush length of 28 feet is assumed.

The potential of the cantilevered configuration (Figure 9-17) is indicated by the lower and the intermediate curves in Figure 9-14. The lower curve is for 8 feet of absorber crush; hence it is generally applicable to transit properties where lateral clearance requirements must be met on curves with radius as short as 145 feet. This curve indicates the following maximum collision closure velocities.

S/W	$V_{c\ max}$
5	21 mph
10	30 mph
15	37 mph

The intermediate curve is for 16 feet of absorber crush, and is therefore generally applicable to transit properties where lateral clearance requirements must be met on curves with radius as short as 250 feet. This curve indicates the following maximum collision closure velocities.

S/W	$V_{c\ max}$
5	30 mph
10	42 mph
15	52 mph

It is evident that the first two energy absorbing configurations (Figures 9-15 and 9-16) have significantly higher potential capacity than the third configuration (Figure 9-17). Thus it appears that the third configuration may be most cost efficient at relatively low levels of required energy absorption, whereas one of the first two configurations would be more applicable at high levels of energy absorption.

In order to make a cost effectiveness comparison of the first two configurations with the cantilevered configuration for levels of energy absorption higher than those which can be handled by the latter, it is necessary to supplement the cantilevered configuration by additional passenger-free crush space taken from the normal passenger compartment. This approach is used in the energy absorber cost estimates which are made in Section 9.4.4.

9.4 APPROXIMATE WEIGHT AND COST ESTIMATES OF DESIGN CONCEPTS

9.4.1 General

In this section, approximate weight and cost estimates are provided for defined improvements in the three priority areas identified in Section 9.2 (car structures, energy absorbers, and interiors).

In establishing relationships between initial costs, recurring costs and weight associated with the design improvements, we note that some portions of the cost of improvement consist of system costs which can be established by other means (e.g., trucks and brake system for vehicle energy absorber). In such cases appropriate sources are identified.

Some design improvements apply to all cars (e.g., basic structural and interior improvements) and other design improvements apply only to particular cars (e.g., lead end and trailing end energy absorbers). It is evident therefor that the most elementary costing methodology must take into account the average number of cars in a train. We have noted from the results of the collision simulations that a very elementary approach to increasing crashworthiness is the provision of passenger-free space at car ends. In evaluating the cost impact of a given design improvement, whether it be an energy absorber or improved car structure or interior, a baseline cost for comparison purpose is therefor the cost of providing this space.

The cost methodology used for evaluating the design improvements is described in the following Section 9.4.2. In the succeeding sections (9.4.3 and 9.4.4) this methodology is applied to specified structural design improvements and energy absorbers.

9.4.2 Cost Methodology:
Initial and Recurring Costs

If a hardware design concept is applicable to each car in the train, as is generally the case for car body structural and interior concepts, the initial cost and the annual recurring costs for an n car train are given by:

$$\text{Initial Cost} = n \; C_{I1} \tag{9-4}$$

$$\text{Annual Recurring Cost} = n \; C_{R1} \tag{9-5}$$

where C_{I1} and C_{R1} are the initial and recurring costs applicable to each car.

If the design concept applies to the train and not to each car, as in the case of a lead car or trailing car energy absorber, the initial and recurring costs for an n car train are given by

$$\text{Initial Cost} = C_{I2}$$

$$\text{Annual Recurring Cost} = C_{R2}$$

where C_{I2} and C_{R2} are costs per train.

The following approach is taken in estimating the cost of providing passenger-free crush space in the lead car of an n car train. If the space provided is defined by x, measured from the front of the car, the fractional reduction in maximum capacity of the car is x/ℓ, where ℓ is the length of one car. If each train has n cars, the effective initial costs and recurring costs, reckoned on a per car basis, are evidently given by

$$\text{Initial Cost} = C_{I3} \; \frac{x}{\ell} \; \frac{1}{n} \tag{9-6}$$

$$\text{Annual Recurring Cost} = C_{R3} \; \frac{x}{\ell} \; \frac{1}{n} \tag{9-7}$$

where C_{I3} and C_{R3} are the initial costs and annual recurring costs for one entire car. These costs reflect the costs of purchasing and running additional cars to make up for the lost passenger space. However the recurring cost shown above applies only if the transit authority runs the additional cars all the time. Actually, since the additional cars are provided to achieve a given level of maximum passenger capacity, it is more realistic to assume that these cars are run only during rush hours. If P is the fraction of total car miles which is accumulated in rush hours, the corrected per car annual recurring cost of providing passenger-free crush space is given by

$$\text{Annual Recurring Cost} = C_{R3} \frac{x}{\ell} \frac{P}{n} \qquad (9\text{-}8)$$

The costs defined in the previous paragraphs are summarized in Figure 9-18 The figure shows how costs per car are calculated in terms of the specific cost elements C_{I1}, C_{I2}, C_{I3}, C_{R1}, C_{R2} and C_{R3} and train parameters n, x and P.

Total annual system cost per car (C_{TAS}) is defined as the average annual cost per car, and includes original cost and recurring cost. If all cars depreciate to zero value over a 20 year period of time and are paid for over the same period, the average annual interest, assuming the principle is reduced in equal amounts each year, is

$$\text{Annual Interest} \approx \frac{C_I}{20} R \qquad (9\text{-}9)$$

where R is the applicable rate of interest.

The average annual cost due to original cost (C_{OA}) over the 20 year time period is the sum of the principle costs and the average annual interest costs

$$C_{OA} = \frac{C_I}{20} + \frac{C_I}{2} R \qquad (9\text{-}10)$$

	Design Concepts Occurring on Every Car	Energy Absorber	Provision of Passenger-Free Crush Space
Initial Cost Per Car	C_{I1}	$\frac{1}{n} C_{I2}$	$C_{I3} \frac{x}{\ell} \frac{1}{n}$
Annual Recurring Cost Per Car	C_{R1}	$\frac{1}{n} C_{R2}$	$C_{R3} \frac{x}{\ell} \frac{p}{n}$

C_{I1} = Initial cost per car of those design changes which occur on every car.

C_{I2} = Initial cost per energy absorber.

C_{I3} = Initial cost of one entire car.

C_{R1} = Annual recurring cost per car due to design changes which occur on every car.

C_{R2} = Annual recurring cost due to one energy absorber.

C_{R3} = Annual recurring cost for one entire car.

n = Number of cars in train.

x = Length of passenger-free crush space.

p = Fraction of car miles accumulated in rush hours.

Figure 9-18. Initial and Annual Recurring Cost Normalized to a Per Car Basis

In this study an annual interest rate of 10 per cent is assumed. Therefore, from equation 9-10

$$C_{OA} = 0.1\ C_I \qquad 9\text{-}11$$

The total annual system cost (C_{TAS}), which includes annual recurring cost, is given by

$$C_{TAS} = 0.1\ C_I + C_R \qquad 9\text{-}12$$

Initial costs (C_I) which arise from the additions of structural material to the car shell or to an energy absorber can be estimated on the basis of the structural weight added. The cost of a structural car shell is normally about 10 per cent of total car cost. At present values (1974) total car cost for a typical transit car is taken as 400,000 dollars . Total weight of a typical transit car shell is taken as 13,000 lb. . The cost of rail vehicle structures per pound of structure is therefor

$$\frac{.10\ (400,000)}{13,000} \approx 3 \text{ dollars per pound}$$

Annual recurring costs (C_R) can be estimated on the basis of added weight, since cost of power, brake replacement and rigging and wheel replacement are very nearly proportional to car weight. The following recurring costs, on a per pound basis (e.g.; per pound of added material for the design change or addition) are used.

Item	Annual Recurring Cost (Dollars per pound per year)
Cost of Power	0.10
Cost of Brake Replacement and Rigging	0.02
Cost of Wheel Replacement	0.02
TOTAL	0.14

9.4.3 Weight and Cost Estimates for Car Body Structural Additions

It has been shown in the previous sections that there are two ways in which car structures can be improved. First, where car designs provide significantly lower strength to weight ratio than the optimum range indicated in Chapter 7 (this range is dependent on interior characteristics), these designs can be made stronger by the provision of additional structural material. Second, given that the car is designed to an appropriate strength to weight ratio, engineering design concepts need to be applied which will minimize override tendency and undesirable structural instabilities associated with initial impact and large longitudinal deformations. This second category of design revisions (discussed in Section 9.3.1) is aimed at providing controlled crush behavior in a crash, and predictable force versus deflection characteristics.

Weights and costs for providing added car strength are calculated with respect to a baseline car with total weight of 70,000 pounds and a relatively low strength to weight ratio of 4. To increase the strength to weight ratio to 12 (the highest ratio studied), the required increase in crush force is approximately given by

$$\Delta S = (12-4)(70,000) \approx 560,000 \text{ pounds}$$

Using steel with a relatively low effective crush stress of 30,000 psi, the required addition in car cross sectional area is

$$\Delta A = \frac{560,000}{30,000} \approx 18.7 \text{ in}^2$$

The added material volume for a 75 foot car is

$$75\ (12)(18.7) = 16,800 \text{ in}^3$$

For steel density of 0.3 pounds per cubic inch, the weight added to the car is

$$\Delta W = 16{,}800\ (0.3) \approx 5000 \text{ pounds}^{*}$$

From Section 9.4.2, the effective initial cost of adding structural material to the original design (not retrofitting) is 3 dollars per pound. The estimated initial cost is therefor

$$C_I = 3\ (5000) = 15{,}000 \text{ dollars}$$

Annual recurring costs, from Section 9.4.2, are equal to 0.14 dollars per pound. Therefor

$$C_R = 0.14\ (5000) = 700 \text{ dollars}$$

The total annual system cost (C_{TAS}), from Section 9.4.2, is given by

$$C_{TAS} = 0.1\ C_I + C_R$$

Therefor, the total annual system cost for increasing a typical transit car from strength to weight ratio of 4 to strength to weight ratio of 12 is given by

$$C_{TAS} = 0.1\ (15{,}000) + 700 = 2200 \text{ dollars}$$

Estimated weights and costs for anti-climbing provisions are based on the design concepts described in Section 9.3.1. It is assumed that two rigid transverse beams are added to the end underframe structure, weighing 1000 pounds per beam. An additional 500 pounds of structure is alloted to joints, bearing points, and local crushing elements. The total estimated weight addition for the anti-climbing provisions is therefor 2500 pounds. Using the appropriate

* Because the car weight is increased from 70,000 pounds to 75,000 pounds, the final S/W is 11.2

cost versus weight factors from Section 9.4.2, the initial cost (C_I), annual recurring cost (C_R) and total annual system cost (C_{TAS}) are given by

$$C_I = 3\ (2500) = 7500 \text{ dollars}$$

$$C_R = 0.14\ (2500) = 350 \text{ dollars}$$

$$C_{TAS} = 0.1\ (7500) + 350 = 1100 \text{ dollars}$$

9.4.4 Weight and Cost Estimates for Energy Absorbers

Three energy absorber design concepts are identified in Section 9.3.2 The energy absorbing potentials of the three concepts, in terms of maximum closure velocity for which full train energy can be absorbed, are indicated by the three curves in Figure 9-14, in which maximum closure velocity is plotted versus strength to weight ratio.

Energy absorbing option (1), a full 75 foot vehicle absorber supported by two trucks, has the maximum energy absorbing potential, as indicated in Figure 9-14. The essential elements of this absorber are:

(1) Trucks and suspension at 2 support points.

(2) Energy absorbing structure and structural attachment elements to trucks and transit car.

(3) Ballast and associated structural elements.

(4) Brake System

The first requirement for the absorber is that it have sufficient restraining forces, one of which is absorber weight, to stay down during severe collisions with similar absorbers, other transit cars, maintenance equipment etc. The weight of the absorber has a rather strong influence on its initial costs (particularly since the weight determines the design of the truck and suspension) as well as on annual recurring costs such as power, brake shoe replacement, etc. Unfortunately it is difficult to estimate what a minimum weight should be, because of the difficulty of predicting climbing forces and resulting climbing behavior. A prudent approach is believed to be that the weight at the rail should be a significant percentage of the weight of typical transit cars, which range from 60,000 pounds (light) to over 100,000 pounds fully loaded. For costing purposes, the weight of the 75 foot absorber is taken as 50,000 pounds at the rail.

The simplest type of truck to consider would be similar to a freight car truck. However such trucks are very stiffly sprung and have primary spring characteristics which would result in relatively unstable lateral ride. Significant lateral inputs would be transmitted to the transit car, and the resulting degradation in ride would be unacceptable for present high ride quality requirements such as those for the Advanced Concept Train (ACT) program.

A truck having equivalent quality to modern transit car trucks is used as a basis for estimating costs. Some suspension modifications might be required because of the relatively light weight of the suspended mass. Propulsion equipment would not be required, but the weight of the absorber is sufficiently high that standard brakes would be required. The approximate cost of such a truck, exclusive of brakes, is estimated to be $15,000[1].

[1] This is based on approximate cost of transit car trucks in 1972-1973 period

From Figure 9-14, required crushing force for an energy absorber designed to be compatible with (for example) the R-44 car corresponds to a car strength to weight ratio of approximately 7. Assuming an 80,000 pound car weight, this is a crush force level of 560,000 pounds. Using an effective material crush allowable of 56,000 psi, the required area of crushable structure is 10 square inches. It is assumed that additional structure required to stablize the crushable elements would require the addition of 10 square inches of equivalent material. The weight of energy absorbing material, exclusive of structural attachments, is given by

$$W = A \ell \varrho$$

where

A = total effective area
ℓ = length of absorber
ϱ = material density

For a length of 75 feet (900 inches) and using 0.3 pounds per cubic inch for steel crushing material

$$W = 20\ (900)\ (0.3) = 5400 \text{ pounds}$$

It is estimated that approximately 5000 pounds of additional weight would be required for structural attachments, including body bolsters, anti-climber and backup structure, coupler and draft gear structure, etc. This would result in a total structural weight of 10,000 pounds for the sprung mass of the energy absorber.

From Section 9.4.2, the cost of rail vehicle structural weight is estimated at 3 dollars per pound. On this basis, the cost of the energy absorber structure is

$$\text{Cost} = 3 \times 10{,}000 = 30{,}000 \text{ dollars}$$

The required amount of ballast is found by subtracting structural weight and truck weight from the design target weight of 50,000 pounds.

Estimated weight of two trucks	16,000 pounds
Structural weight	10,400
Total excluding ballast	26,400 pounds

The required amount of ballast to achieve 50,000 pounds total weight is therefore about 24,000 pounds. The cost of ballast material, including the means of containing and securing the ballast on the vehicle, is estimated to be $0.30 per pound, resulting in a cost of $7200 for the ballast installation.

Estimated brake system cost is based on the cost of a complete brake system for one transit car. This is approximately $15,000 per car*.

The weight and original cost breakdown for the 75 foot vehicle energy absorber (Option 1) is shown in Figure 9-19. The figure also inclues a similar breakdown for Option 2 - an intermediate capacity articulated vehicle energy absorber which is 43 feet in length and has total energy absorbing capacity of 15.7 million foot pounds.

Included in Figure 9-19 is a weight and original cost summary for Option 3 - the cantilevered energy absorber. The length assumed for this absorber is 12 feet, which is about the maximum length which can be accommodated on a transit property having minimum 145 foot curve radii. The weight per foot of the cantilevered absorber, exclusive of transverse structural members, is taken as the same as the weight per foot of typical light weight transit car structures,

* Based on approximate cost of brake system in 1972-1973 period

	Option 1 50 Feet of Available Crush		Option 2 28 Feet of Available Crush		Option 3 8 Feet of Available Crush	
	Weight (lbs.)	Cost ($)	Weight (lbs.)	Cost ($)	Weight (lbs.)	Cost ($)
Trucks	16,000	30,000	8,000	15,000	0	0
Structure	10,400	31,200	6,000	18,000	4,100	12,300
Ballast	22,600	6,900	25,300	7,600	0	0
Brake System	1,000	15,000	700	10,000	---	---
Total	50,000	83,100	40,000	50,600	4,100	12,300

Figure 9-19. Weight and Original Cost Summary for Three Energy Absorbers

Item	Multiplier $ per lb.	$ Option 1 (50,000 lb.)	$ Option 2 (40,000 lb.)	$ Option 3 (4,100 lb.)
Power	0.10	5,000	4,000	410
Brake Replacement and Rigging	0.02	1,000	800	82
Wheel Replacement	0.02	1,000	800	82
TOTAL		7,000	5,600	574

Figure 9-20. Annual Recurring Costs for Three Energy Absorbers

exclusive of transverse members (e.g., 10,000 pounds for 75 feet of structure or 133 pounds per foot). This weight is

$$W = 12\ (133) = 1600 \text{ pounds}$$

The weight of transverse members required for structural stability and prevention of climbing is taken to be equal to the corresponding weight requirement determined in Section 9.4.3 for improvement of car structures (2500 pounds). The total estimated weight of the 12 foot cantilevered absorber is the sum of the weights of longitudinal and transverse structure, or 4100 pounds. Using the cost-weight factor from Section 9.4.2 (3 dollars per pound) the estimated original cost of the 12 foot cantilevered energy absorber is $12,300, as shown in Figure 9-19.

Annual recurring costs for the three energy absorbing options are shown in Figure 9-20. Total annual system costs C_{TAS} (Reference Section 9.4.2) can be calculated from original costs and annual recurring costs as follows:

$$C_{TAS} = 0.1\ C_I + C_R$$

Inserting the original and recurring costs for the three absorbers shown in Figures 9-19 and 9-20 , the total annual system costs for the three absorbers are

	Dollars Per Eight Car Train	Dollars Per Car
Option 1	15,300	1912
Option 2	10,700	1337
Option 3	1,800	225

From Section 9.4.2, the initial cost per car of providing passenger-free end space (x) in the lead car of an n car train is

$$\text{Initial Cost} = C_{I3} \frac{x}{\ell} \frac{1}{n}$$

where C_{I3} is the cost of one complete car and ℓ is car length. For car cost of 400,000 dollars, car length of 75 feet, and for eight cars in a train, the initial cost of providing 5 feet of passenger free end space is

$$\text{Initial Cost} = 400{,}000 \quad \frac{5}{75} \quad \frac{1}{8} \quad = 3{,}330 \text{ dollars}$$

The recurring cost of providing passenger-free end space, from Section 9.4.2, is

$$\text{Recurring Cost} = C_{R3} \frac{x}{\ell} \frac{p}{n}$$

where C_{R3} is the recurring cost of running one standard transit car and p is the fraction of total system car miles which is accumulated in rush hours. Using 70,000 pounds for a standard passenger car weight, the recurring cost of running one car is

$$C_{R3} = .14 \ (70{,}000) = 9800 \text{ dollars}$$

For C_{R3} = 9800 dollars, p = 0.5 and n = 8 cars, the recurring cost per car of providing 5 feet of passenger-free end space is

$$\text{Recurring Cost} = 9800 \quad \frac{5}{75} \quad \frac{0.5}{8} \quad = \$40.83$$

From Section 9.4.2, the total annual system cost per car for providing 5 feet of passenger-free crush space in the lead car is

$$C_{TAS} = 0.1 \ (3330) + 40.83 = \$370.83$$

In Figure 9-21, the total annual system costs of the three energy absorbers are compared to each other, and to the cost of providing passenger-free end space. In the figure, the annual cost of each of the three energy absorbers is shown, along with speed capacity (e.g., maximum closure speed for which energy of colliding eight car trains can be absorbed) of each absorber. Data in the figure are based on a car strength to weight ratio of 7. Note from the figure that the provision of end free passenger space is a more cost efficient means of providing energy absorption than the three absorbers at speeds below the following closure speeds.

Absorber 1	Speeds below 52 mph
Absorber 2	Speeds below 42 mph
Absorber 3	Speeds below 18 mph

For all closure speeds above 18 mph and below 48 mph, the figure shows that the most cost efficient means of absorbing energy is the cantilevered absorber, supplemented by passenger-free space as required. For closure speeds between 48 mph and 55 mph, the most cost efficient means of absorbing energy is the intermediate absorber (absorber 2) and for closure speeds above 58 mph the most cost efficient means of absorbing energy is shown to be the full vehicle energy absorber (absorber 1).

It is noted that the articulated absorber 2 causes a significant amount of additional loading on the forward truck of the lead car (about 10,000 to 20,000 pounds of additional loading, depending on the c.g. location of the energy absorbing vehicle). Hence, a special truck may be required, which would significantly increase the effective cost of absorber 2. The most significant comparison therefor appears to be absorber 1 versus absorber 3. Absorber 3, unsupplemented by passenger-free end space, is most cost efficient at speeds up to about 18 mph. When supplemented by the amount of passenger free end space shown in the figure, absorber 3 is more cost efficient than absorber 1 for all closure speeds below 58 mph.

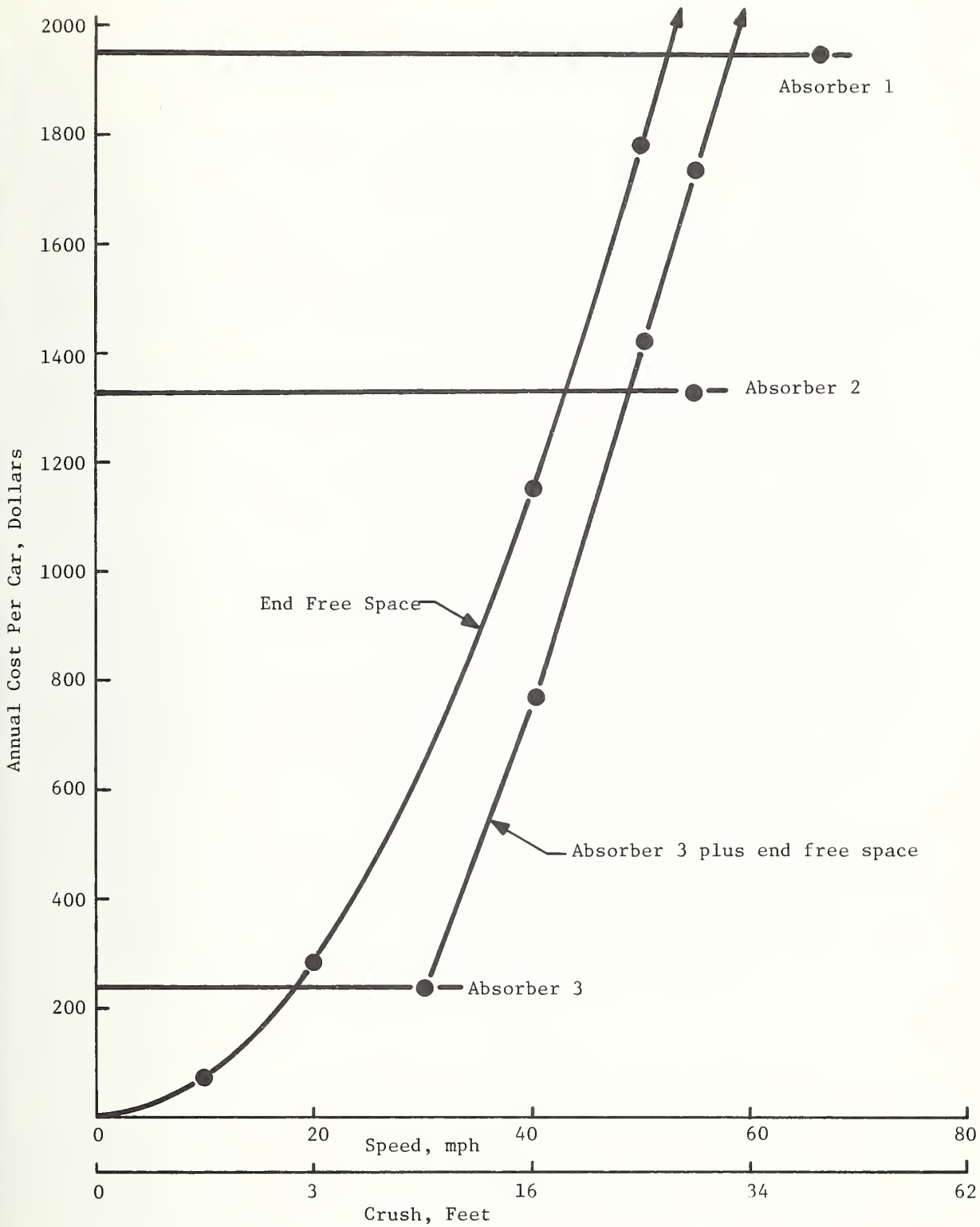

Figure 9-21. Annual Cost of Energy Absorbers 1, 2 and 3 Compared to Annual Cost of Providing Passenger-Free End Space (For Car Strength to Weight Ratio of 7)

It is also noted that an increase in car strength to weight ratio will have the effect of increasing the maximum speed capacity of all of the absorbers, by permitting higher crush forces. If strength to weight ratio is increased from 7 to 12, the maximum closure speed capacity of the cantilevered absorber (with zero supplementary end free space) is increased from 28 mph to 37 mph.

It is emphasized that these calculated energy absorber costs are highly dependent on the assumptions which have been made in regard to the numerous cost elements involved. The relative costs shown, however (for Options 1, 2 and 3) appear to be meaningful, in that relatively large variations in the estimates of the individual cost elements will still result in the conclusion obtained from Figure 9-21 - that Option 3 (the cantilevered absorber) is more cost efficient than the separate vehicle absorber for collision speeds which are likely to occur in practice. It also appears from Figure 9-21 that the best alternative to the cantilevered absorber is the provision of end-free crush space. The final choice between the cantilevered absorber and the provision of end free space will be strongly dependent on the efficiency of the absorber design, and on its demonstrated performance.

The cantilevered energy absorber is selected as the most promising energy absorber for further design studies. In the following section, design studies are performed for the application of a cantilevered energy absorber to the Advanced Concept Train (ACT) and to the State of the Art Car (SOAC).

For the cantilevered energy absorber, bending moments at given car body stations are increased because of the added length associated with the absorber. An important design consideration for the cantilevered absorber is the provision of adequate vertical strength in the absorber itself and in the car body to resist climbing loads. Reasonably accurate estimation of the energy absorber cost is highly dependent on design requirements for vertical strength, which vary considerably depending on the vertical strength of the existing design. This design problem is investigated in considerable detail in Chapter 10.

10. PRELIMINARY DESIGN STUDY OF IMPACT ENERGY ABSORBING DEVICE

10.1 INTRODUCTION

A potentially attractive aspect of the energy absorber is that it may, in theory, be retrofitted to existing cars, thereby increasing the crashworthiness of the cars significantly at a very small percentage of their original cost. However, because of the questionable climbing integrity of many existing cars, the rigidity and strength of the vertical load path from the striking surface of the energy absorber to the car structure should be investigated.

It was noted in the previous section that car axial strength and available length for the energy absorber present limiting conditions on maximum energy absorbing capacity.

In the following section (10.2) the energy absorbing potential of the ACT* car and the SOAC* are investigated, with consideration given to available clearance for the energy absorber, to determine its maximum length, and to existing car strength levels, to determine its maximum permissible strength.

In the preliminary design investigation in section 10.3, the problem of the vertical load path is examined, and an energy absorber design installation is shown which provides significantly more strength and rigidity in the vertical load path than is generally provided by existing car designs.

10.2 ENERGY ABSORPTION POTENTIAL

Figure 10-1 shows the relationship between maximum closure velocity for which the energy of an eight car train can be absorbed, car strength to weight ratio, and available length of crush. The curves shown are obtained from Equation 9-3 and are identical to the curves for corresponding length of crush which are shown in Figure 9-14.

* The Advanced Concept Train (ACT) car and the State-of-the-Art Car (SOAC) are selected as examples of advanced and contemporary car construction.

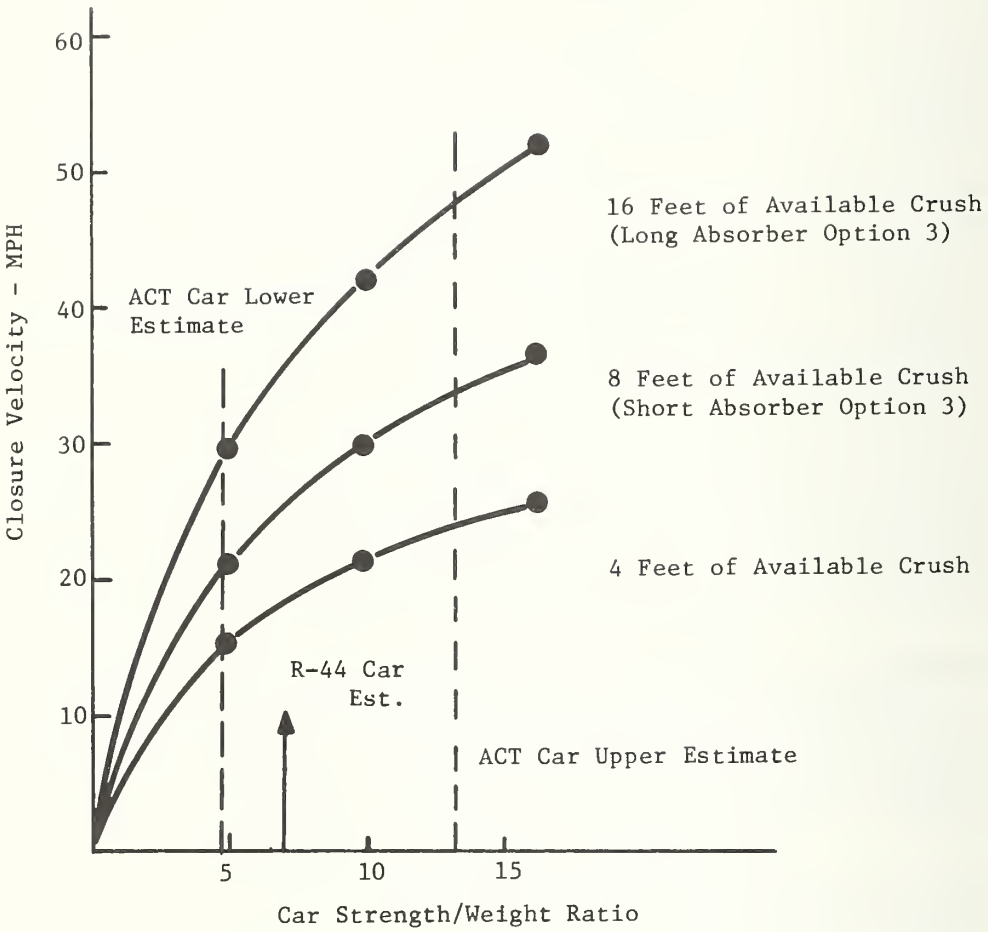

Figure 10-1. Energy Absorption Potential for R-44 and ACT Car

The curves in Figure 10-1 show that energy absorption potential is highly dependent on car strength to weight ratio. The strength to weight ratio of the R-44 car, similar in construction to the SOAC, is shown in the figure. Two strength to weight ratios are shown for the ACT car. The lowest ratio (4.7) is based on light side sill construction, indicated by element (1) in Figure 10-2. The high ratio (13.7) is based on heavy side sill construction, indicated by the combination of elements (1) and (2) in Figure 10-2. Significantly, Figure 10-2 shows that the large change in calculated strength to weight ratio, from 4.7 to 13.7, is obtained solely with the addition of side frame channel (2), and adds only 2.4 percent to the weight of the car.

Additional strength potential in the ACT roof structure is indicated by Figure 10-3. The figure shows a roof corner purlin design with 8.65 square inches of effective material per car side. At 30,000 psi allowable stress, the two corner purlins would provide more than 400,000 pounds of additional strength to the car. Moreover, this estimate of roof strength is evidently conservative, as the fiberglass roof structure joining the corner purlins is not included in the calculation. The large additional strength of the roof is not reflected in Figure 10-1, primarily because the contacting elements in a collision are below floor level, at the level of the side sill. The roof structures are not in contact and are therefore not developing crush force. It was noted in Chapter 9 that for normal car construction (e.g.; no energy absorber outside of the rectangular car outline) the roof structure can be made effective, while also maintaining the structural integrity of the collision post and its attachments to the end underframe structure and the roof structure, by the addition of contacting elements at the top of the collision posts as shown in Figure 9-7. The same principle could be employed in the design of an energy absorber; however it is believed that the complexity required to obtain effective crush at roof level without penalizing operator visibility would be considerable.

The strength to weight ratio selected for this investigation of ACT and SOAC energy absorbers is 7. This force level reflects full development of strength potential below floor level, and is based on the assumption that roof surfaces do not come into effective contact in the course of the collision. In

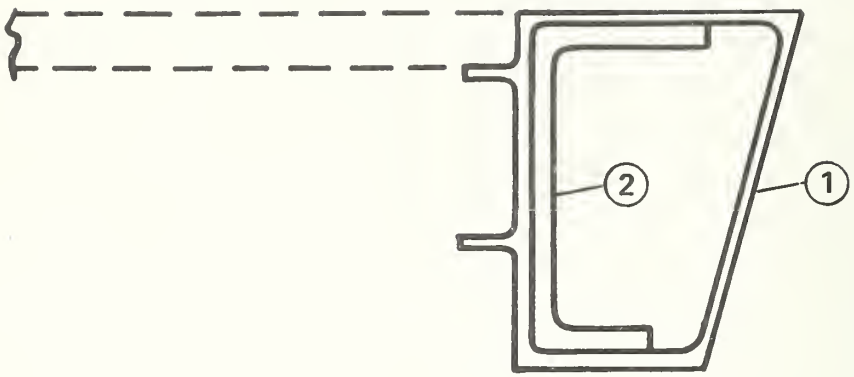

TYPICAL SIDE SILL CONFIGURATION

MEMBER	AREA in^2	I/C in^3	BENDING STRESS (psi)	AXIAL STRENGTH (pounds)	WEIGHT (pounds)
①	5.5	19.7	———	330,000	990
②	8	26.2	———	———	250
TOTAL	13.5	45.9	38,000	330,000	1240

POSSIBLE DESIGN

MEMBER	AREA	I/C	BENDING STRESS	AXIAL STRENGTH	WEIGHT
①	16.5	59.1	29,500	960,000	2900

$$\text{PERCENTAGE INCREASE IN CAR WEIGHT} = \frac{1,660}{70,000}(100) = 2.4\%$$

$$\text{PERCENTAGE INCREASE IN STRENGTH} = \frac{960,000-330,000}{330,000}(100) = 191\%$$

Figure 10-2. Potential for Increased Strength to Weight Ratio

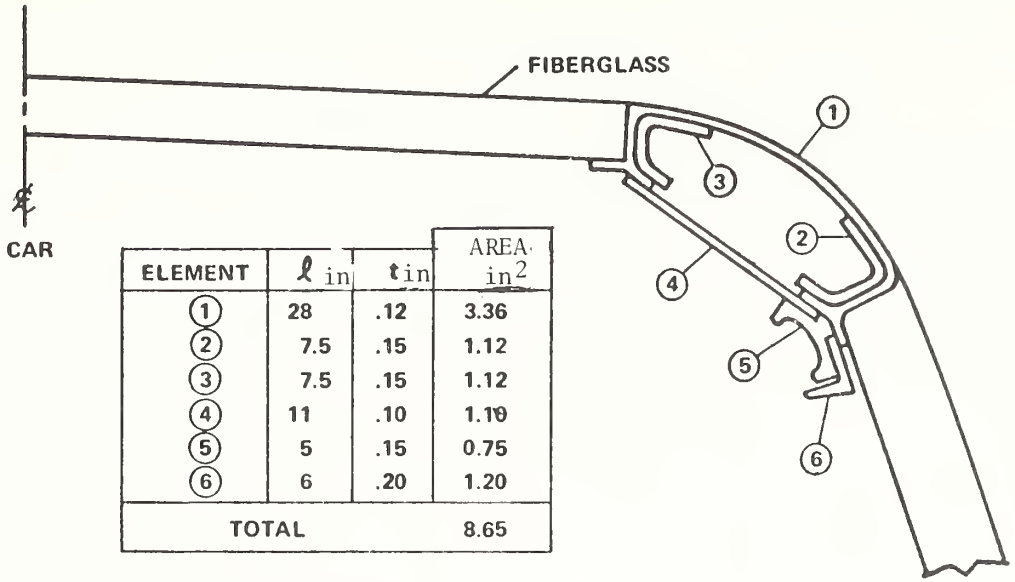

ELEMENT	ℓ in	t in	AREA in^2
1	28	.12	3.36
2	7.5	.15	1.12
3	7.5	.15	1.12
4	11	.10	1.10
5	5	.15	0.75
6	6	.20	1.20
TOTAL			8.65

STRENGTH = 2(8.65) (30,000) = >400,000 LB,

NOT INCLUDING FIBERGLASS

Figure 10-3. Strength Estimate of ACT Roof

selecting this crush force level as a design criterion, previous qualifications in Chapter 5 with regard to accurate prediction of actual crush force levels should be noted.

It is evident from Figure 10-1 that the energy absorbing potential for the ACT car and the SOAC is strongly dependent on useable length of energy absorber, as well as on the strength to weight ratio which can be developed. In this study it is assumed that both cars must operate on properties having minimum curve radii of 145 feet. In Figure 10-4, lateral clearance is shown for an ACT car in a 145 feet radius curve. The figure shows that the length of the cantilevered absorber is limited by available lateral clearance at the end of the car. The absorber shown in the figure extends 5 feet forward of the ACT cab unit, which remains rigid during crushing of the energy absorber.

Figure 10-5 shows an energy absorption design which provides additional useable length of crush by employing a telescoping arrangement. In this design, a 60 inch stroke is obtained by crushing of honeycomb material enclosed in the draft sill structure. A rigid transverse member, shown cross hatched, delivers the longitudinal load to crushable honeycomb members at the sides of the car. To permit the additional stroking of the side members, shown as three feet, the cab structure must be pushed back 3 feet into the car body. This would require that the upper portion of the cab structure and the car roof structure be designed to permit three feet of intrusion by the cab into the roof. In addition, the side structure of the cab would have to peel away laterally to permit the additional motion to take place. Thus, the additional 3 feet of stroke would require additional weight and complexity in the form of the transverse structure and side crushing elements, and would also require design provisions to insure controlled failure of car body roof structure and cab side structure.

The SOAC is shown in Figure 10-6. Employing more conventional design practice, the SOAC cab is contained within the normal rectangular car body outline. Hence the length which is occupied by the cab of the ACT car (81.5 inches) is available for additional crushing on the SOAC. However Figure 10-6 indicates that the controlling design factor for the SOAC energy absorber is

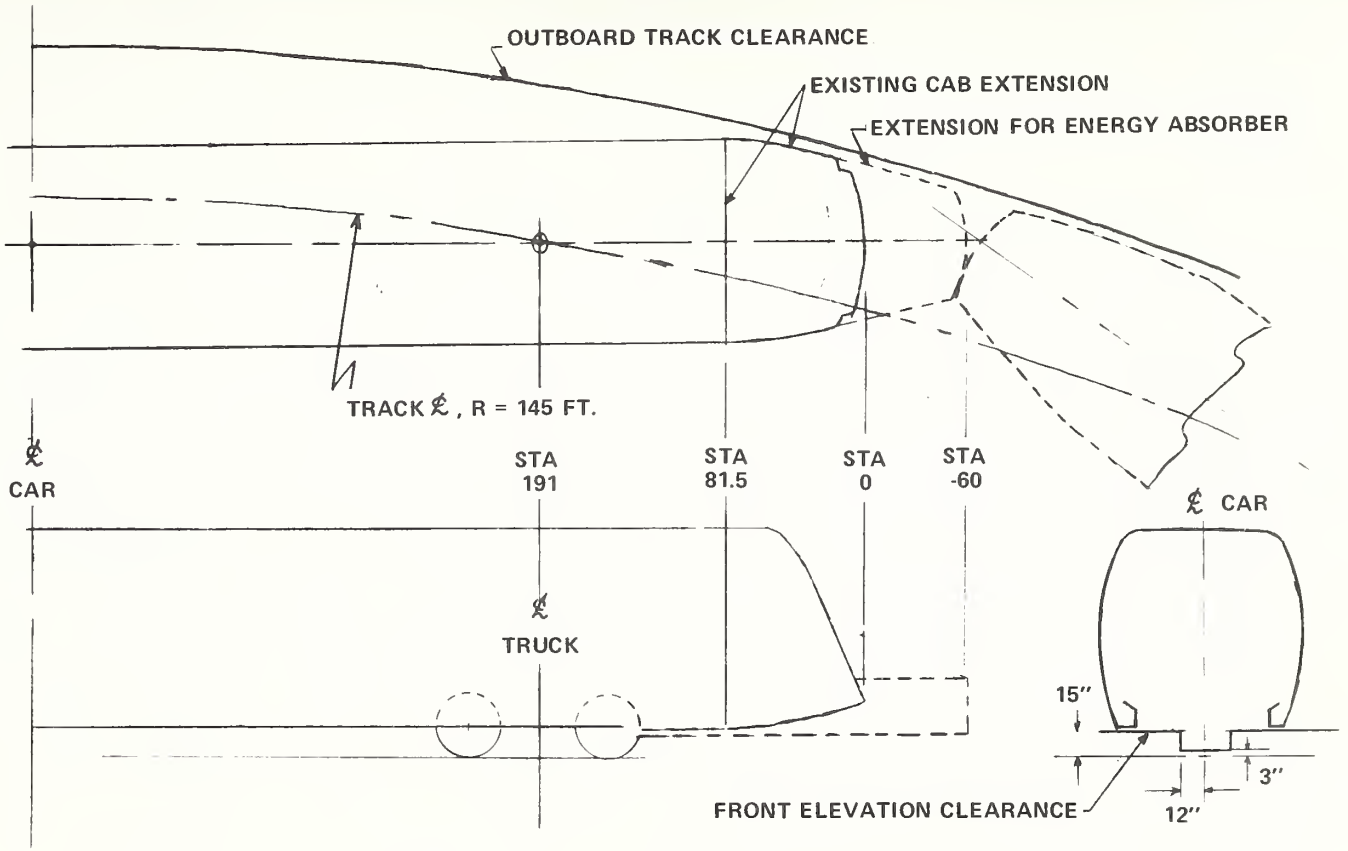

Figure 10-4. Clearance for Energy Absorber on Existing Systems

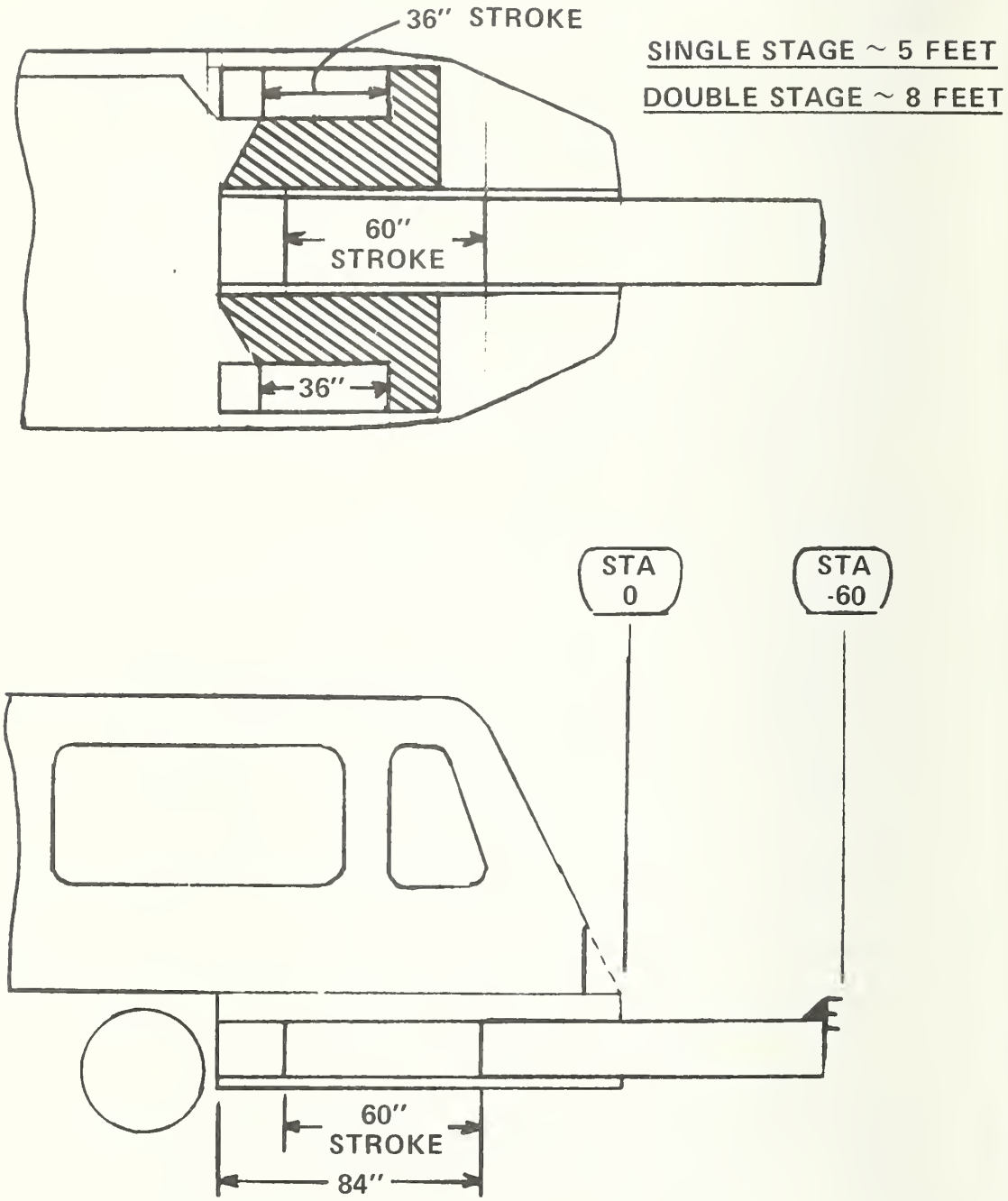

Figure 10-5. Available Stroke (ACT Car)

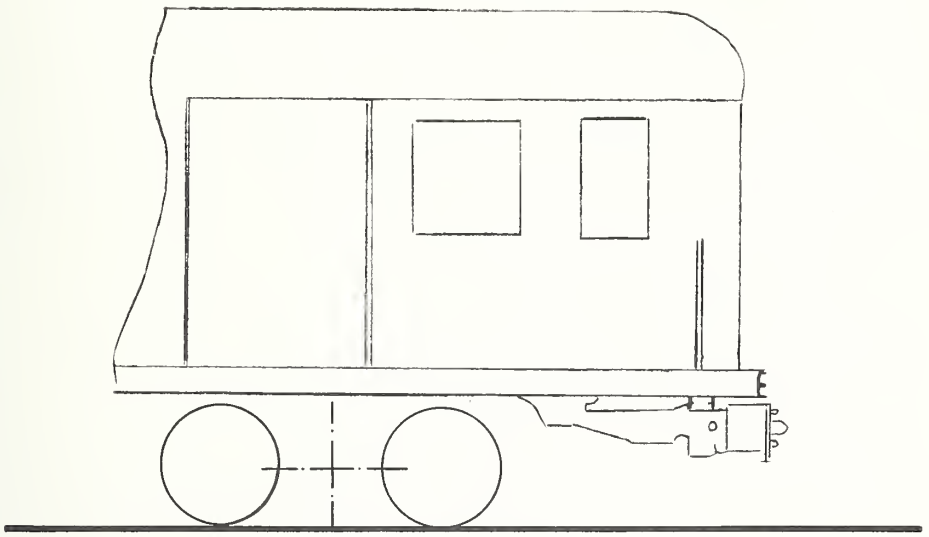

Figure 10-6. Approximate Position of Coupler and Trucks R-44 and SOAC

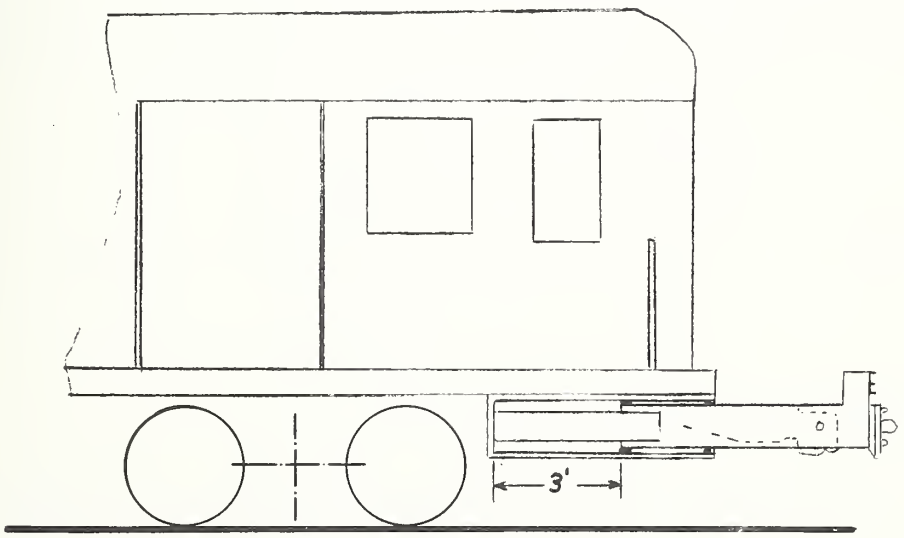

Figure 10-7. Possible Energy Absorbing Configuration

the limited space available between the end of the car and the truck. Though it is possible to obtain energy absorption in the area occupied by the trucks, by providing for shearing of the truck from the car structure, equipment rearrangement to permit free longitudinal truck motion with respect to the car, and probably redesign of the truck supporting structure, these revisions to the existing design would be complex and costly. A possible energy absorber configuration is as shown in Figure 10-7, and employs only 3 feet of available stroke.

In summarizing the energy absorbing potential of the SOAC and the ACT car it is evident that the 145 foot radius requirement permits approximately 8 feet of useable crush on design configurations employing the typical square ended body construction. However this available length tends to be reduced by other factors. In the ACT car, the cab unit occupies space which would normally be available for crush. In the SOAC, the controlling factor is the location of the truck. For both cars, special designs could be utilized to achieve the maximum 8 feet of crush length (e.g.; the use of telescoping arrangements on the ACT car and provision of truck shearing on the SOAC) but these designs would require very significant complexity and cost for the gains obtained. Accordingly, the following specifications are selected for energy absorber preliminary design.

	Useable Length (feet)	S/W	Capacity in MPH (Ref.Eq. 9-3) 8 Car Train	4 Car Train
ACT	5	7	19.7	27.8
SOAC	3	7	15.3	21.6

10.3 DESIGN INVESTIGATION

The addition of a 5 foot energy absorber forward of the ACT cab requires the provision of a rigid vertical load path through the cab into the car body structure in order to provide reasonable assurance that climbing will not take place in severe accidents. The problem is complicated by the design of the side

frame structure between the side door and cab, indicated in Figure 10-8. The shear strength of the side frame, which determines its capacity to deliver body bending loads to the roof structure, is limited by the window cutout between the side door and cab unit. The loads shown in the figure represent a 2g load applied to the car end (80 kips) resisted by vertical car inertia loads. The axial roof load required to resist body bending at the side door center line is 123 kips, as shown in the figure. A conservative estimate of the bending moment at section B-B is indicated by the calculation in Figure 10-8. The moment is given by half of the roof axial load (61.5 kips) acting on a 56 inch arm, indicated in cross section A-A in Figure 10-8. The calculation shows that the section required at B-B to limit bending stress to 30,000 psi is extremely heavy, requiring an area of 6.4 square inches at either end of the 18 inch section. This would require a forging or casting in this area, rather than the usual sheet metal stiffener design typically used in railcar sideframe construction. With the latter form of construction, it is evident that the vertical strength of the car is low compared to its longitudinal strength. It is important to note that this characteristic is generally representative of existing railcar construction, and is not unique to the ACT car. Many new car designs feature large windows, with resulting decrease in potential side frame vertical shear and bending strength.

With the cantilevered energy absorber configuration indicated by Figure 10-4, the vertical loads associated with climbing will produce a significantly larger moment, and resulting larger roof loads, than the same loads applied to the conventional car end shown in Figure 10-8. The proposed solution to the problem is shown by Figure 10-9.

In Figure 10-9a, climbing loads representing 4 g's are shown acting upward on the striking surface, with corresponding inertia loads acting downward on the car body.* The resulting bending moment at the door centerline produces

* The selection of 4g vertical loads as a criterion for vertical strength to eliminate vertical failure and resulting climbing is arbitrary. The conservatism, or lack of conservatism, of this criterion will only be determined by further testing and analysis of the climbing phenomenon.

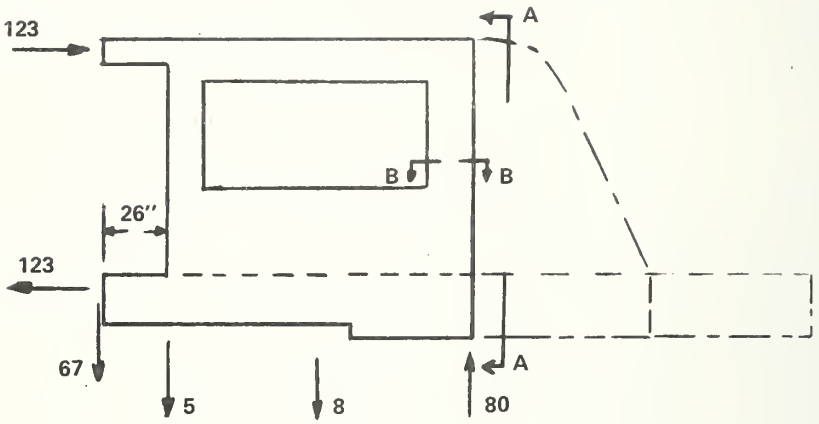

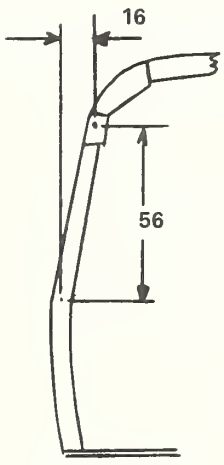

SECT. A-A

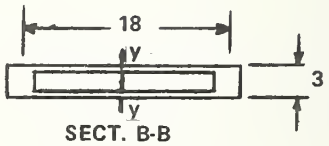

SECT. B-B

M_{yy} = 61.5 (56) = 3440 IN KIP.

$P_{CAP} = \frac{M}{h} = \frac{3.44\ 10^6}{18}$ = 191,000 LB.

FOR f_c = 30,000 PSI, $A_{REQD} = \frac{191,000}{30,000}$ = 6.4 IN^2

$T = \frac{61500\ (16)}{2(18)\ (3)}$ = 9110 LB/IN

$f_s = \frac{9110}{.4}$ = 22,800 PSI

Figure 10-8. Side Frame Shear Stress

an extremely high axial roof load of 319,000 pounds at that point. It is significant to note, however, that this load is less than the estimated inherent strength of the ACT roof-corner purlins acting alone. (See Figure 10-3.)

The major problem remains that of delivering the axial load to the roof. A means of doing this without relying on the relatively weak side frame structure in the window area is indicated by Figure 10-9b. In this figure, the structure housing the energy absorber (called draft sill assembly in the figure) is located in the area normally occupied by the conventional draft sill structure. Attached rigidly to the energy absorber housing is a crash post arch structure, replacing the conventional straight crash post. The arch structure consists of two separate arches, located at the same transverse point on the structure as the normal crash post (at either side of the space normally provided for the end door). These arches provide a rigid central structure around the operators' cabin, and have sufficient strength to deliver the required high axial load to the roof structure. The arch structure therefor has three functions:

(1) Provision of vertical load path to roof, assuring vertical integrity to prevent climbing

(2) Provision of dual collision posts

(3) Provision of rigid structure surrounding central portion of cabin

The combined loads on the roof and side frame structure are shown in Figure 10-9c. Note that a rigid load path for vertical climbing loads is achieved with zero shear load in the relatively weak side frame structure.

A preliminary design layout of the cantilevered energy absorber applied to the ACT car is shown in Figure 10-10, and a perspective view of the energy absorber installation is shown in Figure 10-11.

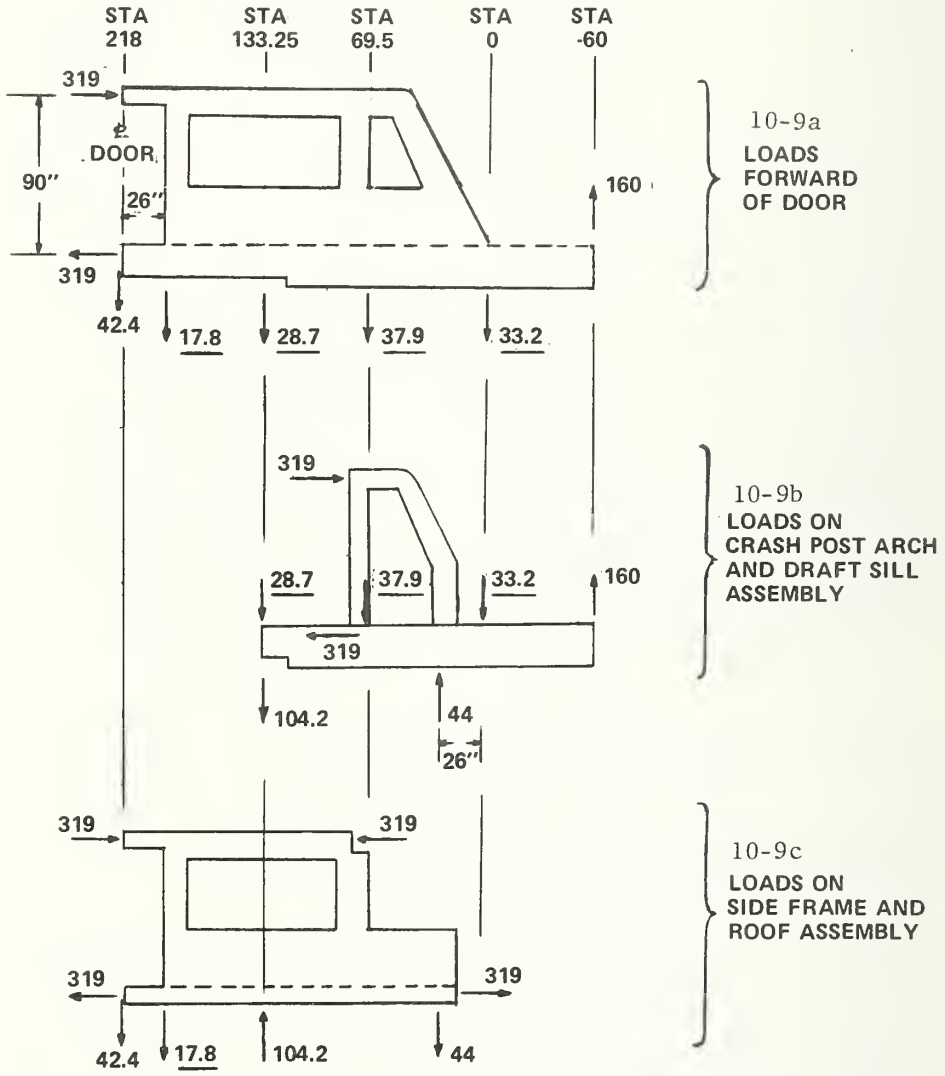

Figure 10-9. Load Path for Climbing Loads (Inertia Loads Underlined)

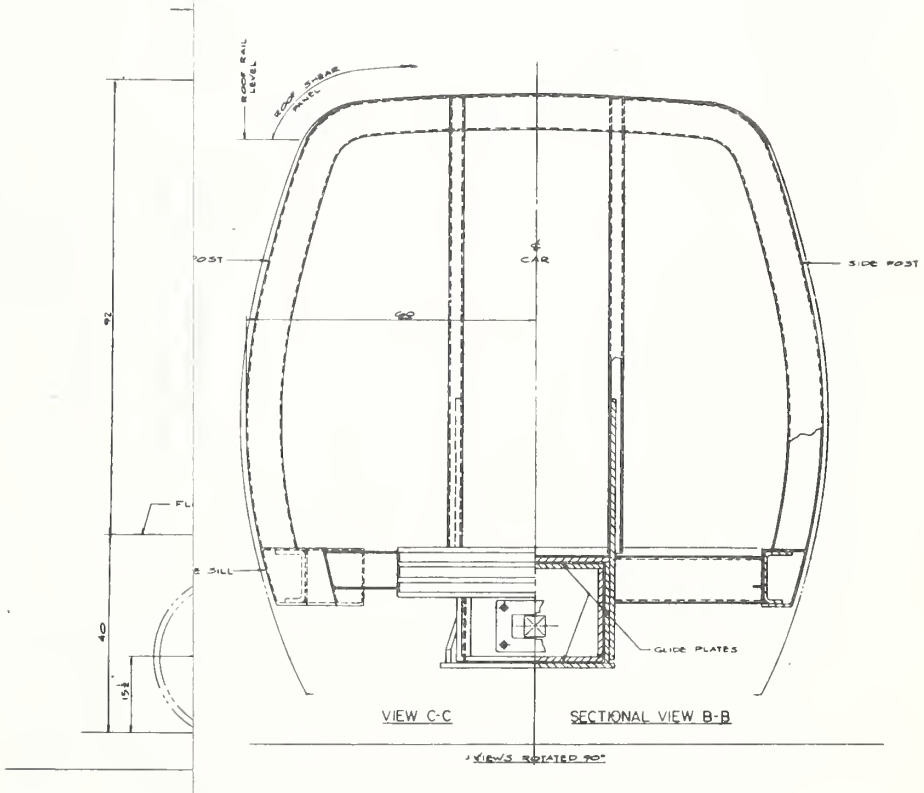

Figure 10-10. Cantilevered Energy Absorber Applied to ACT Car

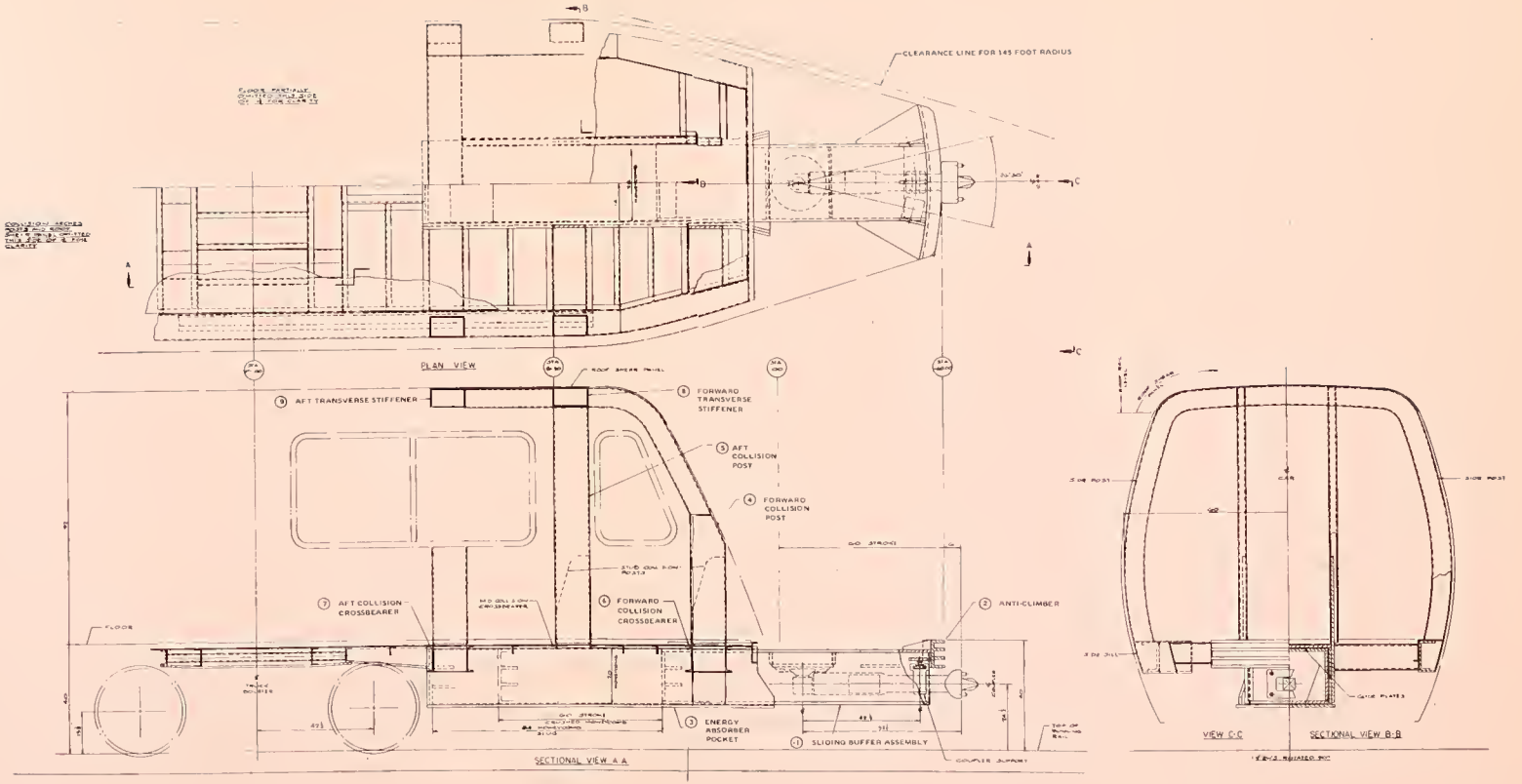

Figure 10-10. Cantilevered Energy Absorber Applied to ACT Car

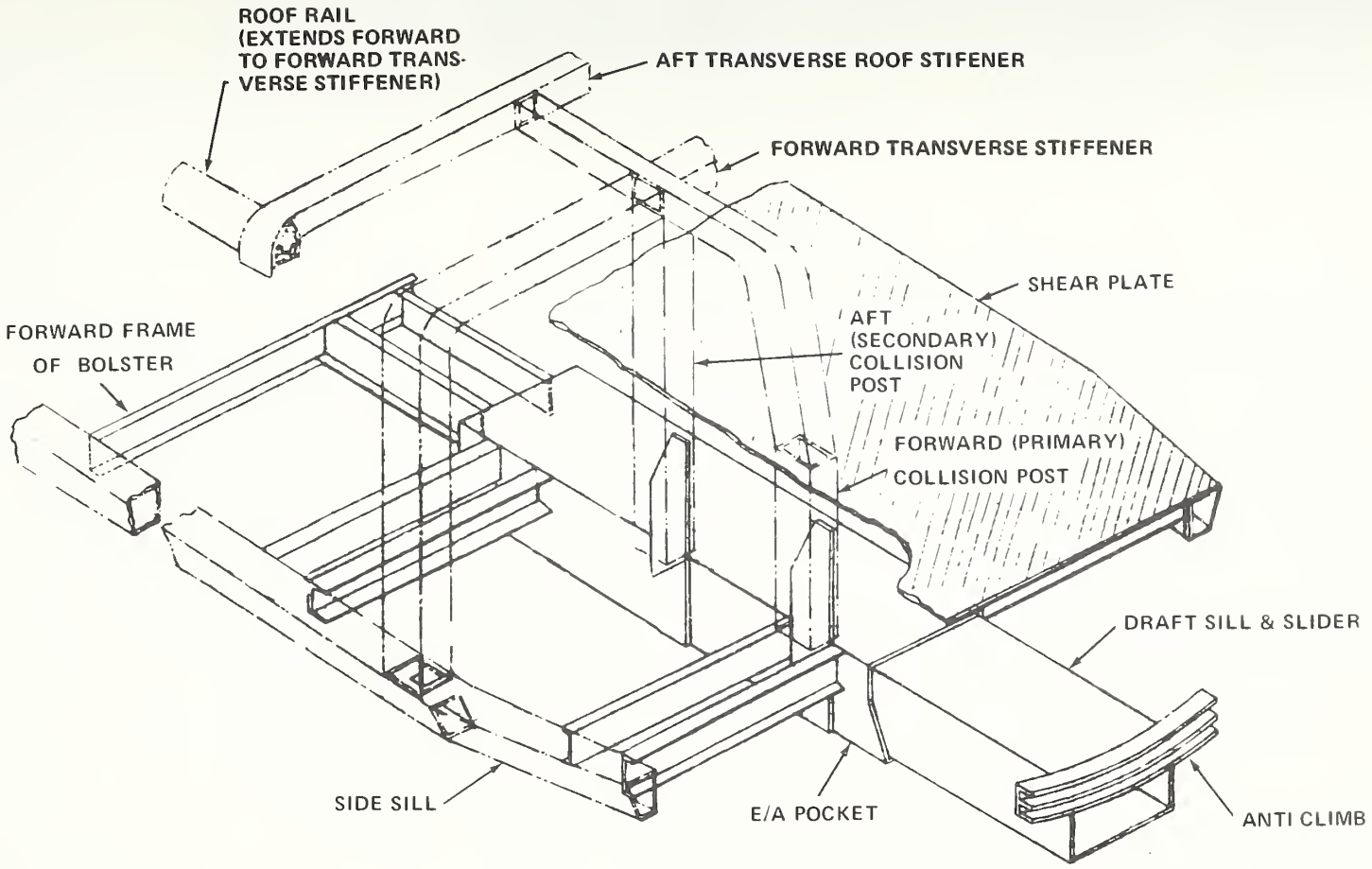

Figure 10-11. Perspective of Cantilevered Energy Absorber

The clearance line in the plan view of Figure 10-10 corresponds to the clearance line for the minimum 145 foot radius. In the end view of Figure 10-10, clearance is assured by maintaining all elements a minimum 15 inches from the rail.

Key elements in the energy absorber itself are (1) sliding buffer assembly, (2) anti climber and (3) energy absorber pocket. During the crushing process, the sliding assembly moves against crushable honeycomb material which is enclosed in the pocket. Available travel shown is 60 inches, with an additional 24 inches of space to accommodate the crushed honeycomb material. Cross section area within the pocket is 625 square inches.

The coupler and a conventional anti climber* are shown mounted to the sliding buffer assembly in such a way that the front end coupling and bearing configuration corresponds to standard car design. Sliding of the buffer assembly within the energy absorber pocket is facilitated by glide plates, indicated in the car end view. A shear pin, not shown, maintains the sliding buffer assembly in its normal extended position. The pin can be designed to shear at a force level slightly in excess of the standard coupler shear pin.

In its normal extended position, the sliding buffer assembly provides a platform to facilitate emergency egress of passengers, by permitting passengers to exit straight ahead, or perpendicular to the vehicle.

The arch structure is formed by (4) forward collision post and (5) aft collision post. The transmission of longitudinal load to the roof causes a pitching moment on the arch structure which is reacted by the energy absorber pocket structure. The pitching moment in the latter structure is reacted by differential vertical loads from (6) forward collision cross bearer and (7) aft collision cross bearer, which transmit vertical loads to the side frame as previously shown in Figure 10-9b.

---

* Such an anticlimber may not be recommended. Further analysis is required (see Chapter 8). The conventional anticlimber is shown in the sketches to illustrate that the standard front end configuration (coupler and anti-climber) can be maintained on the energy absorber, permitting the energy absorber car to be compatible with existing cars.

The roof transverse elements (8) and (9), acting together with the roofing shear material, form a rigid transverse beam to transmit the longitudinal load from the collision post arch structure to the rigid roof corner purlins, previously shown and analyzed in Figure 10-3.

Weight estimates for the SOAC energy absorber of Figure 10-6 and the ACT energy absorber of Figure 10-10 are shown in Figure 10-12. Both absorbers are designed to a car strength to weight ratio of 7 (approximately 500,000 pounds). Stroke of the SOAC absorber is 3 feet, and stroke of the ACT absorber is 5 feet. In calculating the weight for the SOAC energy absorber, no additional structure is provided to increase anti climbing integrity. Whether or not such additional structure would be required would have to be determined by a climbing analysis of the SOAC.

The weight estimate for the ACT absorber includes the additional structure shown in Figure 10-10 to provide the climbing strength required because of the additional 5 foot arm for vertical climbing loads. Vertical loads corresponding to 4 g's were used for sizing of the structural elements. All of the major structural elements are designed by these vertical loads, rather than the longitudinal load of 500,000 pounds. Therefor, longitudinal load capacity significantly greater than 500,000 pounds exists in all the passive (non crushing) elements of the absorber and its supports.

As shown in Figure 10-12, the estimated weight of the ACT absorber and supporting structure is 4750 pounds. The energy absorber pocket and added support structure replace an estimated 1300 pounds of structure, primarily draft sill and lighter collision posts, which would otherwise be required. Therefor the total added weight, as shown in Figure 10-12, is 3450 pounds.

It is interesting to compare the ACT absorber weight estimate with the very approximate weight estimate for a cantilevered absorber made in Section 9.3.4. For the ACT absorber, 5 feet of stroke is achieved with an estimated added weight of 3450 pounds. In section 9.3.4, an absorber having total length of 12 feet and crushable length of approximately 8 feet is estimated to weigh

Element	Weight, Pounds ACT Absorber	SOAC Absorber
Sliding Buffer Assembly and Anti Climber	1000	600
Energy Absorber Pocket	1500	900
Collision Arches (2)	1000	-
Collision Cross Bearers (2)	800	-
Roof Transverse Stiffness (2)	300	-
Honeycomb Crush Material	150	-
TOTAL WEIGHT	4750	1590
Minus Structure Replaced	1300	-
TOTAL WEIGHT CHANGE	3450	1590

Figure 10-12. Estimated Energy Absorber Weights

4100 pounds (see Figure 9-20). Investigation of the weight breakdown in Figure 10-12 shows that the estimates would be approximately equal (in pounds per foot) if the additional structure for anti climbing were not included in the ACT estimate.

The following summary comments on energy absorbers are appropriate

Retrofitting energy absorbers to existing cars may require replacement of some existing structure and addition of other structure to provide for anti-climbing integrity. Each car should be evaluated on its own merits.

For new cars on existing systems, the potential benefits from energy absorption are less than for new systems because

- Many cars on existing systems have very low strength to weight ratio. If the energy absorber is limited in strength to be compatible with the weakest cars, absorption potential is limited.

- Existing systems utilize married pairs of A and B cars. Every A car is a potential lead car in a train. Operational problems are therefore greater than for some new systems (such as BART) where train length is fixed and A cars are always at the end of the train.

In existing systems, maintenance and operational facilities are established. Changes would be required to make them compatible with energy absorber requirements, in particular requirements for changing energy absorbers from one car to another.

Speeds are generally lower on existing systems than on new systems. Consequently potential benefits tend to be less.

11. COST EFFECTIVENESS OF STRUCTURAL IMPROVEMENTS

In this section, the cost of structural improvements recommended in the previous section is investigated in order to develop relationships between structural parameters, passenger safety, vehicle weight and vehicle cost.

The investigation in this section is confined to structural improvements other than the energy absorber. Results of the collision simulations in Chapter 7 showed that increased effective strength to weight ratio, whether accomplished by the addition of structural material or increased structural efficiency, has a very significant effect on reduction of passenger fatalities due to vehicle penetration. These results also indicated that severe second collision injuries can be eliminated at collision closure speeds up to at least 40 mph, and with strength to weight ratios as high as 12, provided that care is taken in the design of safe interiors. Therefore the structural cost effectiveness studies in this section focus on first collision fatalities in cars having an effective strength to weight ratio up to 12.

It is acknowledged that severe second collision injuries and possible second collision fatalities at closure speeds significantly greater than 40 mph can occur; however the computer simulations tend to confirm accident experience - fatalities in severe frontal collisions up to 40 mph or 50 mph are almost entirely due to vehicle penetration.

In the estimation of energy absorber cost (see Chapter 9) a useful baseline for comparing costs was found to be the cost of providing passenger-free end space. The same baseline is used in this investigation, and will provide a common reference point for comparing the potential cost effectiveness of structural improvements to the potential cost effectiveness of the energy absorber.

In Chapter 7, it was noted that the results of the computer simulations showed significant sharing of crush between car ends, and that this tendency has not occurred to any significant extent in actual frontal accidents, even at high closure velocities.* In the following analysis, accident experience is used as the baseline - that is, all crush is assumed to take place in the colliding car. Employing this assumption, if a train having n cars collides with an identical train with closure velocity V_c, the energy balance for each colliding car is given by

$$S \frac{X_c}{2} = \frac{1}{2} n \frac{W}{g} \left(\frac{V_c}{2}\right)^2 \qquad (11\text{-}1)$$

where

X_c = length of total crush for both cars

S = crush strength of cars

W = weight of each car

n = number of cars in train

Regarranging 11-1,

$$X_c = \frac{1}{4ng} \frac{V_c^2}{S/W} = .00777\ n \frac{V_c^2}{S/W} \qquad (11\text{-}2)$$

* It was noted in Chapter 7 that the difference may be due to partial vehicle override, which has the effect of making the lead car weaker than other cars.

The total crush distance of passenger compartment space in both trains (X_F) is equal to X_c minus the total amount of passenger-free end space.

$$X_F = \left\{ .00777\ n\ \frac{V_c^{\ 2}}{S/W} \right\} - 2\ X_s \qquad (11\text{-}3)$$

where X_s is the free end space at the colliding end of each colliding car. Equation 11-3 is plotted in Figure 11-1 for an eight car train, X_s equal to zero, and for closure velocities of 20 mph, 40 mph, 60 mph and 80 mph. Inspection of Figure 11-1 shows that the absolute magnitude of the derivative of X_F with respect to strength/weight ratio increases with increasing velocity and decreasing strength/weight ratio. The significance of the latter is that a given increase in strength/weight ratio is more effective in reducing X_F at low values of strength/weight ratio than at high values.

Figure 11-1 also provides information relating to a trade-off between strength/weight ratio and passenger free end space. For example, at closure speed of 40 mph and strength/weight ratio of 8, the amount of total car crush distance X_c is approximately 27 feet. If strength/weight ratio is increased to 12, the value of X_c is reduced to approximately 18 feet. Thus, it is evident that the vehicle having strength/weight ratio of 8 must have 4.5 more feet of passenger-free crush space than the vehicle with strength/weight ratio of 12 in order to provide equivalent passenger safety in a 40 mph collision.

In determining a reasonable level of strength/weight ratio for a new vehicle design, or in determining the most reasonable combination of vehicle strength and free end space, the collision dynamics information in Figure 11-1 must be considered. A quantitative analysis must also account for the costs of providing given increases in added strength and added end free space, and the corresponding benefits provided in terms of lives saved under specified accident conditions. The analysis should be sufficiently general to permit variations in specific unit costs (e.g.; the initial and recurring costs per pound of added structure) as particular manufacturing and operational requirements dictate. The required relationships are developed in the analysis which follows.

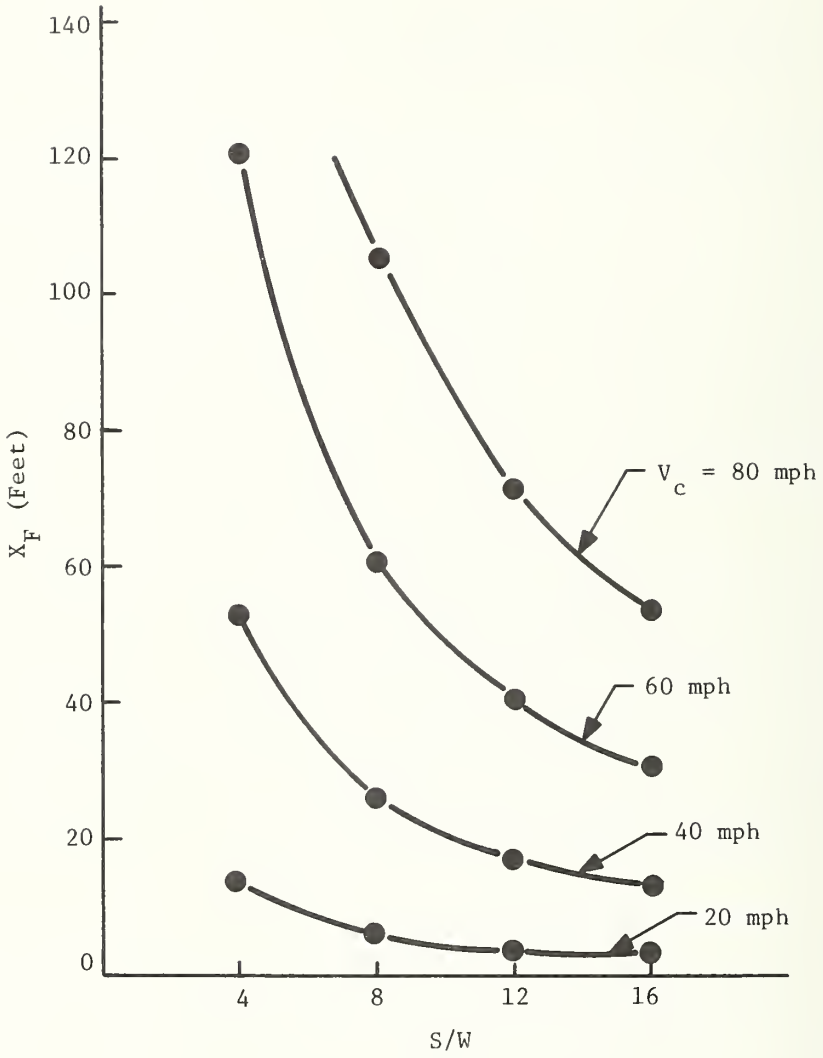

Figure 11-1. Total Crush Distance for Both Colliding Cars (X_F) Versus Strength to Weight Ratio (8 Car Trains)

The partial derivative of X_F with respect to strength/weight ratio is obtained by operating on Equation 11-3.

$$\frac{\partial X_F}{\partial S/W} = -.00777 \frac{n V_c^2}{(S/W)^2} \quad (11\text{-}4)$$

Similarly, the partial derivative of X_F with respect to X_s is

$$\frac{\partial X_F}{\partial X_s} = -2 \quad (11\text{-}5)$$

The corresponding derivatives with respect to cost are given by

$$\frac{\partial X_F}{\partial C_{SW}} = \frac{\partial X_F}{\partial S/W} \frac{\partial S/W}{\partial C_{SW}} \quad (11\text{-}6)$$

and

$$\frac{\partial X_F}{\partial C_s} = \frac{\partial X_F}{\partial X_s} \frac{\partial X_s}{\partial C_s} = -2 \left(\frac{\partial X_s}{\partial C_s} \right) \quad (11\text{-}7)$$

where C_{SW} is the effective annual cost per new car produced (including original cost and recurring cost) associated with strength/weight ratio, and C_s is the effective annual cost per new car produced (also including original cost and recurring cost) associated with the provision of passenger-free end space in the leading and trailing cars of each train.

Based on relationships in Chapter 9, the change in annual cost associated with a change in strength/weight ratio is

$$\Delta C_{SW} = 0.1 \Delta C_I + \Delta C_R \quad (11\text{-}8)$$

where ΔC_I is the change in original cost per new car produced associated with increased strength/weight ratio and ΔC_R is the change in corresponding annual recurring cost per new car produced. The former is given by

$$\Delta C_I = \Delta W \ (C_{IP}) \tag{11-9}$$

where ΔW is the weight increase per car associated with a given $\Delta S/W$ and C_{IP} is the original cost per pound of added weight. Similarly,

$$\Delta C_R = \Delta W \ (C_{RP}) \tag{11-10}$$

where C_{RP} is the annual recurring cost per pound of added weight. From Equations 11-8, 11-9 and 11-10.

$$\Delta C_{SW} = 0.1 \ \Delta W \ (C_{IP}) + \Delta W (C_{RP}) \tag{11-11}$$

Therefor

$$\frac{\partial S/W}{\partial C_{SW}} = \frac{\partial S/W}{\partial W} \left\{ \frac{1}{0.1 \ C_{IP} + C_{RP}} \right\} \tag{11-12}$$

The partial derivative in Equation 11-12 can be obtained from the relationships below

$$S = A \ F_c \tag{11-13}$$

$$W = W_o + \rho A \rho \tag{11-14}$$

where

F_c is the crushing stress allowable for the added material

A is the ratio of vehicle strength to crushing stress allowable (hence ΔA is the change in cross section area required for a change in strength ΔS)

ρ is the density of the added material in weight per unit volume

ℓ is the length of car

W_o is the difference between W and $\ell \rho A$

Manipulation of Equations 11-13 and 11-14 yields

$$\frac{\partial S/W}{\partial W} = \frac{F_c}{W \ell \rho} \left\{ 1 - \frac{S}{W} \frac{\ell \rho}{F_c} \right\} \qquad (11\text{-}15)$$

Combining Equations 11-4, 11-6, 11-12 and 11-15,

$$\frac{\partial X_F}{\partial C_{SW}} = - \frac{.00777\ n\ V_c^2}{(S/W)^2 (0.1\ C_{IP} + C_{RP})} \frac{F_c}{W \ell \rho} \left(1 - \frac{S}{W} \frac{\ell \rho}{F_c}\right) \qquad (11\text{-}16)$$

From section 9.3.2, the initial costs and annual recurring costs per new car produced of providing end free space in the lead car and trailing cars in a train are

$$\text{Initial Cost} = 2\, C_{I3}\, \frac{s}{\ell}\, \frac{1}{n} \tag{11-17}$$

$$\text{Annual Recurring Cost} = 2\, C_{R3}\, \frac{s}{\ell}\, \frac{p}{n} \tag{11-18}$$

where

C_{I3} is initial cost of one entire car

C_{R3} is annual recurring cost of one entire car

p is fraction of total car miles (for system considered) which is accumulated in rush hours

s is length of passenger-free end space at forward end of lead car in train and aft end of trailing car

ℓ is length of car

n is average number of cars per train in system

The annual recurring cost for one entire car can be expressed

$$C_{R3} = C_{RP}\, W \tag{11-19}$$

where C_{RP} is the annual recurring cost per pound of car weight and W is the weight of the car. Combining Equations 11-17 through 11-19 and Equation 9-12 in section 9.3.2

$$\Delta C_S = 0.2\, C_{I3}\, \frac{\Delta X_s}{\ell}\, \frac{1}{n} + 2\, C_{RP}\, W\, \frac{\Delta X_s}{\ell}\, \frac{p}{n} \tag{11-20}$$

From Equations 11-7 and 11-20

$$\frac{\partial X_F}{\partial C_s} = -2\, \frac{\partial X_s}{\partial C_s} = \frac{\ell\, n}{0.1\, C_{I3} + C_{RP}\, W\, p} \tag{11-21}$$

Equations 11-16 and 11-21 provide the partial derivative of passenger compartment crush distance with respect to cost of increased strength/weight ratio and increased passenger free end space, respectively. In Equation 11-16 the magnitude of the derivative represents the reduced length of passenger compartment crush (for the values of n, V_c and S/W specified in the right hand side of the equation) per dollar invested in increasing strength/weight ratio of each new car produced. In Equation 11-21, the magnitude of the derivative represents the reduced length of passenger compartment crush per dollar invested in increasing the passenger-free end space in the lead car and trailing car of each train. In this case, the dollars invested are also with respect to each new car produced. That is, if every train is an n car train and K dollars per train are invested in providing passenger-free end space in the leading and trailing cars, then $\frac{1}{2n}$ (K) dollars are invested for each new car produced.

In order to measure cost effectiveness in terms of dollars per life saved it is necessary to calculate the reciprocal of the derivatives in Equations 11-16 and 11-21. In Equation 11-16 the magnitude of the reciprocal of the derivative represents the cost (per new car produced) of reducing the passenger compartment crush distance 1 foot by means of strengthening the car (again, for the values of n, V_c and S/W specified as accident descriptors in the right hand side of the equation).

If the passenger compartment space is occupied by k passengers per foot when the specified accident occurs, the cost in terms of dollars per new car produced per life saved in a specified accident is obtained by dividing the reciprocal of the derivative by k. If N cars per year are produced in order to maintain the size of the fleet, the annual cost per life saved in a specified frontal accident (whenever it occurs) is given by

$$C_A = N \frac{1}{k} \frac{\partial C}{\partial X} \qquad (11\text{-}22)$$

The derivative used in Equation 11-22 is obtained from Equation 11-16 for costs associated with increased strength/weight ratio, and from Equation 11-21 for costs

associated with end-free passenger space. If the specified accident occurs once in a period of Y years, the total cost per life saved is given by

$$C_T = Y\ N\ \frac{1}{k}\ \frac{\partial C}{\partial X} \qquad (11\text{-}23)$$

The cost per life saved, obtained from Equations 11-16 and 11-23, is plotted in Figure 11-2 as a function of baseline strength to weight ratio for a single collision of identical eight car trains at closure speeds of 20 mph, 40 mph, 60 mph and 80 mph. The curves in Figure 11-2 are based on the following specific cost inputs.

(1) A national total of one collision occurring in all U.S. transit systems every 20 years.

(2) Weight of each car is 70,000 pounds.

(3) Car construction material is steel, with an effective crushing stress of 30,000 psi.

(4) The number of cars produced each year (N) in order to maintain the size of the national fleet (e.g.; the total number of cars in all U.S. transit systems) is 350*.

(5) When the accident occurs, both cars are occupied by three passengers per foot of car length and all passengers within portion of car crushed are killed.

(6) The cost per pound of providing additional structural material in an original design (i.e., not retrofitting) is 3 dollars per pound of added material.

---

* Reference, 73-74 Transit Fact Book, American Transit Association, 465 L'Enfant Plaza West, Washington, D.C.

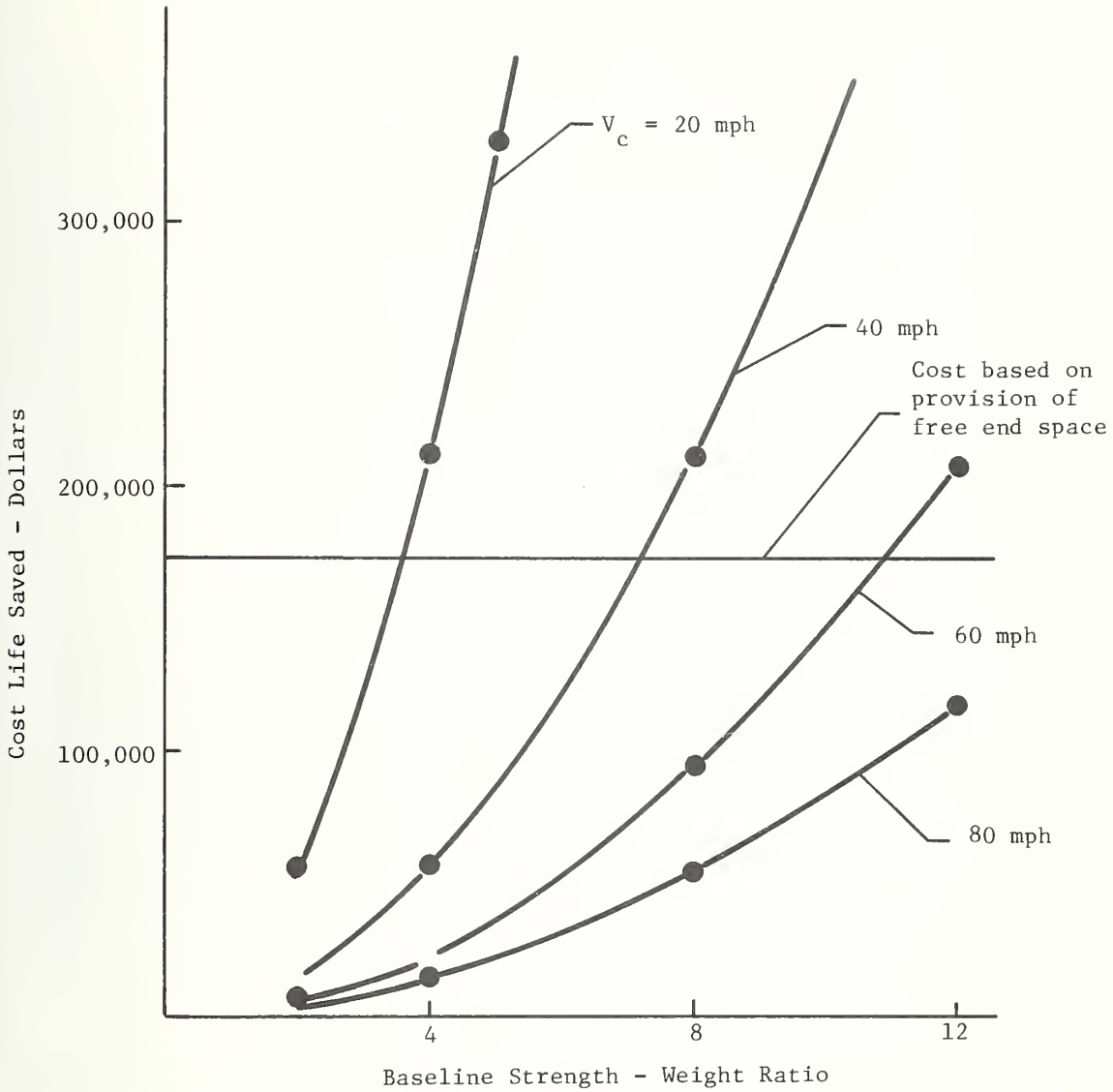

Curves Based on:
- one collision nationally every 20 yr.
- eight cars per train
- C_{13} = 400,000 dollars
- C_{IP} = 3 dollars per pound
- C_{RP} = 0.14 dollars per pound
- W = 70,000 pounds
- F_c = 30,000 psi, steel
- N = 350 cars produced per year
- k - 3 passengers per foot of car length

Figure 11-2. Cost Per Life Saved by Means of Increasing Strength-Weight Ratio

(7) The annual recurring cost of providing added weight is 0.14 dollars per pound.

(8) The annual rate of interest is 10%.

Figure 11-2 provides quantitative information on the following qualitative observations made in regard to Figure 11-1.

(1) Benefits associated with strengthening of cars are highest at low baseline strength to weight ratios and reduce with increasing strength to weight ratio.

Considering a relatively low baseline strength to weight ratio of 4, and a collision closure velocity of 40 mph, Figure 11-2 shows that the cost per life saved by means of strengthening the car (for the accident conditions and cost inputs specified previously) is approximately 50,000 dollars. This increases to approximately 200,000 dollars at a baseline strength-weight ratio of 8, and to approximately 300,000 dollars at a baseline strength-weight ratio of 9.5. In addition, cost benefits increase with increasing speed of collision, as shown in the figure.

(2) A design trade-off exists between strength to weight ratio and passenger free crush space.

This trade-off is indicated by the horizontal line in Figure 11-2. The line shows that the cost per life saved by means of providing additional end-free space is independent of car strength to weight ratio and collision velocity. The particular cost shown (170,000 dollars per life saved) is for the specific cost inputs identified in the figure. The intercept of the horizontal line and each collision velocity line represents the strength to weight ratio at which strengthening of the car and addition of end free space result in equal cost per life saved. For the 40 mph collision the figure shows that this

strength to weight ratio is approximately 7.2. Again, it is noted that the information in Figure 11-2 is for the particular cost inputs specified.

The cost per life saved shown in Figure 11-2 is for the particular baseline strength to weight ratio indicated. If a particular car is strengthened by a large amount, say an increase in strength to weight ratio from 4 to 8, the net cost per life saved is indicated very approximately by the median strength to weight ratio - in this case 6. This can be confirmed by the following specific example, in which the cost inputs are the same as those used in Figure 11-2.

Given that a car is increased in strength to weight ratio from 4 to 8, the reduction in total passenger compartment crush for both colliding cars in a 40 mph (58.7 feet per second) collision of identical eight car trains is obtained from Equation 11-3.

$$\Delta X_F = 26.8 \text{ feet}$$

At a loading of three passengers per foot of car length, the resulting reduction in passenger fatalities is

$$3\ (26.8) \approx 80 \text{ passengers}$$

Assuming a weight (W) of 70,000 pounds per car, the strength increase is given by

$$\Delta S = 4\ (70{,}000) = 280{,}000 \text{ pounds}$$

For an effective material crush strength (F_c) of 30,000 psi, the required increase in cross section area is given by

$$\Delta A = \frac{S}{F_c} = \frac{280{,}000}{30{,}000} = 9.33 \text{ in}^2$$

For a standard car length of 75 feet,the added material volume is equal to

$$9.33\ (75)\ (12) = 8400\ \text{in}^3$$

Using a density for steel of 0.3 pounds per cubic inch, the weight of material added is

$$0.3\ (8400) = 2520 \text{ pounds}$$

For a total construction cost (C_{IP}) of 3 dollars per pound, the initial cost per car (C_I) of providing the added strength is

$$C_I = 3\ (2520) = 7560 \text{ dollars}$$

For an annual recurring cost (C_{RP}) of 0.14 dollars per pound, the annual recurring cost (C_R) is

$$C_R = 0.14\ (2520) = 353 \text{ dollars}$$

From Equation 9-12, the total annual cost (for a 10 per cent rate of interest) per car produced is

$$C_T = 0.1\ (7560) + 353 \approx 1110 \text{ dollars}$$

For a production rate of 350 cars per year and a time period of 20 years, the total cost of strengthening the cars is

$$350\ (20)\ (1110) = 7{,}770{,}000 \text{ dollars}$$

Hence, if the specified accident occurs every 20 years (and no other accident occurs) the cost per life saved is

$$\frac{7{,}770{,}000}{80} = \$97{,}125$$

Figure 11-2 shows that this cost corresponds to a strength to weight ratio of approximately 5.2, slightly less than the median strength to weight ratio of 6. In increasing the strength to weight ratio of the car from 4 to 8, it is evident that the effective average strength to weight ratio for prediction of cost benefits favors the low end value of 4 because of the previously observed fact that more lives are saved by strengthening of the car at low levels of baseline strength to weight ratio.

The unit costs of material and fabrication for increasing the effective crush strength of car structure may vary considerably, depending on the construction material used, the car design and, perhaps most significant, the basis on which the estimates are made. The information in Figure 11-3 focuses on a 40 mph collision, with other collision conditions the same as defined in Figure 11-2, and with a range of unit costs from one dollar per pound of added material to five dollars per pound of added material. As in Figure 11-2, the information is based on the use of steel for construction material. Equation 11-16 shows that the cost of providing additional car strength is proportional to the weight density (ρ) of the construction material used. Aluminum alloys have approximately one third the density of steel alloys. Some of these alloys have effective crush strength as high as the 30,000 psi level on which Figure 11-2 is based. Hence, the one dollar per pound line shown in Figure 11-3 would correspond approximately to three dollars per pound for aluminum alloys with 30,000 psi effective crush stress. Similarly, high strength stainless steel alloys developing 90,000 psi would be in theory equally cost beneficial.

It is important to note that the most cost beneficial means of increasing the effective crush strength of car structure is to design the structure in such a way that the maximum amount of cross section material is effectively used in the crushing process. A good illustration of this was given in Chapter 10, where it was noted that the effective crush strength of the ACT structure could be increased by 400,000 pounds or more by making the roof structure effective in crush by means of adding relatively light contacting elements at the top of the collision posts. The effectiveness of the roof in compression is

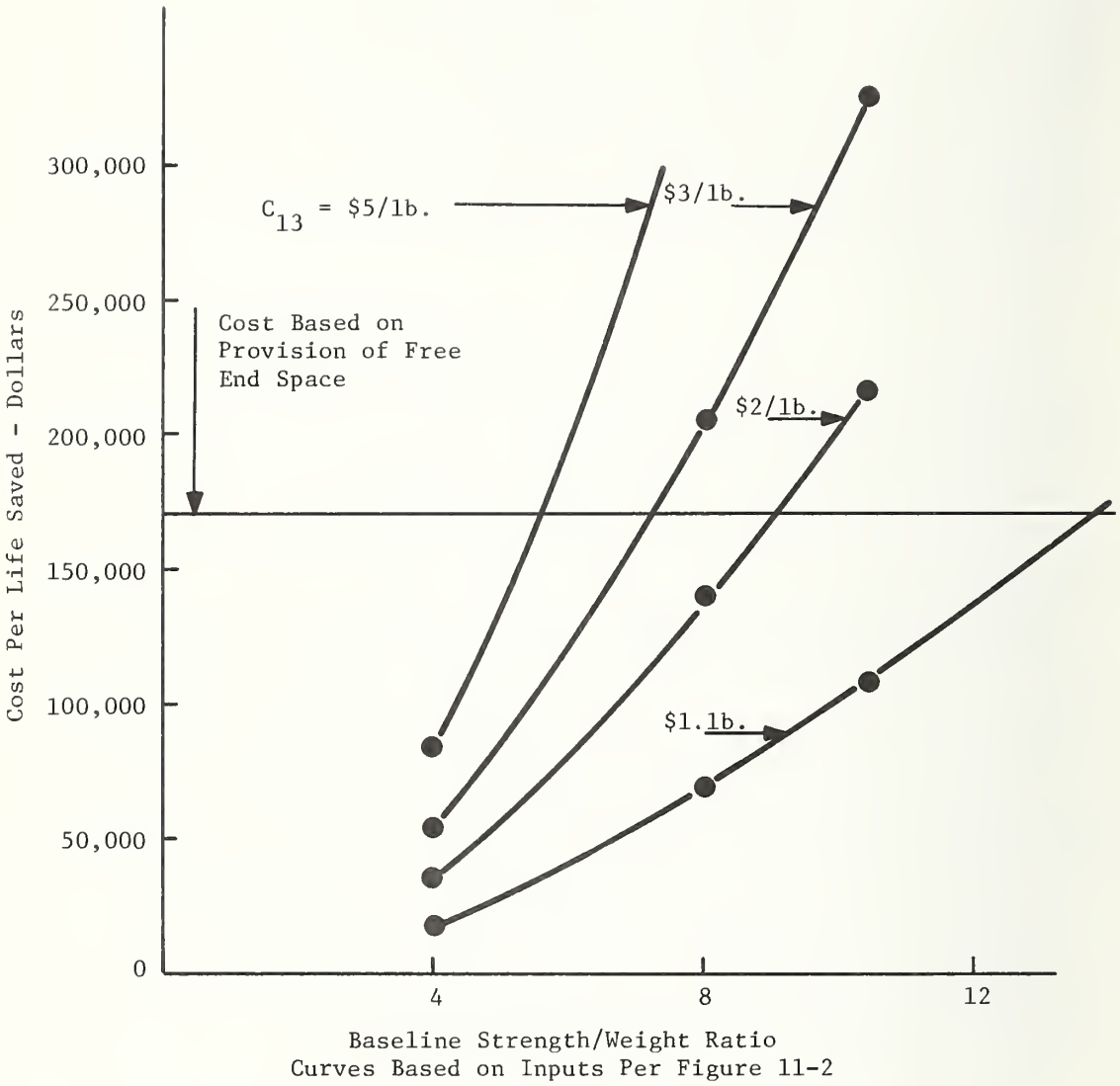

Figure 11-3. Cost Per Life Saved by Means of Increasing Strength-Weight Ratio - 40 MPH Collision

illustrated by Figure 10-3 and is discussed in the accompanying text. Addition of contacting elements to the collision posts is illustrated in Figure 9-7, and discussed in the text accompanying that figure.

By increasing structural efficiency and reducing climbing tendency, it is apparent that the potential gains in terms of cost per life saved would be greater than the best estimate in Figure 11-3, corresponding to one dollar per pound of added structural weight.

The most significant design trade-off appears to be the trade-off between car strength to weight ratio and passenger-free end space. The optimum or most cost beneficial strength to weight ratio is that at which strengthening of the car and provision of free-end space result in equal cost per life saved. In Figure 11-4, optimum strength to weight ratio is plotted as a function of closure velocity and cost per pound of providing stronger structure. As before, the optimum is based on a cost of 400,000 dollars per car for those cars which must be added to the fleet to compensate for the provision of free-end space. Free-end space is again based on the assumption that all crush takes place at the front end of the colliding cars. This space can be reduced if car designs are made such that some crush is distributed to other car ends.

Figure 11-5, based on the curves in Figure 11-4, presents a summary of strength/weight ratio versus free end space trade offs as a function of design criteria and unit cost of providing added structure. The three design criteria shown are based on elimination of first collision (penetration) fatalities in collisions of eight car trains at closure speeds of 20 mph, 40 mph and 60 mph. The upper cost figure shown (3 dollars per pound) is a very approximate estimate of the present total cost of fabricated structure. The lower figure (1 dollar per pound) can generally be taken as an upper limit for the cost of structural material. Since additional longitudinal strength can be provided by increasing the thickness of primary longitudinal members, additional structural members and additional joints should not generally be required. Therefore, the real cost of providing added strength is believed to be closer to the material cost than to the fabricated cost.

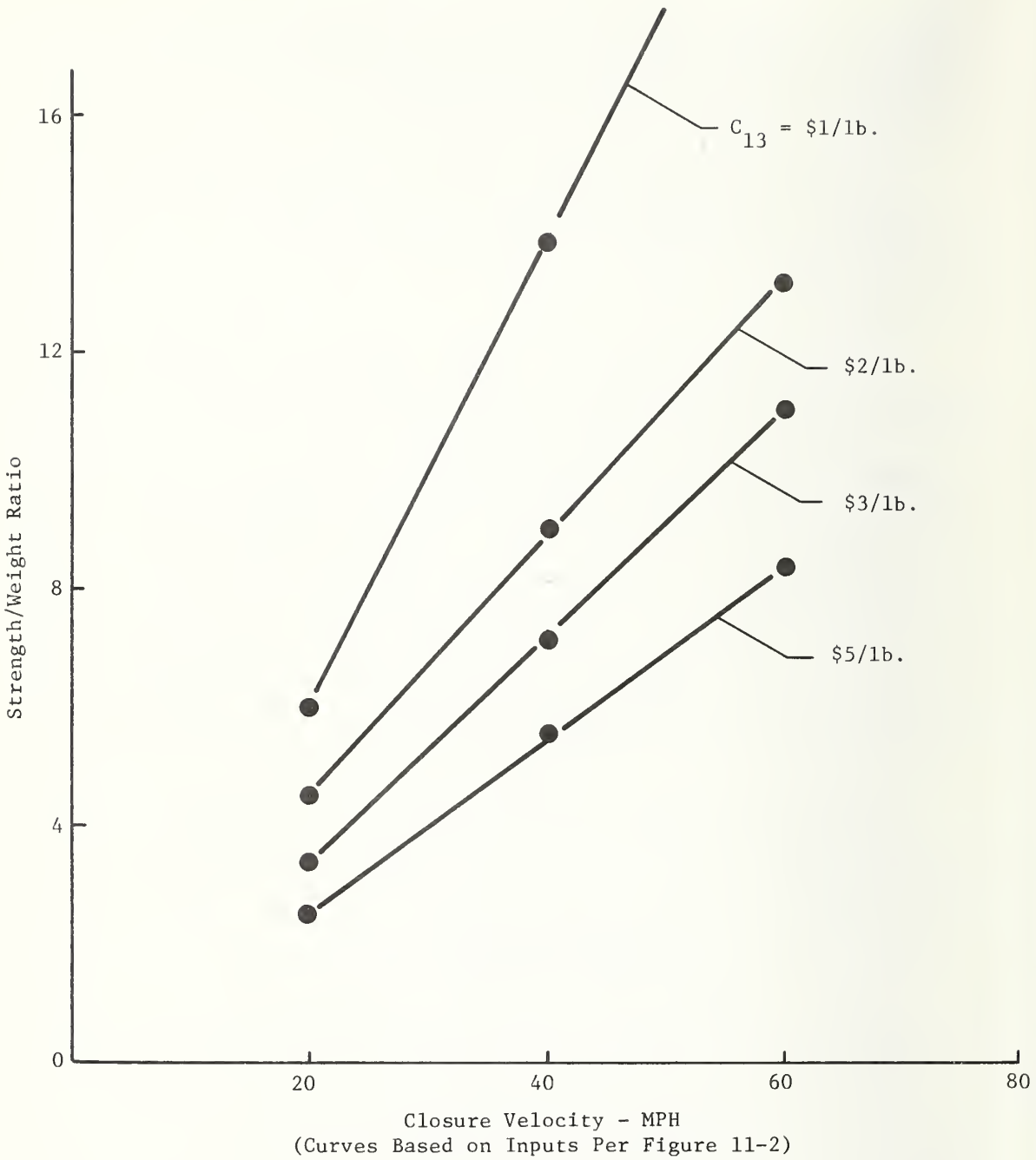

Figure 11-4. Strength to Weight Ratio at Which Strengthening of Car and Addition of End Free Space Result in Equal Cost Per Life Saved (Optimum Strength to Weight Ratio)

DESIGN CRITERIA: For Collisions of 8 Car Trains, Zero Penetration Fatalities at Closure Speeds of:	COST OF STRUCTURE (Dollars Per Pound)	OPTIMUM STRENGTH TO WEIGHT RATIO	END FREE SPACE REQUIRED (Feet)
20 mph	3	3.5	7.5
	2	4.5	6
	1	6	4.5
40 mph	3	7	15.5
	2	9	12
	1	14	7.7
60 mph	3	11	22
	2	13	18.5
	1	21	11

Figure 11-5. Summary of Design Criteria and Strength Versus Passenger-Free End Space Trade Offs

If added strength is obtained by increasing structural efficiency, rather than by adding to structural weight, added cost could be negligible or zero. In such cases, a prudent upper limit on strength to weight ratio should be established based on minimizing minor and moderate second collision injuries.

12. DEVELOPMENT OF UNIFORM STANDARDS

12.1 INTRODUCTION

It is apparent from the accident analyses and cost benefit analyses in previous sections that there is considerable room for improvement in urban railcar crashworthiness, and that significant investment in this improvement is warranted. Results of a severe frontal collision - even if it occurs only once nationally in 20 years - can be catastrophic in terms of lives lost, and will be very damaging to the public acceptance of new and existing transit systems.

Investigation of the five study cars has shown that there are wide differences in their strength levels and structural characteristics. In the following section (12.2) the varying structural specifications which apply to the study cars and 12 additional transit cars are reviewed.

The discussion in section 12.3 describes the difficult problem of coordinating analysis and experiment to form a basis for comprehensive uniform standards and means of determining compliance which are compatible with the economics of the transit car industry. This will require relatively long term development (5-10 years). Accordingly, a basis is suggested in Section 12.3 for the formulation of uniform interim standards which are an outgrowth of the disparate specifications which have been issued by the individual transit authorities.

12.2 REVIEW OF EXISTING STANDARDS

As a background for developing uniform standards for Urban Rail Car Crashworthiness, it is appropriate to consider first the nature and the content of existing structural standards and to proceed from there to a discussion of the factors which will effect the form and content of the new standards.

Present standards for transit system car structures tend to be based generally on particular portions of the existing FRA Equipment Standards. The FRA standards are similar to the earlier Postal Service and Association of American Railroad (AAR) standards, which originated in a set of structural requirements for mail cars at the turn of the century. These standards are almost exclusively aimed at static strength, with little or no provision for energy absorbing characteristics and general structural integrity (e.g., fatigue, corrosion, control of material quality).

The FRA standards and the earlier standards deal with the structural integrity of the car as a rigid shell or compartment, as well as with structural characteristics which can be expected to affect gross behavior in longitudinal collisions.

Specifications dealing with shell integrity include design criteria for side frame and roof assemblies and the vertical and transverse structural elements and sheathing which provide stiffness and strength normal to the plane of these assemblies. The minimum section modulus of the vertical and transverse stiffening members (per foot of car length) is stipulated. However the practice of the railroads has been, and is, to treat requirements not dealing directly with frontal strength as guidelines, in that demonstration of compliance is not generally required, either by analysis or test.

Key elements in the FRA standards dealing with frontal strength are

Car axial strength
Anti-climber strength
Crash post attachment strength
Truck attachment strength

Design substantiation in these areas is required. Car axial strength must be demonstrated by test, whereas stress analysis is generally acceptable as a demonstration of compliance in the other three areas.

The following design requirements in the four areas above are taken from Section 230.457 b-1 of the FRA standards "for trains having a total empty weight of less than 600,000 pounds"*.

Car Axial Strength

"The unit structure shall resist a minimum static end load of 400,000 pounds at the rear draft stops ahead of the bolster on the center line of draft, without developing any permanent deformation in any member of the unit structure."

Anti-Climbing Requirements

"An anti-climbing arrangement shall be applied at each end designed so that coupled units under full compression shall mate in a manner which will resist one unit from climbing the other. This arrangement shall resist a vertical load of 75,000 pounds without exceeding the yield point of its various parts or its attachments to the unit structure.

The coupler carrier and its connections to the unit structure shall be designed to resist a vertical downward thrust from the coupled shank of 75,000 pounds for any horizontal position of the coupler, without exceeding the yield points of the materials used. When a yielding type of coupler carrier is used an auxiliary arrangement shall be provided, designed in accordance with these requirements."

---

* Recent trends have been for more inter-city equipment to be in this lightweight category. However most existing equipment does not fall in this category. Higher FRA strength requirements for heavier equipment are shown subsequently in this section.

Crash Post Attachment Strength

"The outside end of each unit shall be provided with two main vertical members, one at each side of the diaphragm opening. Each main member shall have an ultimate shear value of not less than 200,000 pounds at a point even with the top of the underframe member to which it is attached. The attachments of these members at bottom shall be sufficient to develop their full shear value. If reinforcement is used to provide the shear value such reinforcement shall have full value for a distance of 18 inches up from the underframe connection, then taper to a point approximately 30 inches above the underframe connection."

Truck Attachment Strength

"Strength of locking means of truck to unit body shall be not less than the equivalent of an ultimate shear value of 250,000 pounds."

For trains which exceed 600,000 pounds in weight, strength requirements are generally higher, as shown in the comparison below.

	Trains less than 600,000 pounds	Trains weighing 600,000 pounds or more
Car axial strength	400,000 pounds	800,000 pounds
Anti-climbing strength	75,000 "	100,000 "
Crash Post Attachment Strength	200,000 "	300,000 "
Truck Attachment Strength	250,000 "	250,000 "

With the exception of the longitudinal load requirement, it should be noted that the FRA strength requirements deal with the strength of particular components and attachments, rather than with total structural strength. For example, the strength for "the coupler carrier and its connections to the unit structure" is specified, but equivalent strength in the rest of the structure is not explicitly required. Similarly, crash post attachment strength for a pure shear load is specified, but compatible bending strength of the crash post and its attachments is not specified.

Transit car structural specifications differ from the FRA standards, in that there is no single universal specification applying to all transit cars. Individual transit authorities produce their own specifications. The structural specifications are usually a small portion of the general design specifications which are issued along with Request-for-Bids from car builders.

Transit car structural specifications, though considerably more brief than the FRA standards, are similar to the latter in that they put most emphasis on frontal collision design characteristics - axial strength, crash post strength, and anti climbing strength. The frontal collision requirements of the FRA are used as points of departure by the transit authorities, though not each transit authority has a requirement for each of these design characteristics.

Key specification requirements for the four transit cars which were studied, plus the recently specified NYCTA R-46 car, are shown in Figure 12-1. (The fifth study car - the Silverliner - is not included in this tabulation because it is not a transit car.) It is evident from Figure 12-1 that there are large variations in degree of specification coverage. Early specifications (e.g. R-33 car) have no requirements for crash post strength or anticlimbing strength. Some of the latest specifications (R-46 car) include requirements in these areas as well as for corner posts.

The transit car specifications are similar to the FRA standards in that they deal with the strength of particular components and attachments rather than with total structural strength. For example, crash post requirements,

EXISTING SPECIFICATIONS RE: BUFF LOAD
COLLISION POST
ANTI-CLIMB LOAD

Car	Buff (Kips)	Per Cent FCY *	Buff Test	Collision Post Shear	Anti-Climb Load	Remarks
R-33	200	50	No	No Req.	No Req.	
R-34	250	50	Yes	No Req.	No Req.	
Silver-bird	200	90	Yes	200K Each	75 K	35K to each collision post 18" above floor
BART	180	90	Yes	No Req.	No Req.	
R-46	400	80	Yes	300K Each	100K	300K to each corner post also

* FCY = Allowable compressive yield stress. The percent FCY is the percentage of allowable yield stress which should not be exceeded at the specification buff loads shown.

Figure 12-1. Specifications for Existing Transit Cars

when included in transit car specifications, generally call for shear attachment strength with no corresponding requirements for bending strength of the post or its attachments. In this respect, they are also similar to the earlier standards for inter-city cars.

When particular strength requirements are included in the transit car specifications, there is large variation in level of strength required. A comparison of car buff test requirements, specification ultimate load (calculated from the specified buff test load and the permissible yield stress for which it is specified) and calculated maximum strength for the five study cars is shown below:

Rail Car	Buff Test Load (lb)	% Fy (Yield Strength) Per Spec.	Spec. Ultimate Load (lb)	Calculated Maximum Strength (lb)
R-33	200,000	50	400,000	700,000
R-44	250,000	50	500,000	540,000
Silverbird	200,000	90	222,000	612,000
BART	180,000	90	200,000	285,000
Silverliner	800,000	100	800,000	1,505,000

The average ratio between calculated maximum strength and specification ultimate load for the five cars studied, on the basis of the figures shown above, is 1.72. The maximum ratio is 2.75 (for the Silverbird car), and the minimum ratio is 1.08 (for the R-44 car).

Information on 12 urban rail cars additional to those investigated is shown in Figure 12-2. Although maximum crush load is not available for these additional cars (this would require the same analysis performed in this program for the five study cars), some correlation between the additional cars and the five study cars can be obtained from the last two "strength/weight" columns in the table: "specification ultimate load/weight ratio" and

RAIL-CAR DESIGNATIDN (IF ANY)	USER	MANUFACTURER	YEAR(S) BUILT	AVERAGE LIGHT WEIGHT (lb)*	BUFF TEST LDAD (lb)	SPEC. ULTIMATE LDAD (lb)	MAXIMUM CALCULATED CRUSH LDAD (lb)	BUFF TEST LDAD/ WEIGHT RATIO	MAXIMUM CALCULATED CRUSH LDAD/ WEIGHT RATIO	SPEC. ULTIMATE LDAD/ WEIGHT RATIO	EDUIVALENT STRENGTH/ WEIGHT RATID	RELATIDNSHIP TO RAIL CARS STUDIED
RAPID—TRANSIT CARS												
R-33	NYC TRANSIT AUTHDRITY	ST. LDUIS CAR DIVISIDN	1962-1963	72,653	200,000	400,000	700,000	2.75	9.63	5.50	9.63	(DNE DF RAIL CARS STUDIED)
R-44	NYC TRANSIT AUTHDRITY	ST. LDUIS CAR DIVISIDN	1970-1972	81,000	250,000	500,000	540,000	3.09	6.67	6.17	6.67	(DNE DF RAIL CARS STUDIED)
(BART) A & B CARS	BAY AREA RAPID TRANSIT DISTRICT	RDHR INDUSTRIES	1971-1973	60,000	180,000	200,000	285,000	3.00	4.75	3.33	4.75	(DNE DF RAIL CARS STUDIED)
SILVERBIRD	MASS. BAY TRANSPDRTA-TIDN AUTHDRITY	PULLMAN-STANDARD DIV.	1968	60,800	200,000	222,222	612,150	3.29	10.09	3.65	10.09	(ONE DF RAIL CARS STUDIED)
AIRPDRTER	CLEVELAND TRANSIT SYSTEM	PULLMAN-STANDARD DIV.	1966	64,775	200,000	200,000	--	3.09	--	3.08	5.30	BART /R-44
--	PDRT AUTHDRITY TRANS HUDSON	ST. LDUIS CAR DIVISIDN	1966	58,000	400,000	400,000	--	6.90	--	6.90	11.87	SILVERBIRD/SILVERLINER
--	PORT AUTHDRITY TRANS HUDSDN	ST. LDUIS CAR DIVISIDN	1966	55,300	200,000	400,000	--	7.23	--	7.23	12.44	SILVERBIRD/SILVERLINER
--	DELAWARE RIVER PDRT AUTHDRITY	THE BUDD COMPANY	1966	74,800	200,000	200,000	--	2.67	--	2.67	4.59	BART
EXPD '67 CARS	EXPD '67 (MONTREAL)	HAWKER SIDDELEY CANADA LTD.	1966	62,300	400,000	--	--	6.42	--	--	--	--
	CHICAGO TRANSIT AUTHDRITY	THE BUDD CDMPANY	1967	44,500	200,000	222,222	--	4.49	--	4.98	8.57	R-44/R-33
--	TDRDNTO TRANSIT CDMMISSIDN	HAWKER SIDDELEY CANADA LTD.	1970	55,500	115,000	--	--	2.07	--	--	--	--
--	PDRT AUTHDRITY TRANS HUDSDN	HAWKER SIDDELEY CANADA LTD.	1970	59,000	400,000	400,000	--	6.78	--	6.78	11.66	SILVERBIRD/SILVERLINER
--	CHICAGO TRANSIT AUTHDRITY	ST. LDUIS CAR DIVISION	1958	44,400	100,000	--	--	2.25	--	--	--	--
--	CHICAGD TRANSIT AUTHDRITY	PULLMAN-STANDARD DIV.	1963	46,890	200,000	222,222	--	4.27	--	4.73	8.14	R-44/R-33
--	MASS. BAY TRANSPORTA-TION AUTHDRITY	PULLMAN-STANDARD DIV.	1962	70,600	200,000	222,222	--	2.83	--	3.14	5.40	BART /R-44
MARKET-FRANKFDRD CARS	SDUTHEASTERN PA. TRANSPD. AUTHDRITY	THE BUDD CDMPANY	1959	48,730	200,000	275,000	--	4.10	--	5.64	9.70	R-33/SILVERBIRD

*INCLUDING TRUCKS, BUT WITHDUT PASSENGERS

Figure 12-2. Additional Information on Rail Cars Studied and Other Rail Cars

"equivalent strength/weight ratio." For the additional cars, the figures in the latter column were obtained by multiplying the former by 1.72, which we have noted is the average ratio (for the five study cars) between calculated maximum strength and specification ultimate load.

From Figure 12-2, the highest specification ultimate load/weight ratio of the four transit cars which were studied is 6.17 (R-44 car) and the lowest is 3.33 (BART car). Again, it should be emphasized that these are specified ratios, and do not necessarily represent estimates of maximum car crush strength. The latter are shown in column 8 of Figure 12-2, and the corresponding strength/weight ratios are shown in column 10.

Of the 12 additional transit cars shown in Figure 12-2, the highest specified ultimate load/weight ratio is for the Port Authority Trans-Hudson car (7.23) and the lowest is for the Cleveland Airporter car (3.08). Thus, the total range (3.08 to 7.23) is only slightly larger than for the study cars.

The specification ultimate loads shown in Table 12-2 are equal to maximum compressive yield loads. Though it is possible to develop peak crush strength which is significantly higher than yield strength, it is also possible to develop average crush strength levels (averaged over crush distance) which are significantly lower than yield strength. It is evident that existing specifications permit cars to be built with low strength levels, in terms of crush distance required to absorb collision energy. At a strength to weight ratio of only 3, the crush distance required in each train to absorb the collision energy of two identical eight car trains at closure speed of 40 mph is approximately 36 feet.

In evaluating specification strength requirements, it must be assumed that actual strength levels will not exceed those required by specification; hence it is quite significant that existing specifications call for car

strength levels considerably lower than optimum levels determined by the computer study. The tendency of cars in actual collisions to develop less than calculated strength (because of override) increases this significance.

The status of present transit car structural standards may be summarized as follows:

(1) No single standard applicable to all transit cars exists. Individual transit authorities produce their own structural specifications as part of design specifications for new cars.

(2) Transit car structural specifications, like the FRA structural standards, prescribe static strength levels.

(3) Emphasis is on design characteristics affecting longitudinal strength in frontal collisions.

(4) Strength levels of particular components and attachments are specified, but these strength levels need not be met throughout the structure. The only exception to this is the buff load requirement.

(5) Structural specifications for the different transit systems have large variations in level of coverage. Some standards require only longitudinal strength tests, and others require minimum levels of collision post strength, anti-climbing strength, and truck attachment strength in addition to longitudinal strength tests.

(6) Longitudinal strength requirements are significantly lower than optimum strength levels for minimization of penetration fatalities and second collision injuries at speeds up to 40 or 50 mph.

12.3 PERMANENT STANDARDS AND INTERIM STANDARDS

12.3.1 General Approach

The problem of formulating appropriate uniform standards is made difficult by the need for further research to form a basis for the new standards. The general approach suggested is to proceed with an orderly development of the methodology on which to base permanent standards. Because of the time required for proper analysis and validating experiments, it is suggested that uniform interim standards be formulated, as an outgrowth of the varying specifications which now exist.

The scope of the new standards is described in the following Section 12.3.2. Design criteria for structural standards are suggested in Section 12.3.3. In Section 12.3.4, design guidelines, design standards and performance standards are discussed with respect to the dual problem of developing a methodology for establishing permanent standards and appropriate means of determining compliance, and of formulating appropriate interim standards.

12.3.2 Scope

New structural standards discussed herein are limited to intra-city transit systems and commuter systems, and do not include inter-city systems covered by existing FRA structural standards. The new standards would replace the present non uniform structural specifications which are issued by the individual transit authorities.

Comprehensive standards should include interior safety standards, emergency exit requirements, fire hazard and water hazard requirements, etc. The structural standards discussed herein are limited to the structural integrity and crashworthiness of the basic car shell. Frontal collision integrity as well as general shell integrity are of interest. The latter includes situations where cars are struck from any direction while in a derailed or overturned position.

12.3.3 Design Criteria

The following tentative baselines are suggested for design criteria on which to base structural standards.

(1) Elimination of penetration fatalities in frontal collisions at speeds up to 40 or 50 mph.

(2) For the same collision speeds, limitation of rigid car body decelerations to levels sufficiently low to prevent severe second collision injuries in a defined interior environment.

(3) Establishment of minimum shell intrusion requirements for a limited number of representative crash scenarios.

12.3.4 Applicability of Design Guidelines, Design Standards and Performance Standards

It has been noted that existing FRA standards for inter-city cars are, in effect, a combination of design guidelines (side frame and roof construction) and design standards oriented toward frontal collision strength (strength requirements for longitudinal load, collision post attachments, anti-climbing and truck attachments). Transit car structural specifications issued by the individual transit authorities are essentially design standards and, like the FRA design standards, emphasize frontal collision strength.

One of the requirements of the National Traffic and Motor Vehicle Safety Act of 1966 is that safety standards for motor vehicles be performance oriented rather than design oriented. Thus, if one examines the Federal Motor Vehicle Safety Standards (FMVSS), as promulgated by the National Highway Traffic Safety Administration (NHTSA) of the DOT, one finds that all but a few are performance standards. Many of the standards, however, contain clauses that prescribe that motor vehicles contain certain pieces of equipment (e.g., a brake warning indicator, in FMVSS 105 - Hydraulic Brake Systems, Passenger Cars) and, in this respect, they may be said to mandate "design".

It is evident that any consideration of Federal regulations or standards for urban railcar safety has to deal with the applicability of design guidelines, design standards and performance standards, and the closely related question of destructive versus non-destructive testing in determining compliance to safety standards. A brief examination of these matters as they apply to current Federal standards for motor vehicles should be instructive.

In the case of motor vehicle standards the DOT actually conducts tests (performed by commercial testing laboratories) to determine whether vehicles comply with the FMVSS. The extent to which the DOT funds compliance tests of rail vehicles will undoubtedly depend to a great extent on the cost factors involved. For automobiles, the NHTSA budgeted in F/Y 1974 about 3 million for compliance testing. If one takes the annual passenger car sales at about 9.5 million and assumes an average retail price of $4000 the annual retail new car market amounts to roughly $38 billion. Compliance test costs are then (roughly) less than .01% of annual retail sales market.

The economics of the rail vehicle business are, of course, much different. The 1973-74 Transit Fact Book* states that the average annual production of transit cars in the U.S. is 350 cars per year. At an average annual cost of 400,000 dollars per car, the annual market for transit cars

---

* Reference, 73-74 Transit Fact Book, American Transit Association, 465 L'Enfant Plaza West, Washington, D. C.

amounts to 140 million dollars, or about 0.35 percent of the automobile market.

The cost of an average bare transit car shell is about 40,000 dollars, and the cost of trucks represents an additional 20,000 or 30,000 dollars per car. These figures are many times larger than for a typical automobile. It is evident that the performance standard requiring a destructive test to demonstrate compliance will therefore be many times more expensive than for an automobile.

The development of new urban rail vehicle standards will require a number of non recurring destructive validation tests, but will not necessarily require that every new design be subjected to a destructive test. The following example is given to illustrate this.

A specific design improvement requires additional structural material (or re-configuring of structural material) in the front end of a rail vehicle to prevent vertical deformation during collision (which could lead to override). A destructive validation test could conceivably be designed to demonstrate that, under worst possible misalignment conditions or conditions of anti-climber engagement, the design improvement is successful and no override occurs. Prior to the destructive validation test, a non-destructive vertical load test could be performed to determine the static strength level of the structure. If it could be established that the longitudinal failure mode for certain classes of designs does not destroy vertical load carrying capability (perhaps through a separate series of validation tests), the subsequent performance tests could be limited to non-destructive longitudinal and vertical load tests of the vehicle structure. This is a specific example where destructive validation tests are preceeded by non-destructive tests during the validation program for the purpose of correlating destructive collision behavior with non-destructive test results and providing a basis for relatively economical (non-destructive) conformance tests.

In effect, additional investment in validation tests is made in order to provide a basis for a specification for which compliance can be economically demonstrated. The economic leverage arises from the fact that validation tests are essentially non-recurring, whereas compliance tests must be performed for each new vehicle design.

A combination of design guidelines and design standards can be employed to support the type of approach described above.

Design guidelines supported by analysis and experiments can be effectively used by the car builder to establish gross design characteristics. An example of this is the distribution of mass and longitudinal crush characteristics in a single car. In this case an expanded version of the type of collision model employed in this investigation can be used on a single car to determine a range of desirable force versus deflection characteristics and mass distribution characteristics. Design curves representing the range of desirable distributions can then be used by the car builder. Similarly, guidelines for anti-climbing construction can be provided. In determining the guidelines, analytical calculations should be confirmed by experiment in non-recurring validation tests of various classes of designs.

Design standards would be quantitative, and would require that compliance be demonstrated for each new design, by analysis and non-destructive test. The purpose of the design standards would be to insure that longitudinal crush load falls within the specified range. Results of the analysis and non-destructive test would be compared to destructive and non-destructive validation test results in order to infer car crush characteristics. This is a very general description of a complex methodology - the development of which will require considerable analysis and validation testing.

A significant period of time will be required to develop the new methodology. Because of the wide variation in existing standards, it is therefore suggested that a uniform set of interim design standards and or guidelines be formulated.

It has been noted in previous sections that the force-deflection characteristics of cars in the post-elastic range of interest are very difficult to predict. Since the force-deflection characteristic is extremely important in assessing car crashworthiness, it is recommended that scale model and full scale tests be performed to provide a basis for the formulation of interim standards.

The most comprehensive structural specifications which exist at the present time appear to be the latest specifications for the NYCTA R-46 car. It is suggested that these specifications also be used as a baseline for formulating the interim standards.

APPENDIX A
REVIEW OF INJURY CRITERIA DEFINED IN LITERATURE

A.1 PURPOSE

The injury criteria defined in the literature and presented in Table 2-1 (Chapter 2) were reviewed to determine their applicability to rail crash safety. The review is presented in this appendix.

A.2 HEAD INJURY CRITERIA

Head injury criteria are based upon skull fracture or brain concussion. Data have been obtained to date using cadavers, animals, and human volunteers. Cadavers have been used to obtain levels of skull fracture resulting from being subjected to impacts which fall at the short-duration, high-magnitude end of acceleration/time correlations. Lower-magnitude, long-duration acceleration/time limits have been obtained using human volunteers. Animals are also used in an attempt to extrapolate human data from tolerable to intolerable accelerations and forces.

Injury criteria listed in Table 2-1 are based upon linear deceleration in the longitudinal direction (eyeballs-out in the military vernacular), H_x, or lateral acceleration, H_y; rotational velocity or acceleration of the head, $\dot{\alpha}$ and $\ddot{\alpha}$, respectively; or severity indices, HSI or HIC, which are both acceleration/time integrations.

The earlier Gadd Head Severity Index,[1] HSI, when adopted by DOT, was objected to by the automotive industry because it was based upon a summation of acceleration pulses which occurred over the total crash period. The HIC (Head Injury Criterion) summation method subsequently adopted by DOT to replace the HSI approach does not accumulate separate or distinct pulses occurring during the crash period. In effect, pulses occurring during the primary impact and during rebound are not added to obtain HIC. The industry argued that their safety systems, while adequate in terms of HIC $< 1{,}000$, were failing the criterion HSI $< 1{,}000$ for cases of noninjurious restraint.

Typically, HSI exceeds HIC for representative crash pulses by some 25 to 40%. As a point of interest, at the same time that DOT was being petitioned to accept HIC over HSI, Gadd was suggesting a limit of HSI < 1500 for pulses which occur for durations over a few milliseconds. Essentially, it was recognized that the severity indices were attempting to distinguish between impacts with rigid objects which might cause skull fracture over a period on the order of 5 milliseconds and the longer-duration, "softer" impacts which might cause concussion.

Both HSI (and its revised forms HSI $\leqslant 1{,}000$ with $t < 5$ ms, and HSI $\leqslant 1{,}500$ with $t > 5$ ms) and HIC do not represent all present attempts to devise head injury indices; they are simply the ones receiving the greatest attention at present. At least four others exist: JTI (J*-Tolerance Index), EDI (Effective Displacement Index), MSC (Maximum Strain Criterion), and RBM (Revised Brain Model). An excellent discussion of head injury which compares these indices and also discusses head injury mechanisms in general is presented by Voight R. Hodgson of Wayne State University in Reference 1.

The significance of rotational head velocity ($\dot{\alpha}$) and acceleration ($\ddot{\alpha}$) in injury is perhaps the most controversial consideration. No criterion is presently included in NHTSA FMVSS 208,[2] whereas another study[4] recommends approximately 1800 rad/sec^2 as a tolerable limit based upon data obtained using animals. The latter reference postulates that rotation plays a dominant role in brain injury. Further, in a continuation of this work, A. E. Hirsch (at the Fourteenth Stapp Car Crash Conference) presented data from which he concluded that rotational acceleration is <u>the</u> injury mode to be considered, and that "no convincing evidence has to this date been presented which relates brain injury and concussion to translational motion of the head for short duration force inputs, whether through whiplash or direct impact," to which he adds, "Engineers and safety designers should be aware of this when they employ currently popular head tolerance criteria in the design of head impact-protection devices" (citing Gadd's HSI). However, HSI and, subsequently, HIC

---

*J is the ratio of the maximum-displacement component to the tolerable displacement.

have been supported, both by data taken on tests of frontal impacts to the head and by human-volunteer sled tests for acceleration.[1] The relatively good agreement between these data generated in decidedly different manners suggests that the impact-test results were obtained under conditions where the force was applied over a large enough surface area to justify its interpretation in terms of acceleration and, hence that either HSI or HIC may be used as a valid index of head injury.

Fortunately, we are not in a position in this study where we must choose one proposed injury mode over another or one injury index over another, or even one value of injury index upon which to make a pass/fail judgment. All of these data are being used in helping to evaluate rail crash injury and the effectiveness of proposed improvements.

A.3 FACIAL INJURY CRITERIA

All facial injury data presented in Table 2-1 are concerned with bone fracture within specific areas of the face. The data present maximum force at the threshold of fracture for cadavers and also human-volunteer tolerance levels.

Force levels for skull fracture with a padded impactor can be compared to peak head accelerations at fracture. The force levels, approximately 2,000 lb, appear to be in relatively good agreement with the 150 to 200 g's measured at skull fracture. (See, for example, Reference 12, based upon a nominal head weight of 10 to 12 lb.) This not only allows correlation for the case of head injury but also provides an indication of equivalent acceleration levels for fracture of various parts of the face. Since, for example, the force levels for fracture of some of the more delicate parts of the face are as little as 1/10 the skull fracture levels, we can predict moderate injury for impact with a small-contact-area surface on acceleration/time plots. This, along with other considerations (such as facial laceration), is helping us to project injury levels at conditions below, for example, HSI = 1,000.

A.4 NECK INJURY CRITERIA

Neck injury data have been obtained through torque limits that human volunteers would allow themselves to be subjected to and through slowly applied torques administered to cadavers. (See especially the work of Mertz of G.M. -- for example, Reference 1.) The values of torque presented in Table 2-1 were measured about the occipital condyles, a position located at the base of the skull. The neck injury criteria "hypertension" (chin up) and "hyperflexion" (chin down) have little application to rail crash studies. Hypertension is the "whiplash" injury associated with rear-end automobile collisions which cause high-magnitude, positive longitudinal accelerations. Hyperflexion is an injury associated with a lap- and shoulder-belted occupant experiencing high-magnitude, negative longitudinal accelerations*. In the low-magnitude acceleration environments of train crashes, it is believed that these injuries do not play a significant role. Consequently, these criteria have not been included in the train crash injury criteria.

A.5 CHEST INJURY CRITERIA

Chest injury criteria are presented in terms of longitudinal decelerations (eyeballs-in in the military vernacular) or forces, C_x; vertical acceleration, C_z (eyeballs-down); the resultant of acceleration along all three axes, $C_R = (C_x^2 + C_y^2 + C_z^2)^{1/2}$; or chest severity index, $CSI = \int C_R^{2.5}\, dt$, an offshoot of HSI.

The first two values of C_x presented in Table 2-1 have interesting origins. Acceleration tolerances of 49 g's for 0.10 second were found to be regularly withstood by a professional performer who dove from heights up to 57 feet into foam padding with no apparent discomfort. Thorax rates of deceleration (jerk) were as high as 5900 g's/sec. This diver was brought to

---

*Interestingly enough, such a well-known authority in injury studies as Colonel J. P. Stapp has stated categorically that hyperflexion injuries simply do not occur because of the natural stop or rotation limitor provided by the sternum.

the attention of Mertz and Gadd[13] at G.M. and subsequently instrumented and tested under contract, one purpose being to support G.M.'s disagreement with a proposed safety standard limit (at that time) of 40 g's for automobile crash protection systems.

The second value, 45.4 g's for 0.23 second, represents Colonel J. P. Stapp's most famous rocket sled ride on the Daisy track in New Mexico. Since he experienced considerable discomfort on that ride, the injury value is listed as minor. Both of these results provided a basis for NHTSA's subsequent issuance of safety standards providing for limiting chest resultant acceleration to C_R = 60 g's and chest severity index to CSI = 1000.

The vertical chest acceleration limit, C_Z = 25 g's, has its origin in military jet-aircraft ejection-seat tests and appears to be a condition under which occasional spine injury occurs. Because this condition is not believed relevant to automobile crash injury, the NHTSA allowable tolerance is much higher; 60 g. Likewise, this condition has not been incorporated into the rail crash injury criteria.

The two remaining C_X injury criteria in Table 2-1 are based upon maximum force. Under uniform force distribution, such as occurs with the chest vest, the tolerable forces would be expected to reach chest deceleration equivalent. For a nominal upper torso weight of 100 lb, a total force of 6000 lb (60 g's) appears to be a reasonable limit based upon the 3300-lb load accepted by a volunteer.

As with facial damage data, the force results can also be considered in terms of pressure. For the vest case, the mean pressure would be 23 psi for a 3300-lb load, or 42 psi for a 6000-lb load (the proposed tolerable limit based on 60 g's). Rib fracture occurred for 1200-lb pressure with a 28-in.^{2} impactor, equivalent to a pressure of 43 psi. It appears that tolerance levels fall in the tens of psi range, and that a value on the order of 40 psi is reasonable for use in studies of impact with small contact surfaces.

A.6 PELVIC AND LOWER-EXTREMITY INJURY CRITERIA

Lower-extremity injury criteria in Table 2-1 cover the femur (thigh bone), the patella (knee cap), and the tibia and fibula (leg bones). The data presented in the table are nominal or average values for an adult male, and deviations from the quantities given of as much as ±50% would be expected from person to person.

Studies on cadavers which date back into the 1880's (R. Messerer, "Über Elastizität und Festigkeit der Menschlichen Knochen," cited in Reference 12) have produced data on loading to failure in bending and torsion. These data are of interest primarily to the biomechanist engaged in sports safety -- especially, skiing. Since they involve bending and torsion which is nearly impossible to describe in a rail crash study, it is difficult to apply these criteria. As a general result, we are looking for car interior designs which minimize opportunities for partial entrapment of the lower extremities during a crash sequence.

Axial force data on the patella and femur have been generated through interest in automobile crash protection and involve padded and unpadded impact of the patella. Much of these data have been generated by Patrick at Wayne State University, as cited in, for example, Reference 1. As a general observation, it was found that, if padding is provided, failure of the femur is the dominant injury mode. Without padding, fracture of the patella may be expected to occur first.

These injury studies -- i.e., consideration of the axial force loading of the femur through the patella -- have also provided data on pelvic fracture. In general, the femur is found to be the weaker link. The pelvic injury criteria support this observation in that tolerable pelvis loads applied through seat belts are in excess of twice the tolerable femur loads.

In rail crashes, passengers will not be using lap belts; therefore, it can be assumed that impact forces to the pelvis will likely be transferred from the femur. Since the femur is the weaker link, it is not necessary to consider pelvic injury criteria in the rail crash study.

A.7 UPPER-EXTREMITY INJURY CRITERIA

Upper-extremity injury criteria include consideration of loads to the bone in the upper arm (the humerus) and to the bones in the lower arm (the radius and the ulna). Injury criteria with regard to these body components are presented for torsion and, as with the leg data, are not, in general, applicable to crash injury study. Arm failures may be expected to occur in rail crashes, but the dynamics involved in their injury patterns simply cannot be modeled. These injuries, again, are the type which can be given crash-protection design attention through fairly obvious and straightforward design to avoid entrapment of body-extremity components. These injuries, then, along with others discussed subsequently, must be grouped into areas of injury severity which, as a whole, can be correlated with impact speed and deceleration distance.

A.8 WHOLE-BODY INJURY CRITERIA

Whole-body injury data in Table 2-1 are based entirely on acceleration or acceleration-rate (jerk) limits. These data actually can be placed under the head or chest categories, but, by listing them separately, it is seen that they can be summarily excluded from the rail crash injury criteria. These high acceleration magnitudes (i.e., greater than 40 g's) are not compatible with the train crash deceleration profiles that can be assumed to occur. In a like manner, the very high onset rates of acceleration (1000 to 2000 g's/sec) are inconsistent with possible rail crash injury modes.

A.9 UTILIZATION OF RESULTS

The results of this review were utilized as described in Chapter 2 (subsection 2.3).

APPENDIX B
REPORT OF INVENTIONS

After a diligent review of the work performed under this contract, it was determined that no innovation, discovery, improvement, or invention has been made.

REFERENCES

1. Anon., "Biomechanics and its Application to Automotive Design," Publication P-49, Society of Automotive Engineers, Inc., New York, N.Y., January 1973.

2. Anon., "Occupant Crash Protection in Passenger Cars, Multipurpose Passenger Vehicles, Trucks and Busses," Publication FMVSS 208, National Highway Traffic Safety Administration, U.S. Dept. of Transportation, revision of 17 February 1972.

3. Mertz, H. J. and Gadd, C. W., "Thoracic Tolerance to Whole-Body Deceleration," Paper Published in Proceedings of Fifteenth Stapp Car Crash Conference, Coronado, California, 17 November 1971.

4. Ommaya, A. K., et al., "Comparative Tolerances for Cerebral Concussion by Head Impact and Whiplash Injury in Primates," SAE Paper 700401, 1970 International Automobile Safety Conference Compendium, Society of Automotive Engineers, Inc., New York, N.Y., 1970.

5. Robbins, D. H., Snyder, R. G., and Roberts, V. L., "Injury Criteria Model for Restraint System Effectiveness Evaluation," Report BioM-70-7, Highway Safety Research Institute, Ann Arbor, Mich., October 1970.

6. Eiband, A. M., "Human Tolerance to Radially Applied Acceleration," Memo 5-19-59 E, National Aeronautics and Space Administration, June 1959.

7. Gurdjian, E. S., "Experiences in Head Injury and Skeletal Research," Published in Proceedings of Symposium on Impact Acceleration Stress (held at Brooks Air Force Base, November 27-29, 1961), Publication 977, National Academy of Sciences, National Research Council, 1961.

8. Bahniuk, Eugene, Mack, Robert P., Burstein, Albert H., and Frankel, Victor H., "The Biomechanics of Contemporary Ski Bindings," Journal of Safety Research, December 1972.

9. Anon., "Human Tolerance to Impact Conditions as Related to Motor Vehicle Design," Recommended Practice SAE J885a, published in 1966 SAE Handbook, Society of Automotive Engineers, Inc., New York, N.Y., October 1966.

10. Anon., "Military Troop Seat Design Criteria," Technical Report TCREC TR-62-79, Aviation Crash Injury Research Division, Flight Safety Foundation, Inc., Fort Eustis, Va., November 1962.

11. Schneider, D. C. and Nahum, A. M., "Impact Studies of Facial Bones and Skull," Paper presented at Sixteenth Stapp Car Crash Conference, November 1972.

12. Evans, F. Gaynor, Ph.D., Stress and Strain in Bones - Their Relation to Fractures and Osteogenesis, Charles C. Thomas, Publisher, Springfield, Ill., 1957.

13. Samarco, G. J., Burstein, A. H., Davis, W. Q., and Frankel, V. H., "The Biomechanics of Torsional Fractures: The Effect of Loading on Ultimate Properties," Journal of Biomechanics, 4, pp. 113-450, 1971.

14. DeHaven, H., "The Site, Frequency and Dangerousness of Injury Sustained by 800 Survivors of Light Plane Accidents," Unnumbered document, Crash Injury Research, Department of Public Health and Preventive Medicine, Cornell University Medical College, Ithaca, N.Y., July 1952.

15. Ryan, G. Anthony and Garrett, John W., "A Quantitative Scale of Impact Injury," Report VJ-1823-R34, Calspan Corporation, Buffalo, N.Y., October 1968.

16. Mackay, G. M., Road Accident Research Report No. 4, Human Engineering Section, Dept. of Transportation and Environmental Planning, University of Birmingham (England), December 1966.

17. Robertson, J. S., McLean, A. J., and Ryan, G. A., "Traffic Accidents in Adelaide, South Australia," Special Report No. 1, Australian Road Research Board, Melbourne (Australia), 1966.

18. Safety Investigation Regulations Part 320, Civil Aeronautics Board, U.S. Dept. of Transportation, Washington, D.C., 18 May 1966.

19. States, John D., M.D., "The Abbreviated and the Comprehensive Research Injury Scales," Paper published in Proceedings of Thirteenth Stapp Car Crash Conference, Society of Automotive Engineers, Inc., New York, N.Y., 1969.

20. Reed, Robert C., Train Wrecks, Superior Publishing Company, Seattle, Wash., 1968.